# Dynamic Volunteer Staffing in Multicrop Gleaning Operations[1]

Baris Ata
*Booth School of Business, University of Chicago, 5807 South Woodlawn Ave., Chicago, IL 60637, Baris.Ata@chicagobooth.edu*

Deishin Lee
*Carroll School of Management, Boston College, 140 Commonwealth Ave., Chestnut Hill, MA 02467, deishin.lee@bc.edu*

Erkut Sonmez
*College of Business, University of Nebraska-Lincoln, 730 N. 14th St., Lincoln, NE, 68588, esonmez2@unl.edu*

June 2018

**Abstract**

Gleaning programs organize volunteer gleaners to harvest a variety of leftover crops that are donated by farmers for the purpose of feeding food-insecure individuals. Thus, the gleaning process simultaneously reduces food waste and food insecurity. However, the operationalization of this process is challenging because gleaning relies on two uncertain sources of input: the food and labor supplies. The purpose of this paper is to help gleaning organizations increase the (value-weighted) volume of fresh food gleaned by better managing the uncertainties in the gleaning operation. We develop a model to capture the uncertainties in food and labor supplies and seek a dynamic volunteer staffing policy that maximizes the payoff associated with the amount of food gleaned. The exact analysis of the staffing problem seems intractable. Therefore, we resort to an approximation in the heavy traffic regime. In that regime, we characterize the system dynamics of the multicrop gleaning operation and derive the optimal staffing policy in closed form. The optimal policy is a nested threshold policy that specifies the staffing level for each class of donation (i.e., a donation of a particular crop type and donation size). The policy depends on the number of available gleaners and the backlog of gleaning donations. A numerical study using data calibrated from a gleaning organization in the Boston area shows that the dynamic staffing policy we propose can recover approximately 10% of the volume lost when the gleaning organization uses a static policy. To achieve this improvement, no capital or major process changes would be required – only some small changes to the staffing level requests.

Keywords: Gleaning, volunteer, food bank, food waste, food insecurity, dynamic control.

**Acknowledgements** This work is supported by the Neubauer Family Foundation at the University of Chicago Booth School of Business.

# 1 Introduction

The practice of gleaning combines two societal problems to create an elegant solution for both. Gleaning dates back to ancient times when landowners allowed the poor to gather crop left on the fields after the harvest. This act of generosity alleviated the dual paradoxical problems of food waste and food insecurity. These problems persist and are arguably even magnified in modern times. The amount of food wasted in the U.S. is staggering – almost 40 percent of food fit for human consumption is wasted (Gunders 2012). A significant portion of this waste occurs at the farm level where farmers leave crops unharvested because market conditions make it unprofitable to pay for harvesting labor. For example, the crop could be blemished or misshapen, but perfectly edible and nutritious, or a bumper crop season could drive the market price down. A USDA estimate indicates that 6 percent of fruit and vegetable crops are left unharvested (USDA 2011).

While edible and healthy food was left unharvested in farm fields, 14 percent of U.S. households in 2014 were food insecure. The USDA definition of food insecurity is "a household-level economic and social condition of limited or uncertain access to adequate food" (USDA 2015). This translates to 17.4 million households in which 15.3 million members are children (Coleman-Jensen et al. 2015). It is not simply calories lacking in food insecure households, but insufficient consumption of micronutrient-rich foods such as fruits and vegetables (Davis and Tarasuk 1994; Tarasuk and Beaton 1999). A number of studies have found links between food insecurity and health-related issues such as obesity, diabetes, and hypertension (Gomez et al. 2013; Weinfield et al. 2014; Wilson et al. 2015). Thus, it is not just increasing the quantity of food, but increasing the quantity of the right type of food that will help alleviate the problems associated with food insecurity. In particular, healthy foods such as fresh fruits and vegetables can help improve and balance the diets of food insecure individuals.

Juxtaposing these two societal problems, it seems a natural solution would be to use the unharvested crops that would otherwise go to waste, to help food assistance programs (e.g., food banks) provide healthy, nutritious food to supplement the diet of food-insecure individuals. In fact, many gleaning organizations nationwide have already implemented this solution. For example, in recent years, gleaning programs in California, Ohio, Arizona, Texas, and New York respectively have distributed 127 million, 26 million, 18.5 million, 13 million, and 3.6 million pounds of fruits

and vegetables on an annual basis (California Association of Food Banks 2011; Schuelke et al. 2011; Vitiello et al. 2014).

Although the gleaning solution to food waste and food insecurity is conceptually elegant and appealing, the operationalization of the solution poses distinct challenges. Gleaning relies on two uncertain sources of input: the food and labor supplies. Gleaning donations arrive randomly, as farmers themselves face uncertainty in crop yield, market prices, and labor supply. Donations can be of varying crop types (e.g., apples, lettuce) and of various sizes (measured in pounds of produce). Although the overall gleaning season can be 6 months to year-round depending on geographic location, when the gleaning organization is notified of a gleaning donation (i.e., communication from a farmer for an opportunity to glean unharvested crop), it must schedule a gleaning trip within a short window of time, usually on the order of a few days to a week, in order to reap the crop before it perishes on the field. Moreover, in order to make gleaning economically feasible, gleaning organizations use volunteer gleaners to harvest the crop. Using historical gleaning trip data and current communication with its volunteer pool, the gleaning organization typically has a good idea of how many gleaners are available at a given time. However, since these gleaners are volunteers, they are not obliged to attend a scheduled gleaning trip, even if they are available and sign-up for the trip. Therefore, the labor supply is uncertain.

Clearly, gleaning organizations exist and are successful in their mission to provide healthy food to food assistance programs. There are many ways to measure the performance of a gleaning operation. One metric is the total volume, i.e., the total number of pounds gleaned. However, because of the inherent differences in crop types, there may be differences in "value" per pound across crop types. For example, value could be measured in servings, in which case carrots would have have 2.5 servings per pound whereas lettuce would have 6.3 servings per pound. Value could also be measured in the market value of the crop. The purpose of this paper is to help these organizations increase the value of fresh food gleaned by better managing the uncertainties in a gleaning operation.

We develop a model to capture the uncertainties in food and labor supply and derive a dynamic volunteer staffing policy that maximizes the long run average value of food gleaned. Our policy gives gleaning organizations a simple staffing policy to manage a key tradeoff that arises because of the gleaning operation's reliance on volunteer labor. On the one hand, when a gleaning donation

arrives, the organization would like to maximize the volume gleaned (which translates to a particular value) on the scheduled trip. Each gleaning trip is typically 3 hours long. Each gleaner is able to harvest a certain volume of a given crop type, therefore, the more volunteer gleaners that attend a trip, the higher the output volume (up to the total volume available for harvesting). This would imply requesting a high volunteer staffing level – even higher than the number of gleaners needed to harvest the available crop because some volunteers may not show up. Note, however, that the expected marginal output from each unit increase in volunteer staffing level is decreasing. Moreover, unlike employees who can be required to attend every gleaning trip, volunteers who do show up will likely not attend another gleaning trip for some time. This may cause another gleaning opportunity that arises in the near future to have low volunteer gleaner attendance and low output volume, or even require the gleaning organization to turn down the donation completely because low volunteer availability would delay the scheduling of the trip too far into the future. This could lead to loss of farmer goodwill. Therefore, on the other hand, the organization may want to request a lower volunteer staffing level and sacrifice output on the current trip in order to "save" volunteer labor for anticipated future gleaning trips. The tradeoff between immediate and future output is crucial, especially when gleaner utilization is high, i.e., when the gleaning donation rate is high relative to the rate at which volunteers become available.

In fact, the staffing level tradeoff faced by the gleaning organization is similar to the tradeoff in the Newsvendor model, i.e., the cost versus the benefit of a marginal unit of capacity. However, there is a crucial difference. In the Newsvendor model, the shadow price for the marginal unit of capacity is determined by exogenous parameters such as demand characteristics (or arrival rate of customers), cost, and penalty values. In our setting, the shadow price of a marginal unit of capacity (i.e., an increase in staffing level) also depends on the staffing levels set in previous periods. That is, the shadow price arises endogenously based on the staffing policy deployed. Because of the distinct nature of this process, a dynamic model is required to capture the staffing decision tradeoff.

We characterize the system dynamics of the gleaning operation and derive the optimal staffing policy that maximizes the gleaning organization's net payoff, i.e., the total value of gleaned produce minus penalties incurred for turning down donations (for example, loss of farmer goodwill). We show that the optimal policy is a nested threshold policy that specifies the staffing level for each class of donation (i.e., a donation of a particular crop type and donation size). The policy depends

on the number of available gleaners and the backlog of gleaning donations. Our characterization of the thresholds is almost explicit in the sense that the calculations involved are lightning fast; they only involve finding the roots of strictly monotone functions. We calibrate our model based on volunteer and gleaning trip data from the Boston Area Gleaners (BAG 2016). Using the calibrated model, we perform a simulation study that shows that the dynamic policy improves the net payoff compared to two policies used in practice: the static policy and the unlimited policy. The magnitude of the improvement depends on the penalty for rejecting donations. Within a reasonable range of penalty values, our results showed a net payoff improvement range from approximately 3% to 6% compared to the static policy, and on the order 40% compared to the unlimited policy. This modest improvement in net payoff translates to the recovery of approximately 10% of the volume lost using the static policy and approximately 75% of the volume lost using the unlimited policy. To put this in perspective, for a gleaning organization around the size of the Boston Area Gleaners (BAG 2016) using the static policy, the recovered volume would be equivalent to approximately 18,500 (4-ounce) servings per year.

## 2 Literature Review

Topically, this paper is related to a stream of literature that studies operations that support humanitarian relief organizations. Much of the research in this area focuses on "sudden onset" disasters such as earthquakes and hurricanes (see Altay and Green 2006; Kovacs and Spens 2011; Galindo and Batta 2013; Starr and Van Wassenhove 2014 for reviews). However, there is emerging work on "slow onset" disasters that are not triggered by a specific event, but are severely adverse conditions that create significant hardship for vulnerable segments of the population (Van Wassenhove 2006). The systemic problem of food insecurity is an example of such slow onset disasters. There is a stream of extant literature that focuses on non-profit food bank operations (see Johnson and Smilowitz 2007 for an overview). Most of the research in this area studies tactical decisions in food bank operations such as vehicle routing for food collection and distribution (Gunes et al. 2010; Yildiz et al. 2013; Davis et al. 2014; Lien et al. 2014; Solak et al. 2014), warehouse operations (Mohan et al. 2013), and forecasting techniques for food donation (Davis et al. 2013). In the literature that focuses on food bank gleaning operations, much of the work studies the impact of gleaning

programs on recipients' diet in terms of nutrition and preference (e.g., Teron and Tarasuk 1999; Irwin et al. 2007) and improving food security (Hoisington et al. 2001). The papers most related to ours are Sönmez et al. (2016) and Lee et al. (2017) that examine the operational efficiency of a food bank gleaning operation. Sönmez et al. (2016) and Lee et al. (2017) focus on a particular field study and use a simulation-optimization approach to compare the effectiveness of a given feasible set of fixed trip schedules. In contrast, we model a general setting and derive an (almost) explicit characterization of an optimal dynamic staffing policy.

Similar to our paper, the literature in humanitarian operations has also studied volunteer management. These papers focus on specific settings where volunteer task and scheduling criteria have been critical (see Sampson 2006 for an overview). For example, Falasca and Zobel (2012) develop a spreadsheet model for optimizing volunteer schedules that consider volunteer preferences and task/schedule desirability. Similarly, Gordon and Erkut (2004) develop a scheduling program for a music festival staffed by volunteers. In our setting, the organization cannot schedule volunteers to a particular shift. The challenge is to manage the uncertainty in labor capacity. We develop a model and derive an optimal policy that is generalizable to other volunteer settings where the attendance of volunteers is uncertain.

The gleaning process studied in this paper has similar characteristics to operations in the sharing economy and inventory settings. The research on ride-sharing operations studies queues with self-scheduling capacity. This setting is similar to ours in that the number of servers is stochastic. However, a key difference from our context is that the servers in the sharing economy are compensated, and thus a key managerial lever for managing capacity is setting the compensation level. Banerjee et al. (2015) compare the performance of dynamic and static pricing schemes when there is imperfect information on system parameters. Taylor (2017) investigates how delay sensitivity and agent independence affects the optimal price and server compensation. Ibrahim (2017) jointly optimizes the staffing, compensation, and delay announcement decision of a system with self-scheduling servers. Dong and Ibrahim (2017) provide recommendations on when a firm should use a blended workforce (consisting of full-time and (random number of) contingent workers that are paid different wage levels).

An inventory setting that is related to our paper is the inventory control problem with random yields; Yano and Lee (1995) provides a comprehensive description of the issues in this context and

a review of the literature. The similarity of the random yield setting and ours is the problem of how to set capacity or inventory quantity, i.e., balancing the overage and underage costs when the availability of the relevant resource (inventory or volunteers) is uncertain. Using a modified Newsvendor model with demand uncertainty and production yield uncertainty, early papers focused on the single-period setting, characterizing the optimal order policy, which includes whether to place an order depending on the level of on-hand inventory, and if so what the production/order quantity should be (cf. Karlin 1985, Giffler 1960, Shih 1980, Gerchak et al. 1988, Henig and Gerchak 1990).

A more complex problem addressed in the random yield inventory is the multi-period problem where inventory can be carried over from period to period. Gerchak et al. (1988) show that the solution to the multiperiod random yield problem is not myopic, and Henig and Gerchak (1990) proved the structure of the optimal policy in a general setting (including showing that the order point is higher when the yield is random than when it is certain). Deriving the optimal policy is difficult and the solution approach has been to develop heuristics to determine the optimal order quantity. (cf. Mazzola et al. 1987, Bollapragada and Morton 1999, Zipkin 2000, Inderfurth and Transchel 2007, Huh and Nagarajan 2010, Inderfurth and Vogelgesang 2013, Inderfurth and Kiesmuller 2015). Unlike the inventory setting where the current order quantity is not upper bounded by previous orders, in the volunteer staffing problem, the staffing level requested in the past affects the availability of volunteers currently available. Moreover, unlike the inventory setting where demand and decisions are periodic, donation arrival timing is random and volunteer availability must be synchronized with the arrivals in order to capture the value of the fresh produce, as in a service setting. Thus, we use a queueing model to capture the dynamics of the volunteer gleaning process, and the structure of the optimal policy prescribes positive or negative changes to staffing level to adjust for system congestion. In a similar inventory setting, Huang et al. (2008) studies the optimal policy when there is replacement warranty demand, which depends on demand from previous periods, reduces the capacity to serve the new demand in a given period. A key difference in Huang et al. (2008) is that the reduction in capacity is a fixed fraction of previous demand whereas volunteer availability in our setting is random.

The methodology used in this paper contributes to a stream of literature that studies dynamic resource allocation under uncertainty. At a high level, the abstract mathematical model developed in this paper is related to the literature on (dynamic) service rate control in Markovian queueing

systems. Many papers have been written on different versions of the service rate control problem over the past 50 years (cf. Crabill 1972, 1974, Weber and Stidham 1987, Stidham and Weber 1989, and George and Harrison 2001; see Stidham 1988, 2002 for a survey through circa 2002). More recently, motivated by wireless communications applications, Ata (2005) and Ata and Zachariadis (2007) study this question for a queueing system with a finite buffer where congestion concerns are captured by imposing a constraint on the fraction of blocked jobs. Ata (2005) focuses on choosing the service rate dynamically as a function of the queue length. The cost rate associated with the chosen service rate is convex increasing. Ata and Zachariadis (2007) extend this to a setting where the environment is changing randomly. Both papers derive closed-form formulas for the optimal (dynamic) service rate as a function of the queue length. Ata and Shneorson (2006) consider a setting where both the arrival and service rates are chosen dynamically and characterize the optimal policy in closed form. Hopp et al. (2007) also examine a setting where the service rate can be chosen dynamically and compare it with the fixed service rate case.

Our problem has several important differences from those studied by the aforementioned papers. Arguably, the most important difference is that the service rate (or staffing level for each gleaning donation) chosen in the current period affects the service rate in future periods directly because the volunteers working now will not be available for some time. This process feature is central to the planner's optimization problem.

From a methodological perspective, our work is also related to the control of queueing systems in heavy traffic, pioneered by Harrison (1988). In this literature, one approximates the queueing system with a Brownian model, which is simpler to analyze (see for example, Harrison and Wein 1989, 1990 and Wein 1990). The validity of this approach and the accuracy of the resulting approximation are verified in the literature by simulation studies and heavy traffic limit theorems (see for example, Harrison 1998, Bell and Williams 2001, and Ata and Kumar 2005). Several papers in the heavy traffic literature formulate control problems with delay constraints, and derive more tractable approximations by replacing the delay constraints with upper bounds on the queue lengths in the heavy traffic regime as done in this paper (see for example, Plambeck et al. 2001, Ata 2006, and Rubino and Ata 2009). We follow the same approach and approximate a challenging control problem with a simpler one in the heavy traffic limit. However, the limiting regime we use is the one advanced in the seminal paper, Halfin and Whitt (1981), where the arrival rate and the

number of servers grows simultaneously; also see Browne and Whitt (1995) for a study of related diffusion processes.

The asymptotic analysis of our problem gives rise to a drift-rate control problem. There have been several papers in recent years which consider controlling the drift rate of a diffusion. Ata et al. (2005) study the drift rate control of a reflected diffusion on a bounded interval under general costs of the drift rate chosen; also see Ata (2006), Kim and Ward (2013), Ata and Tongarlak (2013), Ormeci-Matoglu and Vande Vate (2011) and Ghosh and Weerasinghe (2010). Two closely related papers, Rubino and Ata (2009) and Ghamami and Ward (2013), consider scheduling parallel-server queueing systems. Rubino and Ata (2009) consider optimal scheduling and admission control for a general parallel-server system with abandonments under linear holding costs, abandonment penalties, costs for rejecting jobs and delay constraints, which are replaced with bounds on queue lengths in the asymptotic formulation. Rubino and Ata (2009) solve the drift-rate control problem arising in the heavy traffic regime, propose a policy for the general parallel-server system and show its effectiveness through simulations. Ghamami and Ward (2013) consider a similar setting, but also provide a proof of the asymptotic optimality of their proposed policy.

Among the drift-rate control problems mentioned above, the closest to ours is Ata et al. (2005). To be specific, we can use the approach in Ata et al. (2005) whenever there is a positive backlog of gleaning donations and all volunteers are busy. However, when there are available volunteers (i.e., the negative part of the state space), their approach breaks down because the system dynamics are very different in the positive part of the state space. Thus, a novel method is needed to analyze the problem on the negative part of the state space, which we develop. Moreover, combining the solutions on the negative and positive parts of the state space in a smooth fashion is far from straightforward and required us to do the "smooth pasting" with ad hoc arguments from first principles. Hence our paper also contributes to the literature of diffusion control problems by explicitly solving the volunteer staffing problem.

# 3 The Gleaning Operation and the Planner's Dynamic Staffing Problem

We represent the gleaning operation as a queueing process. The process starts with a donation from a farmer. Each donation is of a particular crop type, indexed by $i = 1, ..., I$ (e.g., apples, lettuce, etc.) and a particular size $s_{ij}$, $j = 1, ..., J_i$, measured in pounds of produce. The combination of crop type and the size of donation will define a class. Thus, there are $J_1 + J_2 + ... + J_I$ classes of donations. We will use the double subscript $ij$ to denote the class of a donation. Gleaning donations from farmers of class $ij$ arrive randomly according to a Poisson process of rate $\lambda_{ij}$ to the gleaning organization; we denote the arrival process of class $ij$ gleaning donations by $\{R_{ij}(t); t \geq 0\}$. We refer to the gleaning organization as the *planner* ("she"). When the gleaning donation arrives, the planner schedules a gleaning trip that is staffed by volunteer gleaners who harvest the crop. We refer to volunteer gleaners as *volunteers* ("he").

The entire volunteer pool consists of $n$ volunteers. Each volunteer is capable of harvesting $\alpha_i$ pounds of produce $i$ on a typical 3-hour gleaning trip. Each pound of produce has value $\nu_i$, which can be measured in dollars, number of servings, or another appropriate measure of value. Thus, on a 3-hour trip, each volunteer's gleaning output generates a payoff of $r_i = \nu_i \alpha_i$. To harvest the entire crop associated with a gleaning donation of class $ij$ requires $\tilde{k}_{ij} = s_{ij}/\alpha_i$ volunteers. Therefore, each gleaning donation has a potential total payoff of $r_i \tilde{k}_{ij}$, but the realized value is the minimum of the potential payoff and $r_i$ multiplied by the number of volunteers that attend the gleaning trip.

Volunteers, unlike employees, are not obliged to attend every scheduled gleaning trip. Typically, multiple gleaning trips are scheduled per week during the gleaning season (gleaning seasons are usually 6 to 12 months long). A few very active volunteers may attend a trip every week, whereas many volunteers only attend once or twice a season. Therefore, after an active harvesting time of 3 hours, a volunteer typically has a period of repose that may last weeks to several months during which he is not available for gleaning trips. We consider the combination of the harvest and repose periods as a volunteer's total service time – during his service time, the volunteer is *unavailable* for signing up for gleaning trips. Note that the harvest time for each volunteer is identical, but their repose times differ; moreover, the harvesting time of 3 hours is negligible compared to the repose period. At the end of the entire service time (harvest plus repose), the volunteer becomes

*available* to attend gleaning trips. Because the gleaning organization typically has a good idea of how many gleaners are available (using historical data and through communication with volunteers), we assume that the number of available volunteers is observable. The average rate that a volunteer becomes available after his repose is denoted by $\mu$; and we model the service time of a volunteer as an exponential random variable.

When a gleaning donation arrives, the planner requests a volunteer staffing level, $k$. The request for $k$ volunteers can be sent to the volunteer pool via an online signup portal similar to the one used by the Boston Area Gleaners (BAG 2016). Typically getting volunteers to sign up if they are available is fairly easy. Once the staffing level request is made, those volunteers who are available sign up for the gleaning trip slots, up to the requested staffing level. Thus, we assume that if a staffing level of $k$ is requested, $k$ volunteers will sign up. However, because volunteers are not employees, there is some chance that they will not actually show up, even if they signed up for the trip. We use $q$ to denote the probability that a volunteer attends a gleaning trip if he signs up, and $N_{ij}(k)$ to denote the number of volunteers that attend a class $ij$ gleaning trip when the requested staffing level is $k$. Assuming volunteers act independently, we model $N_{ij}(k)$ as a Binomial random variable with $k$ trials and a success probability of $q$. Thus, for a class $ij$ gleaning trip with requested staffing level $k$, the expected payoff is:

$$\Pi_{ij}(k) = r_i \mathbb{E}[\min\{N_{ij}(k), \tilde{k}_{ij}\}]. \tag{1}$$

Because a class $ij$ gleaning trip uses $N_{ij}(k)$ volunteer servers, we make a flow unit conversion from gleaning donation (trip) to volunteer jobs by breaking down each class $ij$ gleaning donation into $N_{ij}(k)$ volunteer *jobs*.

The service time for a job is the harvest time plus repose time, i.e., the entire time the volunteer is unavailable. If there are not enough volunteers available when a gleaning donation arrives, our model backlogs the jobs, not necessarily the entire donation, unless there are no available volunteers. Thus, this backlog is expressed in units of volunteer jobs, i.e., one backlogged gleaning donation of class $ij$ is equivalent to a backlog of $N_{ij}(k)$ volunteer jobs if the staffing level $k$ is requested. The planner decides the staffing level for gleaning donations of various classes dynamically over time. That is, she chooses a dynamic staffing policy $\{k_{ij}(t) : t \geq 0\}$, for all $i, j$. Given the planner's

dynamic staffing policy $\{k_{ij}(t) : t \geq 0\}$, for all $i, j$, the cumulative number of volunteer jobs (to be served) arriving by time $t$, denoted by $A(t)$, is given as follows:

$$A(t) = \sum_{i=1}^{I} \sum_{j=1}^{J_i} \int_0^t N_{ij}(k_{ij}(s))\, dR_{ij}(s), \;\; t \geq 0.$$

We use $Q(t)$ to denote the number of jobs currently in the gleaning operation at time $t$ and call this the queue-length process. This includes the number of volunteers who are currently unavailable (i.e., actively harvesting or in repose), and the number of virtual jobs that are backlogged. It is easy to see that the process $\{Q(t) : t \geq 0\}$ corresponds to a Markovian queue with arrival process $\{A(t) : t \geq 0\}$ and $n$ exponential servers. Thus, its dynamics can be described by its infinitesimal transition rates.

Gleaning is a time sensitive process because crops must be harvested in a timely manner. When a farmer calls with a gleaning donation, the gleaning trip must be scheduled within a few days to at most a week or else the crop will perish on the field. In other words, there is a constraint on the delay experienced by the backlogged donations. To meet such delay constraints, the planner may choose to reject gleaning donations upon arrival. That is, if the number of backlogged jobs are too high (i.e., there are too many donations already in the queue), the lead time to the scheduled trip will be too long and the planner will have to reject the gleaning donation. If a donation is rejected, the planner not only loses the expected payoff of the trip, she also incurs a loss of farmer goodwill. Farmers are willing to work with gleaning organizations, but they expect a certain level of consistency from the organization. If the gleaning organization often rejects gleaning donations, then farmers will be less willing to expend the extra effort to engage with the organization in the future. To capture that the planner loses more than just the payoff of the current donation when she rejects, we represent the loss of farmer goodwill by a penalty $\tilde{p}_{ij}$ (e.g., in potential future donations) when a class $ij$ gleaning donation is rejected.

The expected payoff of the gleaning trip (Equation (1)) clearly increases in the staffing level, $k$. There are two factors that drive this increase. First, there is a productivity effect: each volunteer is only capable of generating $r_i$ in value. Therefore, the marginal attending volunteer adds $r_i$ to the total payoff of the trip, up to $\tilde{k}_{ij}$ volunteers on a given trip. Second, there is a safety capacity effect: with probability $1 - q$, a volunteer who signs up does not show up for the trip. Up to a

nominal staffing level $k^*_{ij}$, the productivity effect dominates. Beyond $k^*_{ij}$, the safety capacity effect dominates. Thus, the expected payoff function for a class $ij$ donation increases steeply in the requested staffing level $k_{ij}$ up to the nominal staffing level $k^*_{ij}$, then increases less steeply as the productivity effect diminishes and marginal volunteers are only useful if there are no-shows (i.e., the safety capacity effect).

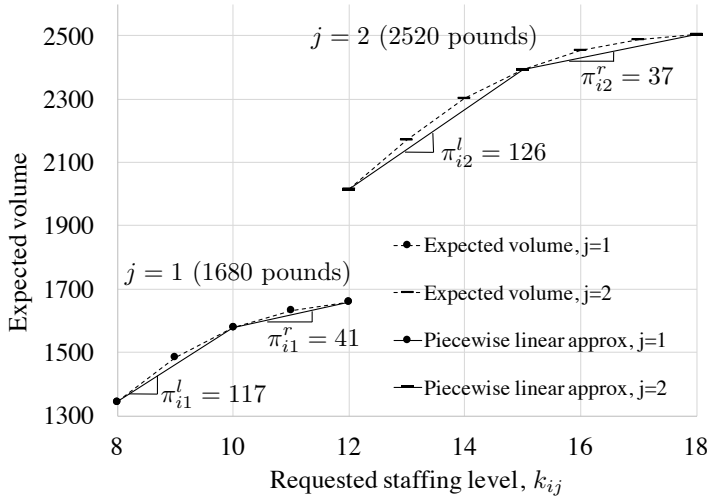


**Figure 1:** Expected payoff functions and piecewise linear approximations for two donation classes of crop type $i = 2$ (apple) with two donation sizes $j = 1$ (1680 pounds) and $j = 2$ (2520 pounds); $q = 0.8$, $\nu_i = 1$, $\alpha_i = 210$ pounds; $\tilde{k}_{i1} = 8$, $k^*_{i1} = 10$, $\underline{k}_{i1} = 8$, $\bar{k}_{i1} = 12$; $\tilde{k}_{i2} = 12$, $k^*_{i2} = 15$, $\underline{k}_{i2} = 12$, $\bar{k}_{i2} = 18$.

Figure 1 shows the expected payoff curves (dotted lines) as a function of the requested staffing level, $k_{ij}$, for a donation of crop type $i = 2$ (apple) with two donation sizes $j = 1$ (1680 pounds) and $j = 2$ (2520 pounds). In the figure, $q = 0.8$, $\nu_i = 1$, and $\alpha_i = 210$ pounds. For $j = 1$, if $\tilde{k}_{i1} = 8$ volunteers are required to harvest the entire crop of 1680 pounds, then setting a nominal staffing level of $k^*_{i1} = \tilde{k}_{i1}/q$ would imply that in expectation, 8 volunteers would show up. The staffing level range is set to $\pm 20\%$ of the nominal (i.e., $k^*_{i1} \pm 0.2k^*_{i1}$) so that $k_{i1} \in [\underline{k}_{i1}, \bar{k}_{i1}]$, where $\underline{k}_{i1} = 8$ and $\bar{k}_{i1} = 12$. Similarly, the staffing level range for $j = 2$ is set to $k^*_{i2} \pm 0.2k^*_{i2}$ such that $\underline{k}_{i2} = 12$ and $\bar{k}_{i2} = 18$.

The payoff functions in Figure 1 show the difference between the productivity effect and the safety capacity effect of the marginal volunteer. For each expected payoff function, $j = 1, 2$, to the left of the nominal staffing level $k^*_{ij}$, the slope of the payoff function is steep (productivity effect), whereas to the right of $k^*_{ij}$, the slope flattens out (safety capacity effect). We approximate the

expected payoff function as a piecewise linear function (solid lines in Figure 1). We approximate the two pieces of the function using the slopes $\pi_{ij}^l = (\Pi_{ij}(k_{ij}^*) - \Pi_{ij}(\underline{k}_{ij}))/(k_{ij}^* - \underline{k}_{ij})$ and $\pi_{ij}^r = (\Pi_{ij}(\bar{k}_{ij}) - \Pi_{ij}(k_{ij}^*))/(\bar{k}_{ij} - k_{ij}^*)$. We use such a piecewise linear approximation of the expected payoff to derive the optimal staffing policy. However, to assess the performance of the policy in the simulation study in Section 6, we use the realizations of the payoff of each trip.

The planner seeks to maximize the total value generated through gleaning. Because of volunteer attendance uncertainty, she may want to build some safety capacity in the requested staffing level ($k_{ij}$ for class $ij$). The downside to this is that there may be excess volunteers on an early trip and not enough volunteers for a later trip. In fact, the planner may have to reject future gleaning donations if volunteer availability drops too low, resulting in long delays – this would further reduce the volume of crops gleaned. This tradeoff is crucial when the system is critically loaded, i.e., when it is in heavy traffic. In other words, the demand rate for volunteers is close to the rate at which they become available.

Given the tradeoff between increasing the value of crops gleaned on the immediate trip versus a future trip, the planner can potentially improve her long-run average performance by dynamically adjusting the volunteer staffing level based on the congestion in the system. If there is low congestion, then she can afford to request a high staffing level because the shadow price for volunteer capacity is low. If congestion is high, she needs to be more frugal with volunteer capacity and request a lower staffing level. To state the planner's problem, let $\pi_{ij}$ denote the piecewise linear approximation of the expected payoff $\Pi_{ij}$ on the relevant range of $[\underline{k}_{ij}, \bar{k}_{ij}]$ (as illustrated in Figure 1). That is, for $k_{ij} \in [\underline{k}_{ij}, \bar{k}_{ij}]$ and nominal staffing level $k_{ij}^*$, we define

$$\pi_{ij}(k) = \begin{cases} \Pi_{ij}(k_{ij}^*) + \pi_{ij}^r(k_{ij} - k_{ij}^*), & k_{ij} \in [k_{ij}^*, \bar{k}_{ij}], \\ \Pi_{ij}(k_{ij}^*) + \pi_{ij}^l(k_{ij} - k_{ij}^*), & k_{ij} \in [\underline{k}_{ij}, k_{ij}^*]. \end{cases} \tag{2}$$

Within a reasonable staffing level range $[\underline{k}_{ij}, \bar{k}_{ij}]$, the planner's problem is to find the optimal control $k_{ij}(t) \in [\underline{k}_{ij}, \bar{k}_{ij}]$ for $t \geq 0$ and all $i, j$, such that the staffing level maximizes the net payoff over the long run. To be more specific, for each class $ij$, she chooses the dynamic staffing policy $\{k_{ij}(t) \in [\underline{k}_{ij}, \bar{k}_{ij}] : t \geq 0\}$ so as to maximize her average net payoff (i.e., maximize the total payoff from scheduled trips, taking into account the effect of rejection penalties), subject to the delay constraints of the backlogged gleaning donations. Unfortunately, this formulation is not tractable

analytically. Therefore, in the next section, by considering a sequence of closely related systems in heavy traffic, we formulate an approximate, yet far more tractable formulation.

# 4 An Approximating Brownian Control Problem

The dynamic staffing problem is not tractable in its *exact* form, as discussed earlier. Therefore, by considering a sequence of closely related systems indexed by the total number of volunteers $n$, we formulate a more tractable approximation. To be specific, we study this sequence of systems as the number of volunteers $n$ gets large under the so-called heavy traffic assumption; a superscript $n$ will be attached to the quantities of interest in the $n^{th}$ system. In particular, $\lambda_{ij}^n$ is the average arrival rate of class $ij$ gleaning donations and $\mu^n = n\mu$ is the average rate at which volunteers become available in the $n^{th}$ system.

The traffic intensity $\rho^n$ of the $n^{th}$ system is given by $\rho^n = \sum_{i=1}^{I} \sum_{j=1}^{J_i} \lambda_{ij}^n k_{ij}^* q/(n\mu)$. Next, we state the assumption on how the traffic intensity $\rho^n$ changes as the number of volunteers increases.

**Assumption 1** *(Heavy traffic assumption) We assume that $\rho^n < 1$ for all $n$, and that*

$$\lim_{n\to\infty} (1-\rho^n)\sqrt{n} = \beta > 0. \tag{3}$$

*Letting $\rho_{ij}^n = \lambda_{ij}^n k_{ij}^* q/(n\mu)$ for all $ij$, we also assume that $\lim_{n\to\infty} \rho_{ij}^n = \rho_{ij} > 0$, where $\rho_{ij}$ is defined as the limit on the left-hand side. In particular, we have that*

$$\sum_{i=1}^{I} \sum_{j=1}^{J_i} \rho_{ij} = 1. \tag{4}$$

We focus on this regime because when the volunteer gleaner capacity is close to the demand rate (resulting from the arrival rate of gleaning donations), the planner benefits most from being able to dynamically adjust her staffing policy. If the volunteer gleaning capacity was much higher than the demand rate, the planner could always request a high staffing level without worrying about adversely affecting the volunteer attendance on future gleaning trips. On the other hand, if volunteer gleaning capacity was much lower than the demand rate, then the planner would always set safety capacity to zero because there would always be a future gleaning trip where the volunteer capacity would be productively used. In the regime where the relative values of volunteer capacity

and the demand rate are close so that the demand rate can sometimes be greater than volunteer capacity because of fluctuations in volunteer availability, the ability to adjust the staffing level based on the number of jobs in the system can have a significant impact on the output.

As mentioned above, the planner dynamically adjusts the requested staffing level, denoted by $k_{ij}(t)$ for each class $ij$ of gleaning donations and $t \geq 0$. We focus our attention on the following functional form for $k_{ij}^n(t)$:

$$k_{ij}^n(t) = k_{ij}^* \left(1 - \frac{\theta_{ij}(t)}{\sqrt{n}}\right), \;\; t \geq 0, \; i = 1, ..., I, \; j = 1, ...J_i, \tag{5}$$

where $\theta_{ij}(\cdot)$ is the control for class $ij$. This functional form is natural because the congestion is of second order relative to the system size as the number of volunteers $n$ gets large in the heavy traffic regime. Thus, as the backlog in the system varies, only second order adjustments to the requested staffing level per trip are warranted. In particular, the adjustment proposed in Equation (5) to the nominal staffing level $k_{ij}^*$ is $k_{ij}^* \theta_{ij}(t)/\sqrt{n}$ in the $n^{th}$ system; and the assumed decay rate of $1/\sqrt{n}$ translates to a drift rate reduction in the approximating Brownian control problem.

Recall that $Q^n(t)$ denotes the number of jobs currently in the gleaning operation at time $t$, which includes the number of volunteers currently unavailable and the number of virtual jobs that are backlogged. We define the scaled version of $Q^n(t)$ as follows:

$$Z^n(t) = \frac{Q^n(t) - n}{\sqrt{n}}, \;\; t \geq 0. \tag{6}$$

If $Z^n(t) > 0$, it means there are backlogged jobs and no available volunteers, whereas if $Z^n(t) < 0$, then there is no backlog of jobs and there are volunteers available.

The infinitesimal drift and variance of $Z^n(\cdot)$, denoted by $m_n$ and $\sigma_n^2$, respectively, are defined as follows:

$$m_n(z,t) = \lim_{h \downarrow 0} \mathbb{E}\left[\frac{Z^n(t+h) - Z^n(t)}{h} \mid Z^n(t) = z\right],$$
$$\sigma_n^2(z,t) = \lim_{h \downarrow 0} \mathbb{E}\left[\frac{(Z^n(t+h) - Z^n(t))^2}{h} \mid Z^n(t) = z\right],$$

see Chapter 15 of Karlin and Taylor (1981).[2]

Defining $\sigma^2 = \mu\left[2 + q\sum_{i=1}^{I}\sum_{j=1}^{J_i}\rho_{ij}(k_{ij}^* - 1)\right]$ and

$$m(z) = \begin{cases} -\mu z, & z < 0, \\ 0, & z \geq 0, \end{cases}$$

the following proposition characterizes the asymptotic behavior of $m_n$, $\sigma_n$.

**Proposition 1** *We have that* $\lim_{n\to\infty}\sigma_n^2(z,t) = \sigma^2$ *and*

$$\lim_{n\to\infty} m_n(z,t) = m(z) - \mu(\beta + \sum_{i=1}^{I}\sum_{j=1}^{J_i}\rho_{ij}\theta_{ij}(t)).$$

In light of Proposition 1, as done in Theorem 2 of Halfin and Whitt (1981), one can check Stone's criterion (see for example, Theorem 3.2 of Iglehart (1965)) to conclude that $Z^n$ converges weakly to a diffusion process with the drift rate and variance parameters as characterized in Proposition 1.

Because crops must be harvested in a timely manner, another important feature of the volunteer staffing problem is that the planner has congestion concerns and wishes to limit the delay between the time a donation arrives and the time at which gleaning occurs. The delay constraint is not really meaningful in a conventional queueing model, because the delays are random variables. Nonetheless, it becomes meaningful in an asymptotic sense. That is, it is met with probability one because the law of large numbers implies an equivalence between (scaled) bounds on the number of jobs in the system and (scaled) bounds on delays as one approaches the heavy traffic limit. Therefore, one tractable surrogate model for the delay constraint is to impose an upper bound on the queue length process[3] as done in Plambeck et al. (2001), Ata (2005), and Rubino and Ata (2009). This corresponds to imposing an upper bound on the backlog of jobs, i.e.,

$$Q^n(t) - n \leq b^n. \tag{7}$$

In the asymptotic regime we consider, the deviations of the queue length process $Q^n$ from $n$ are of order $\sqrt{n}$. So we will assume that in the $n^{th}$ system, we have that

$$b^n = \sqrt{n}b,$$

where $b > 0$ is a parameter to be chosen by the planner. Note that by Little's Law and the

heavy traffic assumption, the upper bound imposed on the backlog corresponds to delays of order $b/(\mu\sqrt{n})$. This can be used to calibrate $b$ so as to incorporate the planner's congestion concerns.

To impose an upper bound on the queue length process, the planner turns away donations when the queue length reaches its upper bound, exercising admission control. Turning away a donation of class $ij$ at time $t$ results in a rejection penalty of $\tilde{p}_{ij}$ and turning away $N_{ij}(k_{ij}^n(t))$ volunteer jobs, where

$$\mathbb{E}[N_{ij}(k_{ij}^n(t))] = qk_{ij}^n(t) = qk_{ij}^* \left(1 - \frac{\theta_{ij}(t)}{\sqrt{n}})\right) \approx qk_{ij}^*. \tag{8}$$

In what follows, we approximate the number of volunteer jobs turned away with each such class $ij$ donation that is rejected by $qk_{ij}^*$, ignoring the lower order (random) terms. This is a reasonable approximation because our method of analysis is crude enough that such differences are washed away under the heavy traffic scaling as we pass to the limit.

Moreover, for mathematical convenience, we model the admission control as if the planner can turn off the clock for the arrival process (when the queue length reaches its upper bound). In particular, we let $U_{ij}^n(t)$ denote the cumulative amount of time that the arrival process is turned off for class $ij$ during the interval $[0, t]$.

As mentioned above, we consider a sequence of closely related systems indexed by the number of volunteers $n$ whose formal limit is the Brownian control problem. The original dynamic staffing problem can be viewed as a specific element of this sequence of problems, which is determined by the number of volunteers. The underlying assumption of the Brownian approximation is that the number of volunteers (for the original problem of interest) is large enough so that various (scaled) performance-relevant processes of the original system can be approximated by the corresponding processes of the Brownian control problem.

Passing to the limit formally as the number of volunteers $n$ gets large, we assume that[4]

$$(Z^n(\cdot), \sqrt{n}\, U_{11}^n(\cdot), ..., \sqrt{n}\, U_{IJ_I}^n(\cdot)) \Rightarrow (Z(\cdot), U_{11}(\cdot), ..., U_{IJ_I}(\cdot)) \text{ as } n \to \infty, \tag{9}$$

where $\Rightarrow$ denotes weak convergence; see Billingsley (1999).

Given the rejection and arrival processes of class $ij$ denoted by $U_{ij}^n(\cdot)$ and $R_{ij}^n(\cdot)$, respectively, we approximate the cumulative number of donations of class $ij$ rejected by time $t$, i.e., $R_{ij}^n(t) -$

$R_{ij}^n(t - U_{ij}^n(t))$, as follows:

$$R_{ij}^n(t) - R_{ij}^n(t - U_{ij}^n(t)) \approx \lambda_{ij}^n U_{ij}^n(t) \approx \frac{\sqrt{n}\mu\rho_{ij}}{k_{ij}^* q}\, U_{ij}(t),$$

where we used (9) and the approximation $\lambda_{ij}^n \approx n\mu\rho_{ij}/(k_{ij}^* q)$; see Assumption 1 for a justification of the latter approximation. Then using the approximation in Equation (8), we approximate the cumulative number of volunteer jobs of class $ij$ rejected until time $t$ by $\sqrt{n}\mu\rho_{ij}\, U_{ij}(t)$. Scaling this further by $\sqrt{n}$, in accordance with the scaling of $Z^n$ (see Equation (6)), and defining

$$U(t) = \sum_{i=1}^{I} \sum_{j=1}^{J_i} \rho_{ij} U_{ij}(t), \;\; t \geq 0,$$

and building on Proposition 1, we assume that the processes $Z$ and $U$ jointly satisfy the following:

$$dZ(t) = \left[ m(Z(t)) - \mu \left( \beta + \sum_{i=1}^{I} \sum_{j=1}^{J_i} \rho_{ij} \theta_{ij}(t) \right) \right] dt + \sigma\, dB(t) - \mu\, dU(t), \;\; t \geq 0, \tag{10}$$

$$Z(t) \leq b, \;\; t \geq 0, \tag{11}$$

$$\int_0^\infty \mathbb{1}_{\{Z(t)<b\}}\, dU(t) = 0, \tag{12}$$

$$U(\cdot) \text{ is nondecreasing with } U(0) = 0, \tag{13}$$

where $B$ is the standard Brownian motion.

To repeat, the controlled process $Z$ described in Equation (10) is (the limit of) the scaled version of the queue length process $Q^n$. Similarly, $U_{ij}$ is (the limit of) the scaled version of the cumulative rejection process $U_{ij}^n$. Equation (13) states the natural constraint that $U$ must be nondecreasing, whereas Equation (12) ensures that it increases only when the (scaled) backlog $Z$ reaches its upper bound $b$.

Equation (11) imposes an upper bound on the backlog of jobs $Z$, ensuring that delays do not become excessive. Note, however, that the backlog $Z(t)$ is not observable to the planner at time $t$, because it is the sum of the number of volunteer jobs for all of the currently backlogged gleaning donations. Moreover, the number of volunteer jobs for each gleaning donation is not known until the trip for the donation takes place. Only then does the planner know if a volunteer shows up or not. However, $Z(t)$ can be approximated closely in the asymptotic regime by multiplying each

donation by the expected number of volunteers attending, given the requested staffing level for the donation, and summing over all donations in the backlog.

Equations (10)-(13) describe the evolution of the system state in the approximating Brownian control problem given the controls $\theta_{ij}(\cdot)$ for all $ij$. To complete the description of the approximating problem, it only remains to specify its objective. To this end, recall our approximation $\pi_{ij}(k)$ from Equation (2). Then we let $\tilde{\pi}_{ij}(x) = \pi_{ij}(k^*_{ij} - x) - \pi_{ij}(k^*_{ij})$ for $x \in [k^*_{ij} - \bar{k}_{ij}, k^*_{ij} - \underline{k}_{ij}]$. That is,

$$\tilde{\pi}_{ij}(x) = \begin{cases} -\pi^r_{ij} x, & x \in [k^*_{ij} - \bar{k}_{ij}, 0], \\ -\pi^l_{ij} x, & x \in [0, k^*_{ij} - \underline{k}_{ij}]. \end{cases}$$

Figure 2 displays an illustrative $\tilde{\pi}_{ij}(\cdot)$ function.

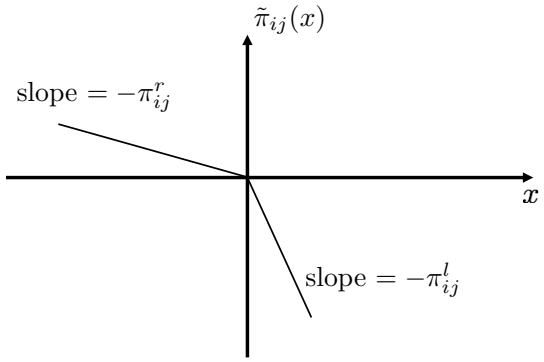


**Figure 2:** An illustrative $\tilde{\pi}_{ij}(\cdot)$ function.

To facilitate the analysis to follow, we make the following assumption; see Appendix C.2 for a discussion of how to relax this assumption.

**Assumption 2** *We have that $\tilde{p}_{ij} = pk^*_{ij}$ where $p > 0$ is a parameter.*

Appendix C.3 provides an approximation of the planner's expected payoff. Building on that approximation and defining

$$\underline{\theta}_{ij} = \frac{\sqrt{n}(k^*_{ij} - \bar{k}_{ij})}{k^*_{ij}} < 0 \text{ and } \bar{\theta}_{ij} = \frac{\sqrt{n}(k^*_{ij} - \underline{k}_{ij})}{k^*_{ij}} > 0 \text{ for all } i, j,$$

we arrive at the following formulation for the planner's problem: For $s \geq 0$, choose $\theta_{ij}(s) \in [\underline{\theta}_{ij}, \bar{\theta}_{ij}]$

for all $i, j$ so as to

$$\text{Maximize } \underline{\lim}_{t\to\infty} \frac{1}{t}\,\mathbb{E}\left[\int_0^t \frac{\mu}{q}\sum_{i=1}^{I}\sum_{j=1}^{J_i}\tilde{\pi}_{ij}(\rho_{ij}\theta_{ij}(s))\,ds - p\frac{\mu}{q}\,U(t)\right]$$

subject to (10)-(13).

To facilitate the analysis to follow, define $\hat{\pi}_{ij}(x) = -\tilde{\pi}_{ij}(x)$ for $x \in [\underline{\theta}_{ij}, \bar{\theta}_{ij}]$ and all $i, j$. Then we formulate the following problem: choose $\theta_{ij}(s) \in [\underline{\theta}_{ij}, \bar{\theta}_{ij}]$ for all $s \geq 0$ and $i, j$ so as to

$$\text{Minimize } \overline{\lim}_{t\to\infty}\,\mathbb{E}\left[\frac{1}{t}\int_0^t \sum_{i=1}^{I}\sum_{j=1}^{J_i}\mu\,\hat{\pi}_{ij}(\rho_{ij}\theta_{ij}(s))\,ds + \mu p\,U(t)\right] - \mu\sum_{i=1}^{I}\sum_{j=1}^{J_i}\pi_{ij}^{r}\rho_{ij}\underline{\theta}_{ij} \qquad (\tilde{P})$$

subject to (10)-(13).

It is straightforward to argue that this formulation is equivalent to the previous one. To be more specific, to arrive at $(\tilde{P})$, one multiplies the objective of the previous one by $-q$ and formulates the problem as one of minimization. Lastly, the constant term $\sum_{i=1}^{I}\sum_{j=1}^{J_i}\pi_{ij}^{r}\rho_{ij}\underline{\theta}_{ij}$ is subtracted from the objective. None of these mathematical operations change the nature of the problem, nor its optimal solution. However, this transformation helps us streamline the analysis to follow. Let $\mathscr{A} = \{(i, j, d) : i = 1, ..., I, j = 1, ..., J_i, d = l, r\}$.

**Assumption 3** *The elements of the set* $\{\pi_{ij}^{d} : (i, j, d) \in \mathscr{A}\}$ *are all distinct.*

**Remark.** Otherwise, one may combine the identical values "suitably" to arrive at a case where the assumption is satisfied. ■

Let $M = 2(J_1+J_2+...+J_I)$ and consider the set $\{\pi_{ij}^{d} : (i, j, d) \in \mathscr{A}\}$ and let $\text{rank}(\pi_{ij}^{d})$ denote the rank of $\pi_{ij}^{d}$ among the elements in that set. In addition, for $m = 1, ..., M$, let $i(m), j(m)$ denote the crop type and the size of the donation, respectively, for the $m^{th}$ smallest element, i.e., the element with rank $m$. Similarly, let $d(m) \in \{l, r\}$ denote whether the $m^{th}$ smallest element corresponds[5] to the "left slope" or the "right slope".

In particular, let $c_m$ denote the $m^{th}$ smallest element of the set $\{\pi_{ij}^{d} : (i, j, d) \in \mathscr{A}\}$. That is,

$$c_m = \pi_{i(m),j(m)}^{d(m)} \text{ for } m = 1, ..., M. \qquad (14)$$

Similarly, for $m = 1, ..., M$, let

$$\eta_m = \begin{cases} \rho_{i(m),j(m)}\bar{\theta}_{i(m),j(m)} & \text{if } d(m) = l, \\ \rho_{i(m),j(m)}|\underline{\theta}_{i(m),j(m)}| & \text{if } d(m) = r. \end{cases}$$

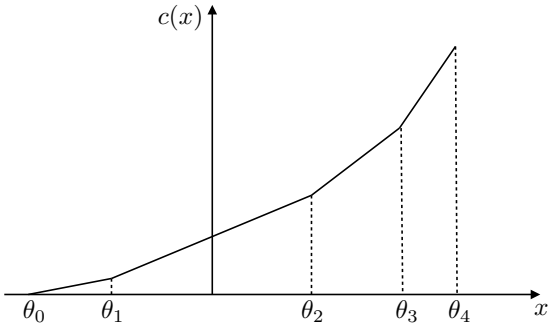


**Figure 3:** An illustrative $c(\cdot)$ function.

To facilitate the analysis to follow, define $\underline{\theta} = \sum_{i=1}^{I} \sum_{j=1}^{J_i} \rho_{ij}\underline{\theta}_{ij}$, $\theta_0 = \beta + \underline{\theta}$, and

$$\theta_m = \theta_0 + \sum_{l=1}^{m} \eta_l \text{ for } m = 1, ..., M.$$

Note that $\theta_M > 0$ because $\beta > 0$ by the heavy traffic assumption and that $\bar{\theta}_{ij} > 0$ for all $ij$. Also note that $0 < c_1 < c_2 < ... < c_M$ and define the piecewise linear, convex and increasing function $c(\cdot)$ on $A = [\theta_0, \theta_M]$ as follows: $c(\theta_0) = 0$, and

$$c(x) = \sum_{i=1}^{m-1} c_i(\theta_i - \theta_{i-1}) + c_m(x - \theta_{m-1}),\ \theta_{m-1} < x \leq \theta_m,\ m = 1, ..., M.$$

Figure 3 displays an illustrative $c(\cdot)$ function with $M = 4$.

Then consider the following minimization problem: For $s \geq 0$, choose $\theta(s) \in [\theta_0, \theta_M]$ so as to

$$
\begin{aligned}
&\text{Minimize } \overline{\lim}_{t\to\infty} \frac{1}{t}\, \mathbb{E}\left[\int_0^t \mu\, c(\theta(s))\, ds + \mu\, pU(t)\right] \\
&\text{subject to} \\
&dZ(t) = [m(Z(t)) - \mu\theta(t)]\, dt + \sigma\, dB(t) - \mu dU(t), \;\; t \geq 0, \\
&Z(t) \leq b, \;\; t \geq 0, \qquad\qquad (P) \\
&\int_0^t \mathbb{1}_{\{Z(t)<b\}}\, dU(t) = 0, \;\; t \geq 0, \\
&U(\cdot) \text{ is nondecreasing with } U(0) = 0.
\end{aligned}
$$

The following proposition establishes the equivalence of the formulations $(\tilde{P})$ and $(P)$.

**Proposition 2** *The problems $(\tilde{P})$ and $(P)$ are equivalent in the following sense. For every feasible policy $\tilde{\theta}(\cdot)$ of $(\tilde{P})$, there exists a feasible policy $\theta(\cdot)$ for $(P)$ that has lower (or the same) cost. In particular, given $\tilde{\theta}(\cdot)$ feasible for $(\tilde{P})$, one can define such a policy $\theta(\cdot)$ as follows:*

$$\theta(s) = \sum_{i=1}^{I} \sum_{j=1}^{J_i} \rho_{ij} \tilde{\theta}_{ij}(s) \text{ for } s \geq 0.$$

*Similarly, every feasible policy $\theta(\cdot)$ of $(P)$ yields a feasible policy $\tilde{\theta}(\cdot)$ for $(\tilde{P})$ that has the same cost. To be more specific, given the feasible policy $\theta(\cdot)$ for $(P)$, one can define the corresponding policy $\tilde{\theta}(\cdot)$ for $(\tilde{P})$ as follows: For $s \geq 0$, if $\theta(s) = \theta_M$, then $\tilde{\theta}_{ij}(s) = \bar{\theta}_{ij}$ for all $i, j$. Otherwise, $\theta(s) \in [\theta_m, \theta_{m+1})$ for some $m = 0, 1, ..., M-1$. For each $ij$, letting $r_1(i,j) = rank(\pi^r_{ij})$ and $r_2(i,j) = rank(\pi^l_{ij})$, we have that*

$$
\tilde{\theta}_{ij}(s) = \begin{cases}
\bar{\theta}_{ij} & \text{if } r_2(i,j) \leq m, \\
\frac{\theta(s)-\theta_m}{\rho_{ij}} & \text{if } r_2(i,j) = m+1, \\
0 & \text{if } r_2(i,j) > m+1,\ r_1(i,j) \leq m, \\
\underline{\theta}_{ij} + \frac{\theta(s)-\theta_m}{\rho_{ij}} & \text{if } r_1(i,j) = m+1, \\
\underline{\theta}_{ij} & \text{if } r_2(i,j) > m+1.
\end{cases} \qquad (15)
$$

The next section solves the formulation $(P)$ and characterizes the optimal policy as a nested threshold policy on $Z$. However, as discussed above, the planner does not directly observe $Z$

in practice. Nonetheless, she can observe the backlog of gleaning donations. Therefore, she can estimate the backlog of volunteer jobs by summing the expected number of gleaners (which is a function of the requested staffing level $k$) that will attend each of these backlogged donations, $\mathbb{E}[N(k)]$. In the heavy traffic regime, this approximation is not only asymptotically accurate, but also leads to an implementable policy in practice. In Section 6, to assess the performance of the dynamic policy, we simulate the actual gleaning process where $Z$ is unobservable and use $\mathbb{E}[N(k)]$ to determine the staffing level, and show that the dynamic policy still offers significant performance gains. Therefore, in what follows, we proceed as though the backlog process $Z$ is observable to the planner.

# 5 Solution to the Limiting Brownian Control Problem

This section characterizes the optimal policy. To minimize technical complexity, we shall restrict attention to stationary, Markov control policies. That is, the (excess) staffing level requested at any time $t$ is assumed to depend on past history only through the current backlog $Z(t)$. Thus, an admissible control policy is then a function $\theta(\cdot) : (-\infty, b] \to A$. To characterize the optimal policy analytically, consider the associated Bellman equation: Find a twice-continuously differentiable, convex increasing function $f$, and the constant $\gamma > 0$ that jointly satisfy the following (second order, nonlinear) differential equation:

$$\gamma = \min_{x \in A} \left\{ \frac{1}{2}\sigma^2 f''(z) + (m(z) - \mu x) f'(z) + \mu c(x) \right\} \tag{16}$$

subject to the boundary conditions

$$\lim_{z \to -\infty} f'(z) = 0 \qquad \text{and} \qquad f'(b) = p. \tag{17}$$

We interpret $\gamma$ as a guess at the optimal average cost; and the unknown function $f$ is the so-called relative value function in average cost dynamic programming. The properties of the Bellman equation used in our analysis will be proved from first principles (see Proposition 3 and Theorem 1).

To facilitate the analysis to follow, define the convex conjugate of the cost function $c(\cdot)$ as

follows:

$$\phi(y) = \sup_{x \in A}\{yx - c(x)\}, \quad y \geq 0. \tag{18}$$

It is straightforward to prove that there exists a smallest $x^* \in A$ that achieves the supremum which is denoted by $\psi(y)$, i.e.,

$$\psi(y) = \inf \operatorname*{argmax}_{x \in A}\{yx - c(x)\}, \quad y \geq 0. \tag{19}$$

See Appendix C.4 for further elaborations of the $\phi(\cdot)$ and $\psi(\cdot)$ functions.

Note that the Bellman equation (16)-(17) does not involve the function $f$ itself. So it is possible to reduce it to a first-order differential equation by setting $v(x) = f'(x)$ for $x \leq b$. Then using the definition of $\phi$, we express the Bellman equation equivalently as follows: Choose a non-decreasing, continuously differentiable function $v$ and a constant $\gamma > 0$ that jointly satisfy the following:

$$\gamma = \frac{1}{2}\sigma^2 v'(z) + m(z)v(z) - \mu\phi(v(z)) \tag{20}$$

subject to the boundary conditions

$$\lim_{z \to -\infty} v(z) = 0 \qquad \text{and} \qquad v(b) = p. \tag{21}$$

The following proposition establishes the existence of a solution to the Bellman equation; see Appendix B for its proof. Appendix A provides a constructive proof and a rather explicit characterization of the function $v(\cdot)$. That characterization of $v(\cdot)$, in turn, facilitates the rather explicit description of the optimal policy in Section 5.1.

**Proposition 3** *The Bellman equation (20)-(21) has a solution $(\gamma^*, v)$ where $\gamma^* > 0$ and $v$ is increasing and continuously differentiable.*

Then, defining

$$f(x) = -\int_x^b v(y)dy, \qquad x \leq b, \tag{22}$$

and noting that $f'(x) = v(x)$, the following corollary is immediate from Proposition 3 and it provides a solution to (16)-(17).

**Corollary 1** *The pair $(f, \gamma^*)$ solves the Bellman equation (16)-(17).*

In each state $z \leq b$, our candidate policy chooses

$$\theta^*(z) = \psi(v(z)). \tag{23}$$

Because $v(\cdot)$ is strictly increasing, it is invertible. Denoting that inverse by $v^{-1}(\cdot)$, let

$$\tau_i^* = v^{-1}(c_i),\ i = 1, 2, ..., M. \tag{24}$$

Then, it follows from Equation (19) (see also Equation (92) in Appendix C.4) that the candidate policy $\theta^*(\cdot)$ (see Equation (23)) is a nested threshold policy with thresholds $\tau_1^* < \tau_2^* < ... < \tau_M^* < b$. That is,

$$\theta^*(z) = \begin{cases} \theta_0, & \text{if } z < \tau_1^*, \\ \theta_m, & \text{if } \tau_m^* \leq z < \tau_{m+1}^*,\ m = 1, ..., M-1, \\ \theta_M, & \text{if } \tau_M^* \leq z \leq b. \end{cases} \tag{25}$$

The following result establishes that the candidate policy is indeed optimal; see Appendix B for its proof.

**Theorem 1** *The candidate policy $\theta^*(\cdot)$ given in (25) is optimal and has average cost of $\gamma^*$.*

Given the optimal thresholds $\tau_1^*, ..., \tau_M^*$ for the Brownian control problem $(P)$, define

$$Q_j^* = n + \sqrt{n}\,\tau_j^* \quad \text{for } j = 1, ..., M.$$

Then recalling that $r_1(i,j) = \text{rank}(\pi_{ij}^r)$ and $r_2(i,j) = \text{rank}(\pi_{ij}^l)$, and combining Proposition 2, Theorem 1, and Equations (5)-(6) leads to the following proposed policy for the original system.

*Proposed staffing policy for the multicrop gleaning operation*: For $t \geq 0$ and class $ij$, we have the following three cases:

(i) $Q(t) < Q_1^*$, then set $k_{ij}(t) = \bar{k}_{ij}$,

(ii) $Q(t) \geq Q_M^*$, then set $k_{ij}(t) = \underline{k}_{ij}$,

(iii) $Q(t) \in [Q^*_m, Q^*_{m+1})$ for $m = 1, ..., M-1$, then set

$$k_{ij}(t) = \begin{cases} \underline{k}_{ij} & \text{if } r_2(i,j) \leq m, \\ \bar{k}_{ij} & \text{if } r_1(i,j) \geq m+1, \\ k^*_{ij} & \text{otherwise (i.e., } r_2(i,j) \geq m+1, r_1(i,j) \leq m). \end{cases}$$

**An outline of the solution to the Bellman Equation.** Our analysis of the limiting Brownian control problem proceeds by studying the Bellman equation in two intervals separately. This is because the system behavior, namely, the drift-rate (without control) of the diffusion process that governs the evolution of the system is rather different depending on whether the state is positive or negative. As observed also in Halfin and Whitt (1981) when the system state is positive, it evolves (locally) as a Brownian motion. In contrast, when the state is negative, it evolves (locally) as an Ornstein-Uhlenbeck process with a linear drift towards the origin. This, of course, causes the Bellman equation to behave differently in these two cases. Indeed, the analysis for $z \geq 0$ closely mimics that of Ata et al. (2005) whereas the analysis for $z < 0$ is novel. Moreover, whether one can "paste" the solutions for the two parts suitably (see Equation (28) below) so as to solve the Bellman equation over the entire state space is unclear a priori. Therefore, a technical contribution of the paper is to construct a solution to the Bellman equation for $z \leq 0$ and combine that with the solution for $z \geq 0$ in a smooth fashion. Along the way, we also come up with a rather explicit characterization of the optimal policy. To this end, let

$$\phi_* = -\inf_{0 \leq u \leq p} \phi(u). \tag{26}$$

Also let

$$\underline{\gamma} = \mu\phi_* \quad \text{and} \quad c_* = \inf\{x \geq 0 : \phi(x) = -\phi_*\}. \tag{27}$$

Then, for $\gamma > \underline{\gamma}$, consider the following two initial value problems. The first one is on the negative real line and is denoted by IVP$_-(\gamma)$:

$$\begin{aligned} &\gamma = \frac{1}{2}\sigma^2 w'(z) - \mu z w(z) - \mu\phi(w(z)) \\ &\text{subject to } \lim_{z \to -\infty} w(z) = 0. \end{aligned} \tag{IVP$_-(\gamma)$}$$

The second one is on the positive interval $[0, b]$ and is denoted by $\text{IVP}_+(\gamma)$:

$$\gamma = \frac{1}{2}\sigma^2 u'(z) - \mu\phi(u(z))$$
$$\text{subject to } u(b) = p. \qquad (\text{IVP}_+(\gamma))$$

For each $\gamma > \underline{\gamma}$, we derive the solutions to both problems, thereby establishing the existence and uniqueness of a smooth solution for each by construction. These solutions will be denoted by $w(\cdot, \gamma)$ and $u(\cdot, \gamma)$, respectively. Ultimately, we pin down the optimal long-run average cost $\gamma^*$ by setting

$$u(0, \gamma^*) = w(0, \gamma^*), \tag{28}$$

and will set (the derivative of) the relative value function to be

$$v(z) = \begin{cases} w(z, \gamma^*), & z < 0, \\ u(z, \gamma^*), & z \in [0, b]. \end{cases} \tag{29}$$

Ensuring that Equation (28) has a unique solution and that $(\gamma, v)$ given by Equations (28)-(29) solves the Bellman equation (20)-(21) require a careful analysis involving several steps, which also yields a rather explicit characterization of $v(\cdot)$ and the corresponding optimal policy, i.e., the thresholds $\tau_1^*, \tau_2^*, ..., \tau_M^*$, as by-product. Indeed, Section 5.1 provides a closed-form characterization of the thresholds $\tau_1^*, \tau_2^*, ..., \tau_M^*$ in terms of the optimal average cost $\gamma^*$ and the problem primitives.

## 5.1 Further Characterization of the Thresholds and the Proposed Staffing Policy

The analysis outlined immediately above yields an explicit characterization of the optimal thresholds $\tau_1^*, ..., \tau_M^*$. To facilitate this characterization, define the auxiliary function $H(v, \gamma)$ for $\gamma > \underline{\gamma}$ and $v \in [0, p]$ as follows:

$$H(v, \gamma) = b - \frac{\sigma^2}{2} \int_v^p \frac{dy}{\gamma + \mu\phi(y)}. \tag{30}$$

Also define $g_i$ and $G_i$ as the pdf and cdf, respectively, of a Normal random variable with mean $-\theta_i$ and variance $\sigma^2/(2\mu)$, for $i = 0, 1, ..., M$. The characterization also involves the function $w(\cdot, \gamma^*)$.

Proposition 6 shows that $w(\cdot, \gamma^*)$ is increasing on $(-\infty, 0]$, hence, it is invertible; denote that inverse by $w^{-1}(\cdot, \gamma^*)$, whereas Propositions 5 and 9 provide explicit characterizations of it; see Appendix A.1 for the statements and the proofs of the propositions.

**Proposition 4** *The following $M+1$ cases characterize the thresholds of the optimal policy, $\tau_1^*, ..., \tau_M^*$:*
*Case 0.* $2\gamma^* \leq c_1\sigma^2 \frac{g_0(0)}{G_0(0)}$;
*Case j.* $(j = 1, ..., M-1)$ $2\gamma^* > c_1\sigma^2 \frac{g_0(0)}{G_0(0)}$, $H(c_{j+1}, \gamma^*) > 0$, *and* $H(c_j, \gamma^*) \leq 0$;
*Case M.* $2\gamma^* > c_1\sigma^2 \frac{g_0(0)}{G_0(0)}$ *and* $H(c_M, \gamma^*) \leq 0$.

*In Case 0, we have that $\tau_i = H(c_i, \gamma^*)$ for $i = 1, ..., M$. Moreover, in Case j $(j = 1, ..., M)$, we have the following two subcases*[6]*:*
*Case j(a).* $\tau_i^* = H(c_i, \gamma^*)$ *for* $i = j+1, ..., M$, *and*
*Case j(b).* $\tau_i^* = w^{-1}(c_i, \gamma^*)$ *for* $i = 1, ..., j$.
*In particular, in the subcase j(b), the thresholds $\tau_1^*, ..., \tau_j^*$ can be computed as follows:*

$$\tau_1^* = \left(\frac{G_0}{g_0}\right)^{-1} \left(\frac{c_1\sigma^2}{2\gamma^*}\right) < 0. \tag{31}$$

*Then given $\tau_{i-1}^* < 0$, the next threshold $\tau_i^* < 0$ for $i = 2, ..., j$ is computed by solving the following equation:*

$$c_{i-1}\frac{g_{i-1}(\tau_{i-1}^*)}{g_{i-1}(\tau_i^*)} + \frac{2(\gamma^* - \mu c(\theta_{i-1}))}{\sigma^2}\frac{G_{i-1}(\tau_i^*) - G_{i-1}(\tau_{i-1}^*)}{g_{i-1}(\tau_i^*)} = c_i. \tag{32}$$

# 6 Numerical Study

To study the effectiveness of our proposed policy, we conduct a numerical study using parameters based on the process characteristics of the Boston Area Gleaners (BAG 2016), a gleaning organization that operates in the Boston metropolitan area. Currently, when deciding the staffing level for a gleaning trip, BAG primarily considers the type of crop and the characteristics of the farm (Caldwell et al. 2017). In the context of our model, this would correspond to a fixed staffing level for each class $ij$ trip. Another staffing policy that is used by the Food Bank of the Southern Tier in New York (FBST 2015) is to send out a broadcast email to the entire volunteer list for each gleaning trip and not set any limit on the number of volunteers that can attend each trip. We

compare our dynamic staffing policy to the class-dependent static policy used by BAG and the unlimited policy used by FBST.

To assess the effectiveness of the dynamic policy, we construct a simulation model for the gleaning process that reflects the actual gleaning process flow (i.e., without making the simplifying assumptions used to derive the dynamic policy). Specifically there are four simplifying assumptions made in the analytical model that we do not incorporate into the simulation. First, the payoff for each gleaning trip is calculated using the actual realizations for gleaner attendance, not the piecewise linear approximation shown in Figure 1. Second, instead of breaking donations into volunteer job flow units, the simulation uses donations as the flow unit, so that volunteers attending the same trip are synchronized in their gleaning timing (as would be the case in practice). Third, if there are not enough available volunteers during the gleaning window to fill the requested staffing level, the gleaning trip proceeds with however many are available, and we lose a part of the payoff proportional to the number of missing volunteers. Fourth, because the planner cannot observe $N(k)$ of a backlogged donation until the gleaning trip occurs (note that the planner can observe the backlog of gleaning donations though), we use $\mathbb{E}[N(k)]$ instead of $N(k)$ to estimate the backlog for the purpose of deciding the staffing level. Thus, even though we used simplifying process assumptions to derive the dynamic policy, we assess the performance of this policy relative to the static and unlimited policies by applying them in a simulation model that reflects the reality of the gleaning process (without process simplifications).

In Appendix E, we compare our simulation output to the actual output of the 2014 BAG gleaning season and verify that the actual output measures are within the 95% confidence intervals of the simulation output measure. In the numerical analysis below, we use our simulation model applied to the process parameters of the 2016 BAG gleaning season to compare the performance of our dynamic policy with static and unlimited policies. The 2016 season reflects the growth in the gleaning operation (increased number of donations and volunteers), where the dynamic policy can be helpful in managing system congestion.[7]

**Calibrating the simulation model parameters.** To compare the performance of the dynamic policy to the static and unlimited policies, we chose three crop types, corn, apple, and chard (indexed by $i = 1, 2$, and 3, respectively), and use the distribution of these crop-type donations

from 2016. Appendix D provides the values for specific gleaning parameters. We assumed that values for the three crop types are $\nu_1 = \nu_2 = \nu_3 = 1$ so that the payoffs represent the number of pounds gleaned. This is consistent with the way BAG reports its output and gives a straightforward interpretation of the results, but obviously $\nu_i$ can be set to translate pounds gleaned into another performance metric of interest such as serving size or wholesale price. Additionally, by using pounds gleaned as the output metric, these very different crops with very different payoff functions illustrate some interesting properties of the dynamic policy.

We base the number of volunteers off of BAG's volunteer pool size in 2016: $n = 400$. We use an estimate from BAG of the rate at which volunteers become available as $\mu = 0.0253$ (i.e., each volunteer becomes available approximately every 40 days) (Caldwell et al. 2017). The productivity of a volunteer ($r_i$, the number of pounds gleaned per volunteer per trip) varies depending on the type of crop. These productivity numbers were estimated based on productivity numbers of actual gleaning trips of these crop types (see Appendix D).

Typically, when a farmer calls with a gleaning donation, the gleaning trip must be scheduled within a 7-day window – this implies that the backlog of jobs cannot exceed $b_n = 7n\mu \approx 70$ jobs. Although the data is not available to determine the probability that a gleaner will attend a trip, estimates from BAG indicate that this probability is fairly high (Caldwell et al. 2017), thus we assume that $q = 0.8$.

We compare the dynamic policy to two policies used in practice: the unlimited policy and the static policy. The unlimited policy allows any number of volunteers to attend a gleaning trip. The gleaning organization simply sends out a trip announcement to the entire email list of volunteers, and whoever is available can attend the trip. Under the static policy, the gleaning organization posts a sign-up page with a specified number of volunteer slots for each gleaning trip. The number of slots depends on the donation class (crop type and donation size).

Clearly, the static policy staffing level and also the staffing levels in the dynamic policy (i.e., $k^*_{ij}$, $\underline{k}_{ij}$, and $\bar{k}_{ij}$ for each class $ij$) are parameters that can be optimized. However, we use straightforward heuristics to determine the values of these parameters in our simulation to reflect the process used by BAG. That is, we use a static staffing level that depends on the crop type and size of the donation, with some safety capacity built-in to compensate for volunteers who potentially may not show up for the gleaning trip. In particular, we use the static policy that sets the number of slots

to $\tilde{k}_{ij}/q$ for all $ij$. For the staffing parameters of the dynamic policy, we take the static policy for each class as the nominal level, and consider a range that is plus or minus 20% of the nominal, a reasonable range based on discussions with BAG (Caldwell et al. 2017). That is, we set the nominal staffing level in the dynamic policy to $k^*_{ij} = \tilde{k}_{ij}/q$, and the lower and upper bounds of staffing level to $\underline{k}_{ij} = k^*_{ij} - 0.2k^*_{ij}$ and $\bar{k}_{ij} = k^*_{ij} + 0.2k^*_{ij}$, respectively. We use the results from Proposition 4 to determine the optimal thresholds for the dynamic policy. The most interesting regime is when the system is congested, i.e., in heavy traffic, therefore we set the overall gleaning donation arrival rate to $\lambda^n = \sum_{ij} \lambda^n_{ij} = 0.93$ arrivals per day. The fraction of arrivals that are corn, apple, and chard, respectively, are determined by the actual distribution of donations of these crop types during the 2016 gleaning season.

To compare the performance of the dynamic, static, and unlimited policies, we develop a discrete event simulation model of our setting using the Arena© simulation software. We select the simulation run times and number of replications such that the estimate of a given performance metric of interest reaches steady state and the half-width of a 95% confidence interval on this estimate is at most 0.5% of the mean. Each simulation scenario is replicated 100 times using a replication run time of 110,000 days with the first 10,000 days used as warm-up. The steady state was confirmed by plotting the performance metric estimate versus the run time.

Figure 4 shows the structure of the dynamic policy for this example with three crop types and 10 classes. The requested staffing level for each class is shown as a function of the queue length $Q(t)$, with the thresholds $Q^*_1, ..., Q^*_M$, where $M = 20$, indicated on the $x$-axis. Notice that for each crop type $i$, as the size of the donation size increases, the threshold queue length to switch from the nominal staffing level $k^*_{ij}$ to the low staffing level $\underline{k}_{ij}$ increases, and the threshold queue length to switch from the nominal staffing level $k^*_{ij}$ to the high staffing level $\bar{k}_{ij}$ decreases. We can see this by looking at, for example, the corn staffing levels in Figure 4. The solid arrow that indicates the queue lengths for which the nominal staffing level $k^*_{ij}$ is optimal, gets longer as the donation size increases. This is intuitive because $\pi^l_{i1} < \pi^l_{i2} < \pi^l_{i3}$ (see Appendix D), which means that below the nominal staffing level, it is very costly for large size trips to lose volunteers. Thus, the queue length threshold for switching from $k^*_{ij}$ to $\underline{k}_{ij}$ is higher for larger size trips. Similarly, $\pi^r_{i1} > \pi^r_{i2} > \pi^r_{i3}$, which means that above the nominal staffing level, the benefit of more volunteers decreases in donation size. Therefore, the queue length threshold for switching from $k^*_{ij}$ to $\bar{k}_{ij}$ is

lower for larger size trips.

Comparing the staffing levels across crop types can also be instructive. For example, for a given congestion level, chard staffing levels for almost all donation sizes are lower than apple staffing levels. Comparing the staffing levels for class 24 (large apple donation) and class 31 (small chard donation) in Figure 4, we see that at congestion level $Q_4^*$, the dynamic policy would switch to the low staffing level $\underline{k}_{31}$ for class 31 chard donations, but still remain at the high staffing level $\bar{k}_{24}$ for class 24 apple donations. This is because the value (measured by number of pounds) of chard donations is much smaller than apple donations. Thus, the dynamic policy assigns higher staffing levels to the higher value apple donations. This, of course, could change under a different metric (e.g., serving size or wholesale price).

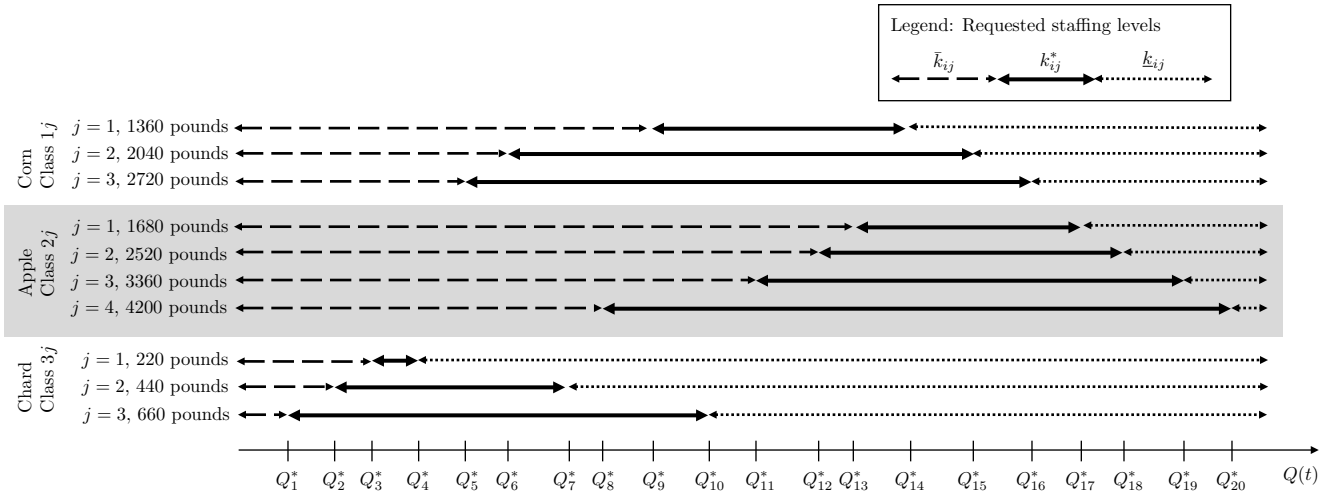


**Figure 4:** Structure of the dynamic policy

Figure 5 shows the performance of the dynamic policy compared to the static staffing policy. In particular, Figure 5 shows the percentage increase in net payoff (i.e., the total volume gleaned minus the total penalty for rejected donations) as a function of the penalty parameter $p$. Recall that the penalty for a rejected donation of class $ij$ is $\tilde{p}_{ij} = pk^*_{ij}$, which is roughly proportional to the size of the donation. Our conversations with gleaning organizations indicate that a reasonable range for the penalty is approximately the volume of one trip. That is, if a farmer's gleaning donation is rejected, the loss of goodwill results in roughly the loss of one future gleaning donation. In fact, the penalty could be considerably higher, depending on the willingness of a farmer to engage with the gleaning organization. Making the extra effort to coordinate with the gleaning organization

and allowing amateur pickers onto the fields create additional work and risk for the farmer. If in addition to those issues, the gleaning organization rejects well-intentioned donations, farmers may not find it worthwhile to participate in the gleaning network at all. Therefore, the gleaning organization needs to be responsive to farmers. To capture a range of penalty values, we show the performance of the dynamic policy relative to the static and unlimited policies for a range of $p$ values.

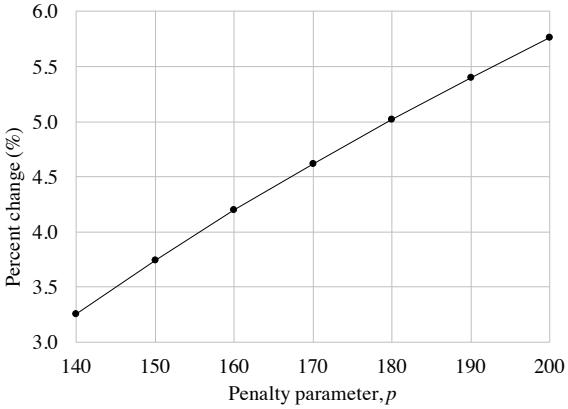


**Figure 5:** Percent increase in net payoff achieved by the dynamic policy compared to the static policy; $n = 400$, $q = 0.8$, $\mu = 0.0253$.

Our simulation results show that the percentage increase in average net payoff of the dynamic policy (for staffing range $k^*_{ij} \pm 0.2k^*_{ij}$)[8] over the static policy ranges from slightly over 3% to slightly under 6% for penalty values ranging from $p = 140$ to $p = 200$, respectively (Figure 5). Moreover, the relative performance increases in $p$. This is intuitive because as the penalty increases, the static cannot adjust for it, whereas the dynamic policy can. The percentage improvement of the dynamic policy over the unlimited policy is much higher – approximately 40% – because the unlimited policy is very inefficient in using volunteer capacity. Many trips are overstaffed which then causes later trips to be understaffed, thus resulting in low overall volume gleaned. However, similar to the comparison to the static policy, the percentage improvement of the dynamic policy over the unlimited policy increases in the penalty parameter, $p$.

Figure 6 shows how the dynamic policy adjusts the staffing policy to improve performance. Figure 6(a) shows the percentage breakdown of trips for all classes combined as a function of the penalty. When the penalty is low, the percentage of rejected donations is relatively high. As the penalty increases, the the dynamic policy shifts the staffing level allocation for each class $ij$ from

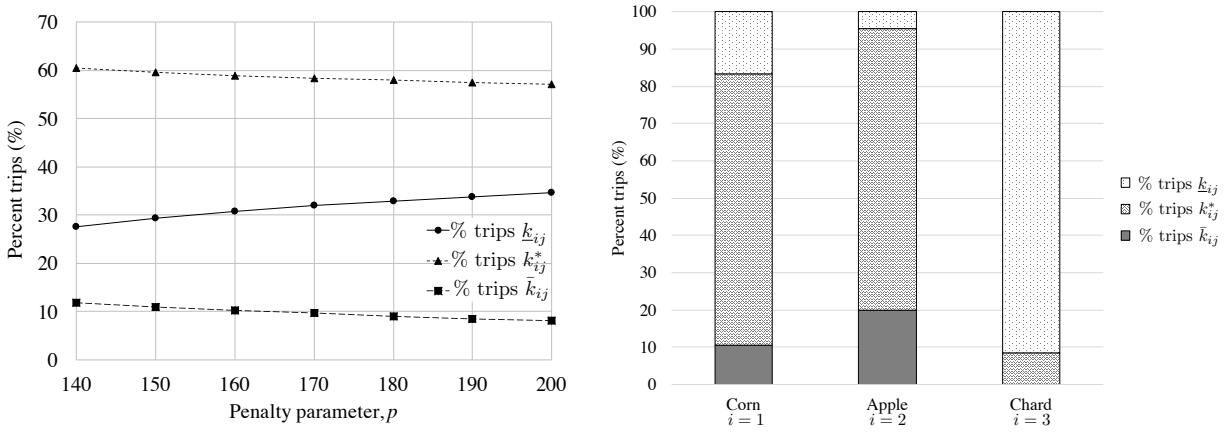


(a) All crop types combined.

(b) By crop type for $p = 150$.

**Figure 6:** Percentage breakdown of trips at each staffing level for the dynamic policy; $n = 400$, $q = 0.8$, $\mu = 0.0253$.

$\bar{k}_{ij}$ and $k^*_{ij}$ to $\underline{k}_{ij}$ to "save" volunteers for later trips. This reduces the average number of donations in the queue, thereby reducing the probability of having to reject future gleaning donations, thus avoiding the penalty. Figure 6(b) shows the trip breakdown by crop for $p = 150$. Recall that since $\nu_1 = \nu_2 = \nu_3 = 1$, the heavier crops (i.e., corn and apple) are higher value crops than the lighter crop, chard. Thus, we see that the dynamic policy mostly allocates $k^*_{ij}$ and $\bar{k}_{ij}$ staffing levels to the heavier crops, whereas it allocates mostly the $\underline{k}_{ij}$ staffing level for the lighter chard crop. In fact, during the simulation, there was not an instance of the high staffing level $\bar{k}_{ij}$ being assigned for chard. This is because whenever a chard donation arrived (i.e., a class 31, 32, or 33 arrival), the queue length was always greater than the threshold for staffing level $\bar{k}_{3j}$, $j = 1, 2, 3$. Figure 4 shows that the thresholds corresponding to $\bar{k}_{31}$, $\bar{k}_{32}$, and $\bar{k}_{33}$ are the lowest thresholds, $Q^*_1$, $Q^*_2$, and $Q^*_3$, respectively. Thus the staffing levels $\bar{k}_{31}$, $\bar{k}_{32}$, and $\bar{k}_{33}$ would not be assigned unless the system congestion was quite low – a condition that was not satisfied whenever a chard donation arrived.

Note that the net payoff includes the penalty cost for rejecting donations (to account for loss of farmer goodwill). Another important performance metric is how much of the volume lost under the static or unlimited policy can be recovered by using the dynamic policy. Figure 7 shows the dynamic policy can recover approximately 10% of the volume lost under the static policy. The percent recovered starts to decrease for higher penalties because the policy emphasizes reducing rejections, therefore, more trips are assigned $\underline{k}_{ij}$ staffing levels, thereby reducing the volume gleaned per trip. If we breakdown the recovered volume by crop, we see that the recovered corn and apple

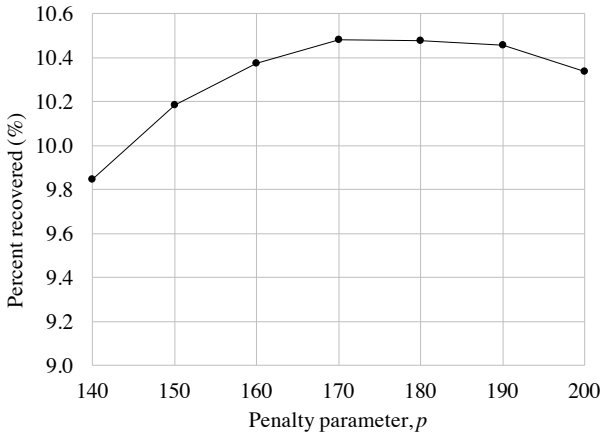


**Figure 7:** Percent of static policy volume loss recovered under the dynamic policy; $n = 400$, $q = 0.8$, $\mu = 0.0253$.

crops come at the expense of chard. For example, for $p = 150$, the dynamic policy recovers 6.4% and 25.3% of the volume of corn and apple, respectively, that are lost under the static policy. However, the volume of chard gleaned under the dynamic policy is only 88.8% of the volume gleaned under the static policy. Thus, even though the total volume gleaned increases under the dynamic policy, at the crop level, the volume changes could be positive or negative. Additionally, compared to the unlimited policy, the percentage of the volume loss recovered by the dynamic policy is considerably higher – in the range of 74-75% – because the volume loss under the unlimited policy is so much higher.

Our numerical study parameters represent an organization approximately the size of the Boston Area Gleaners. To put these recovery numbers in perspective, running a static policy similar to BAG's policy would imply an annual volume loss of 46,328 pounds. In this case, the dynamic policy would recover 4633 pounds or an equivalent of 18,532 four-ounce servings. To achieve this increase in volume, no capital or major process changes would be required – only some small changes to their staffing level requests.

# 7 Conclusion

Organizing gleaning operations is a worthwhile endeavor that benefits society by alleviating food insecurity and reducing food waste. The gleaning operation presents an interesting operational challenge because the demand for gleaning services (the arrival of donations from farms) and the

labor supply (volunteer gleaner capacity) are both stochastic. This uncertainty is particularly challenging when the demand rate and gleaner capacity are close. The gleaning organization needs to trade off safety capacity on the current trip with gleaner capacity for future trips.

This paper characterizes the gleaning process under the heavy traffic assumption and derives an (almost explicit) staffing policy that depends on the congestion in the system and allows for multiple donation classes (for different crop types and donation sizes). This policy is a nested threshold policy that specifies the staffing level for each donation class. In a numerical study with parameters for volunteer and donation characteristics calibrated using data from a gleaning organization in the Boston area, we found that the dynamic staffing policy can recover approximately 10% of the volume lost under the static policy and approximately 75% of the volume lost under the unlimited policy. The dynamic policy also increases the net payoff, and this improvement increases in the rejection penalty. Thus, our analysis can help gleaning organizations increase the volume gleaned by changing their staffing policy based on the congestion in the process. Moreover, these improvements do not require major investments or process changes – only small adjustments to the staffing request are required. We also provide a methodological contribution by explicitly solving the associated drift-rate control problem.

Our focus in this study was on volunteer staffing under congestion, however, there are several avenues of future research that can enrich our understanding of gleaning operations. First, we assumed that there would be demand for whatever is gleaned. However, the outlets for some crops, even if they are free, are limited. Therefore, the model could be extended to consider the demand side of the gleaning operation. Second, another resource that can constrain the output of the gleaning operation is the paid staff who coordinate and lead the gleaning trips. The number of trips that can be scheduled also depends on the capacity of the paid staff. This constraint can be added to capture another realistic dimension of the gleaning operation.

**References**


Altay, N. and W. G. Green (2006, November). Or/ms research in disaster operations management. *European Journal of Operational Research 175*(1), 475–493.

Ata, B. (2005). Dynamic power control in a wireless static channel subject to a quality of service contract. *Operations Research 53*, 842–851.

Ata, B. (2006). Dynamic control of a multiclass queue with thin arrival streams. *Operations Research 54*, 876–892.

Ata, B., J. M. Harrison, and L. A. Shepp (2005). Drift rate control of a brownian processing system. *The Annals of Applied Probability 15*(2), 1145–1160.

Ata, B. and S. Kumar (2005). Heavy traffic analysis of open processing networks with complete resource pooling: Asymptotic optimality of discrete review policies. *Annals of Applied Probability 15*, 331–391.

Ata, B. and S. Shneorson (2006). Dynamic control of an m/m/1 service system with adjustable arrival and service rates. *Management Science 52*, 1778–1791.

Ata, B. and M. Tongarlak (2013). On scheduling a multiclass queue with abandonments under general delay costs. *Queueing Systems 74*, 65–104.

Ata, B. and K. Zachariadis (2007). Dynamic power control in a fading downlink channel subject to an energy constraint. *Queueing Systems 55*, 41–69.

BAG (2016). *Boston Area Gleaners*. Boston Area Gleaners. http://www.bostonareagleaners.org, Accessed September 25, 2016.

Banerjee, S., C. Riquelme, and R. Johari (2015). Pricing in ride-share platforms: A queueing-theoretic approach. Working paper. Available at SSRN: https://ssrn.com/abstract=2568258 or http://dx.doi.org/10.2139/ssrn.2568258.

Bell, S. L. and R. Williams (2001). Dynamic scheduling of a system with two para servers in heavy traffic with resource pooling: Asymptotic optimality. *Annals of Applied Probability 11*, 608–649.

Billingsley, P. (1999). *Convergence of Probability Measures* (2nd ed.). Wiley.

Bollapragada, S. and T. E. Morton (1999, Sep - Oct). Myopic heuristics for the random yield problem. *Operations Research 47*, 713 – 722.

Boyce, W. E. and R. C. DiPrima (1992). *Elementary differential equations and boundary value problems*. Wiley.

Bramson, M. (1998). State space collapse with application to heavy traffic limits for multiclass queueing networks. *Queueing Systems 30*, 89 – 140.

Browne, S. and W. Whitt (1995). Piecewise-linear diffusion processes. In J. H. Dshalalow (Ed.), *Advances in Queueing Theory, Methods, and Open Problems*, Probability and Statistics Series, pp. 463–480. CRC Press.

Caldwell, L., D. Frazier, and M. Crawford (2017). *Personal Communications*. Boston Area Gleaners.

California Association of Food Banks (2011). *Utilizing New Methods of Crop Harvesting to Introduce Nutrient-Dense Specialty Crops to Low Income Consumers*. California Association of Food Banks. http://www.cafoodbanks.org/sites/default/files/concurrent-harvesting-report.pdf. Accessed May, 2015.

Coleman-Jensen, A., M. P. Rabbitt, C. Gregory, and A. Singh (2015). *Household Food Security in the United States in 2014*. U.S. Department of Agriculture. ERS Report. http://www.ers.usda.gov/media/1896841/err194.pdf.

Crabill, T. (1972). Optimal control of a service facility with variable exponential service times and constant arrival rate. *Management Science 18*, 560–566.

Crabill, T. (1974). Optimal control of a maintenance system with variable service rates. *Operations Research 22*, 736–745.

Davis, B. and V. Tarasuk (1994). Hunger in canada. *Agriculture and Human Values 11*(4), 50–57.

Davis, L. B., S. X. Jiang, S. D. Morgan, and C. Harris (2013). Forecasting donated goods for a local food bank. Proceedings of the Southeast Decision Sciences Institute 2013 Annual Meeting. Charleston SC, 20-22 February.

Davis, L. B., I. Sengul, J. S. Ivy, L. G. Brock III, and L. Miles (2014, September). Scheduling food bank collections and deliveries to ensure food safety and improve access. *Socio-Economic Planning Sciences 48*(3), 175–188.

Dong, J. and R. Ibrahim (2017). Flexible workers or full-time employees? on staffing systems with a blended workforce. Working paper. Available at SSRN: https://ssrn.com/abstract=2971841.

Falasca, M. and C. Zobel (2012, December). An optimization model for volunteer assignments in humanitarian organizations. *Socio-Economic Planning Sciences 46*(4), 250–260.

FBST (2015). *Food Bank of the Southern Tier*. Food Bank of the Southern Tier. http://www.foodbankst.org, Accessed December 6, 2015.

Galindo, G. and R. Batta (2013, October). Review of recent developments in or/ms research in disaster operations management. *European Journal of Operational Research 230*(2), 201–211.

George, J. M. and J. M. Harrison (2001). Dynamic control of a queue with adjustable service rate. *Operations Research 49*, 720–731.

Gerchak, Y., R. G. Vickson, and M. Parlar (1988). Periodic review production models with variable yield and uncertain demand. *IIE Transactions 20*, 144 – 150.

Ghamami, S. and A. R. Ward (2013). Dynamic scheduling of a two-server parallel server system with complete resource pooling and reneging in heavy traffic:asymptotic optimality of a two-threshold policy. *Mathematics of Operations Research 38*, 761–824.

Ghosh, A. and A. Weerasinghe (2010). Optimal buffer size and dynamic rate control for a queueing network with reneging in heavy traffic. *Stochastic Processes and their Applications 120*, 2103–2141.

Giffler, B. (1960). Determining an optimal reject allowance. *Naval Research Logistics Quarterly 7*, 201 – 206.

Gomez, M., C. Barrett, T. Raney, P. Pinstrup-Andersen, J. Meerman, A. Croppenstedt, B. Carisma, and B. Thompson (2013, October). Post-green revolution food systems and the triple burden of malnutrition. *Food Policy 42*, 129–138.

Gordon, L. and E. Erkut (2004, October). Improving volunteer scheduling for the edmonton folk festival. *Interfaces 34*(5), 367–376.

Gunders, D. (2012, August). *Wasted: How America is Losing Up to 40 Percent of Its Food from Farm to Fork to Landfill*. National Resources Defense Council. NRDC Issue Paper 12-06-B. http://www.nrdc.org/food/files/wasted-food-IP.pdf.

Gunes, C., W.-J. v. Hoeve, and S. Tayur (2010). Vehicle Routing for Food Rescue Programs: A Comparison of Different Approaches. In A. Lodi, M. Milano, and P. Toth (Eds.), *Integration of AI and OR Techniques in Constraint Programming for Combinatorial Optimization Problems*, Number 6140 in Lecture Notes in Computer Science, pp. 176–180. Springer Berlin Heidelberg.

Halfin, S. and W. Whitt (1981, May – Jun). Heavy-traffic limits for queues with many exponential servers. *Operations Research 29*(3), 567–588.

Harrison, J. (1988). Brownian models of queueing networks with heterogenous customer populations. In W. Fleming and P. L. Lions (Eds.), *Stochastic Differential Systems, Stochastic Control Theory and Applications*, pp. 147–186. Springer-Verlag.

Harrison, J. (1998). Heavy traffic analysis of a system with parallel servers: Asymptotic optimality of discrete review policies. *Annals of Applied Probability 8*, 822–848.

Harrison, J. and L. Wein (1989). Scheduling network of queues: Heavy traffic analysis of a simple open network. *Queueing Systems 5*, 265–280.

Harrison, J. and L. Wein (1990). Scheduling networks of queues: Heavy traffic analysis of a two-station closed network. *Operations Research 38*, 1052–1064.

Harrison, J. M. (2013). *Brownian Models of Performance and Control* (1st ed.). Cambridge University Press.

Henig, M. and Y. Gerchak (1990). The structure of periodic review policies in the presence of random yield. *Operations Research 38*, 634 – 643.

Hoisington, A., S. N. Butkus, S. Garrett, and K. Beerman (2001, January). Field Gleaning as a Tool for Addressing Food Security at the Local Level: Case Study. *Journal of Nutrition Education 33*(1), 43–48.

Hopp, W. J., S. M. R. Iravani, and G. Y. Yuen (2007). Operations systems with discretionary task completion. *Management Science 53*, 61–77.

Huang, W., V. Kulkarni, and J. M. Swaminathan (2008). Managing the inventory of an item with a replacement warranty. *Management Science 54*, 1441 – 1452.

Huh, W. T. and M. Nagarajan (2010). Linear inflation rules for the random yield problem: Analysis and computations. *Operations Research 58*, 244 – 251.

Ibrahim, R. (2017). Managing queueing systems where capacity is random and customers are impatient. Working paper. Available at SSRN: https://ssrn.com/abstract=2623502 or http://dx.doi.org/10.2139/ssrn.2623502.

Iglehart, D. (1965). Limit diffusion approximations for the many-server queue and the repairman problem. *Journal of Applied Probability 2*, 411–429.

Inderfurth, K. and G. P. Kiesmuller (2015). Exact and heuristic linear-inflation policies for an inventory model with random yield and arbitrary lead times. *European Journal of Operational Research 245*, 109 – 120.

Inderfurth, K. and S. Transchel (2007). Note on "myopic heuristics for the random yieid probiem". *Operations Research 55*, 1183 – 1186.

Inderfurth, K. and S. Vogelgesang (2013). Concepts for safety stock determination under stochastic demand and different types of random production yield. *European Journal of Operational Research 224*, 293 – 301.

Irwin, J. D., V. K. Ng, T. J. Rush, C. Nguyen, and M. He (2007, January). Can Food Banks Sustain Nutrient Requirements? A Case Study in Southwestern Ontario. *Canadian Journal of Public Health / Revue Canadienne de Sante'e Publique 98*(1), 17–20.

Johnson, M. P. and K. Smilowitz (2007, September). Community-Based Operations Research. In *OR Tools and Applications: Glimpses of Future Technologies*, INFORMS Tutorials in Operations Research, pp. 102–123. INFORMS.

Karlin, S. (1985). One stage models with uncertainty. In K. J. Arrow, S. Karlin, and H. Scarf (Eds.), *Studies in the Mathematical Theory of Inventory and Production*, Chapter 14. Stanford University Press.

Karlin, S. and H. Taylor (1981). *A Second Course in Stochastic Processes*. Academic Press.

Kim, J. and A. R. Ward (2013). Dynamic scheduling of a gi/gi/1+gi queue with multiple customer classes. *Queueing Systems 75*, 339–384.

Kovacs, G. and K. M. Spens (2011). Trends and developments in humanitarian logistics – a gap analysis. *International Journal of Physical Distribution & Logistics Management 41*(1), 32–45.

Lee, D., E. Sönmez, M. I. Gómez, and X. Fan (2017). An operational analysis of multi-crop food bank gleaning programs. *Food Policy 68*, 40–52.

Lien, R. W., S. M. Iravani, and K. R. Smilowitz (2014, March). Sequential resource allocation for nonprofit operations. *Operations Research 62*(2), 301–317.

Mandl, P. (1968). *Analytic Treatment of One-Dimensional Markov Processes*. Berlin: Springer-Verlag.

Mazzola, J. B., W. F. McCoy, and H. M. Wagner (1987). Algorithms and heuristics for variable-yield lot sizing. *Naval Research Logistics 34*, 67 – 86.

Mohan, S., M. Gopalakrishnan, and P. J. Mizzi (2013, June). Improving the efficiency of a non-profit supply chain for the food insecure. *International Journal of Production Economics 143*(2), 248–255.

Ormeci-Matoglu, M. and J. Vande Vate (2011). Drift control with changeover costs. *Operations Research 59*, 427–439.

Plambeck, E., S. Kumar, and S. Harrison (2001). A multiclass queue in heavy traffic with throughput time constraints: Asymptotically optimal dynamic controls. *Queueing Systems 39*, 3–54.

Reed, J. and A. Ward (2004). A diffusion approximation for a generalized jackson network with reneging. Proceedings of the $42^{nd}$ Annual Allerton Conference on Communication, Control and Computing, Sept 29 – Oct 1, 2004.

Reed, J., A. Ward, and D. Zhan (2013). On the generalized drift skorokhod problem in one dimension. *Journal of Applied Probability 50*, 16–28.

Royden, H. (1998). *Real Analysis* (3rd ed.). Englewood Cliffs, New Jersey: Prentice-Hall.

Rubino, M. and B. Ata (2009). Dynamic control of a make-to-order, parallel-server system with cancellations. *Operations Research 57*, 94–108.

Sampson, S. E. (2006, June). Optimization of volunteer labor assignments. *Journal of Operations Management 24*(4), 363–377.

Schuelke, R., M. Hoffmann, and M. Gómez (2011, July). Cause marketing opportunities: Gleanny, donating food from farms to ny's hungry. Smart Marketing. http://agribusiness.dyson.cornell.edu/SmartMarketing/pdfs/SmrtMkg20July2012.pdf.

Shih, W. (1980). Optimal inventory policies when stockouts result from defective products. *International Journal of Production Research 18*, 677 – 685.

Solak, S., C. Scherrer, and A. Ghoniem (2014, October). The stop-and-drop problem in nonprofit food distribution networks. *Annals of Operations Research 221*(1), 407–426.

Sönmez, E., D. Lee, M. I. Gómez, and X. Fan (2016). Improving food bank gleaning operations: An application in new york state. *American Journal of Agricultural Economics 98*(2), 549–563.

Starr, M. and L. Van Wassenhove (2014, June). Humanitarian operations and crisis management. *Production and Operations Management 23*(6), 925–937.

Stidham, S. (1988). Scheduling, routing, and flow control in stochastic networks. In W. Fleming and P. L. Lions (Eds.), *Stochastic Differential Systems, Stochastic Control Theory and Applications*, pp. 529–561. Springer-Verlag.

Stidham, S. (2002). Analysis, design, and control of queueing systems. *Operations Research 50*, 197–216.

Stidham, S. and R. R. Weber (1989). Monotonic and insensitive optimal policies for control of queues with undiscounted costs. *Operations Research 37*, 611–625.

Tarasuk, V. and G. Beaton (1999). Household food insecurity and hunger among families using food banks. *Canadian Journal of Public Health 90*(2), 109.

Taylor, T. (2017). On-demand service platforms. Working paper. Available at SSRN: https://ssrn.com/abstract=2722308 or http://dx.doi.org/10.2139/ssrn.2722308.

Teron, A. C. and V. S. Tarasuk (1999, November). Charitable Food Assistance: What are Food Bank Users Receiving? *Canadian Journal of Public Health / Revue Canadienne de Sante'e Publique 90*(6), 382–384.

USDA (2011). *Crop Production Annual Summaries (principal crops and vegetables)*. USDA. U.S. Department of Agriculture National Agricultural Statistics Service, http://usda.mannlib.cornell.edu/MannUsda/viewDocumentInfo.do?documentID=1047, accessed June 12, 2016.

USDA (2015). *Definitions of Food Security.* USDA. U.S. Department of Agriculture, http://www.ers.usda.gov/topics/food-nutrition-assistance/food-security-in-the-us/definitions-of-food-security.aspx, accessed December 19, 2015.

USDA (2018). *Agricultural Prices).* USDA. U.S. Department of Agriculture, http://usda.mannlib.cornell.edu/usda/nass/AgriPric//2010s/2018/AgriPric-02-27-2018.pdf, accessed May 15, 2018.

Van Wassenhove, L. N. (2006). Humanitarian aid logistics: Supply chain management in high gear, blackett memorial lecture. *Journal of the Operational Research Society 57*(5), 475–489.

Vitiello, D., J. A. Grisso, K. L. Whiteside, and R. Fischman (2014, November). From commodity surplus to food justice: Food banks and local agriculture in the united states. *Agriculture and Human Values*, 1–12. http://link.springer.com/article/10.1007/s10460-014-9563-x.

Weber, R. R. and S. Stidham (1987). Optimal control of service rates in network of queues. *Advances in Applied Probability 19*, 202–218.

Wein, L. (1990). Brownian networks with discretionary routing. *Operations Research 37*, 1065–1078.

Weinfield, N. S., G. Mills, C. Borger, G. Maeve, T. Macaluso, J. Montaquila, and S. Zedlewski (2014). *Hunger in America 2014.* Feeding America. http://www.feedingamerica.org/hunger-in-america/our-research/hunger-in-america/.

Wilson, N., B. Wansink, J. Swigert, and E. Waxman (2015). Hunger relief programs and behavioral economics: An introduction. Paper Presented at 2015 AAEA Annual Meeting. San Francisco CA, 26-28 July.

Yano, C. A. and H. L. Lee (1995). Lot sizing with random yields: A review. *Operations Research 43*, 311 – 334.

Yildiz, H., M. P. Johnson, and S. Roehrig (2013, October). Planning for meals-on-wheels: algorithms and application. *Journal of the Operational Research Society 64*(10), 1540–1550.

Zipkin, P. H. (2000). *Foundations of Inventory Management.* McGraw-Hill.

**Notes**

1. An earlier version of this paper was circulated with the title "Dynamic Staffing of Volunteer Gleaning Operations", and is available from SSRN: https://ssrn.com/abstract=2873250 or http://dx.doi.org/10.2139/ssrn.2873250.

2. Our definition allows time-dependent infinitesimal drift and variance. So, it is slightly more general. However, we will ultimately focus attention on stationary Markov control policies; see Section 4. Hence, our definition will coincide with that of Karlin and Taylor (1981).

3. Moreover, by virtue of the state space collapse results, imposing an overall delay constraint as done in (7) also imposes the same delay constraint for every class $ij$ separately; see Appendix C for a justification of this.

4. The weak convergence result assumed in Equation (9) can be proved by combining Stone's Lemma (see for example, Theorem 3.2 of Iglehart (1965)) and the continuous mapping theorem for weak convergence (see Billingsley (1999)), provided a certain regulator map (similar to the one given in Equations (10), (12), and (13)) is continuous. Reed and Ward (2004) and Reed et al. (2013) establish various useful properties of a closely related regulator map, including its Lipschitz continuity. The results of Reed and Ward (2004) and Reed et al. (2013) do not apply to our setting because we allow discontinuous drift terms in Equation (10). However, one may be able to extend their results to our setting, which would pave the way for proving a rigorous heavy traffic limit theorem. The study of these intricate technical issues is beyond the scope of this paper.

5. Note that $\pi_{ij}^r$ corresponds to the "left slope" whereas $\pi_{ij}^l$ corresponds to the "right slope" as shown in Figure 2.

6. For the case $j = M$, we only have the subcase (b).
7. We use the BAG data from 2014 to compare the simulation and actual outputs because the data from this year includes donation arrivals and volunteer attendance on gleaning trips. Thus, we were able to compare the simulation and actual outputs for pounds gleaned and volunteer attendance. Moreover, we could use this data to estimate the volunteer productivity for various crops. In 2016, we only have the donation arrival data, but this more recent data better reflects the distribution of the crops and the growth in the operation. Therefore, in the simulation study, we use the 2016 donation data to compare the performance of the dynamic policy to the static and unlimited policies, and assume that volunteer service rates and productivity remain the same as in 2014.
8. Appendix F presents a sensitivity analysis and discussion of how the staffing level range affect the policy performance.

# A Solution to the Bellman Equation

This appendix solves the Bellman equation, tackling the two intervals $(-\infty, 0]$ and $[0, b]$ separately at first, and then pasting the solutions obtained from each in a smooth fashion. In the next subsection, we study IVP$_-(\gamma)$ followed by an analysis of IVP$_+(\gamma)$ in Subsection A.2.

## A.1 Solving IVP$_-(\gamma)$

As a preliminary, we first study what happens when $z$ is sufficiently small. In that range, $w(\cdot, \gamma)$ admits an elegant closed-form solution. To facilitate the derivation of that solution, let

$$T_1(\gamma) = \inf\{z \leq 0 : w(z, \gamma_1) \geq c_1\} \qquad \text{for} \qquad \gamma \geq \underline{\gamma}, \tag{33}$$

where $\inf \phi = \infty$. Then let $x_1(\gamma) = \min\{0, T_1(\gamma)\}$ for $\gamma \geq \underline{\gamma}$, and consider the initial value problem on $(-\infty, x_1(\gamma)]$:

$$\gamma = \frac{1}{2}\sigma^2 w'(z) - \mu(z + \theta_0)w(z), \tag{34}$$

subject to the boundary condition

$$\lim_{z \to -\infty} w(z) = 0.$$

The initial value problem IVP$_-(\gamma)$ reduces to this one because $\phi(y) = \theta_0 y$ for $y \in [0, c_1]$; see Equation (92).

Recall that $g_i$ and $G_i$ denote the pdf and cdf, respectively, of a Normal random variable with mean $-\theta_i$ and variance $\sigma^2/2\mu$ for $i = 0, 1, ..., M$. The following proposition characterizes $w(z, \gamma)$ on $(-\infty, x_1(\gamma))$.

**Proposition 5** *For $\gamma \geq \underline{\gamma}$, we have that*

$$w(z, \gamma) = \frac{2\gamma}{\sigma^2} \frac{G_0(z)}{g_0(z)} \qquad \textit{for} \qquad z \in (-\infty, x_1(\gamma)).$$

**Proof.** Rearranging the terms in Equation (34) gives

$$\frac{2\gamma}{\sigma^2} = w'(z) - \frac{2\mu}{\sigma^2}(z + \theta_0)w(z) \qquad \text{for} \qquad z \in (-\infty, x_1(\gamma)).$$

Multiplying both sides with the integrating factor $\exp\left(\int_y^{x_1(\gamma)} \frac{2\mu}{\sigma^2}(\theta_0+y)dy\right)$ leads to

$$\frac{2\gamma}{\sigma^2}\,\frac{\exp\left(\frac{\mu}{\sigma^2}(\theta_0+x_1)^2\right)}{\exp\left(\frac{\mu}{\sigma^2}(\theta_0+y)^2\right)} = \left[\frac{\exp\left(\frac{\mu}{\sigma^2}(\theta_0+x_1)^2\right)}{\exp\left(\frac{\mu}{\sigma^2}(\theta_0+y)^2\right)}\,w(y)\right]'.$$

Integrating both sides over $[z, x_1(\gamma)]$ and using the definition of $g_0$, $G_0$ gives

$$\frac{2\gamma}{\sigma^2}\,\frac{1}{g_0(x_1(\gamma))}\int_z^{x_1(\gamma)} g(y)dy = w(x_1(\gamma)) - w(z)\,\frac{g(z)}{g(x_1(\gamma))}.$$

Multiplying both sides by $g_0(x_1(\gamma))$ gives

$$\frac{2\gamma}{\sigma^2}\int_z^{x_1(\gamma)} g_0(z)dz = w(x_1(\gamma))g_0(x_1(\gamma)) - w(z)g(z).$$

Equivalently, we write

$$w(z) = \left[w(x_1(\gamma))g_0(x_1(\gamma)) - \frac{2\gamma}{\sigma^2}\,G_0(x_1(\gamma))\right] + \frac{2\gamma}{\sigma^2}\,G_0(z), \tag{35}$$

from which it is clear that setting

$$w(z) = \frac{2\gamma}{\sigma^2}\,\frac{G_0(z)}{g_0(z)} \qquad \text{for} \qquad z \le x_1(\gamma)$$

solves (35), hence (34). To conclude the proof, it suffices to show that

$$\lim_{z\to-\infty} \frac{G_0(z)}{g_(z)} = 0.$$

Because both the numerator and the denominator tend to zero, by L'Hôpital's rule, we conclude that

$$\lim_{z\to-\infty} \frac{G_0(z)}{g_(z)} = \lim_{z\to-\infty} \frac{g_0(z)}{g_0'(z)} = \lim_{z\to-\infty} \frac{g_0(z)}{\frac{2\mu(\theta_0+z)}{\sigma^2}\,g_0(z)} = 0.$$

■

The following lemma facilitates the analysis below.

**Lemma 1** *The function $G_0/g_0$ is strictly increasing.*

**Proof.** Letting $\hat{\phi}$ and $\hat{\Phi}$ denote the pdf and cdf, respectively, of a standard Normal distribution, note that

$$g_0(z) = \frac{1}{\hat{\sigma}}\,\hat{\phi}\left(\frac{z-\hat{\mu}}{\hat{\sigma}}\right) \qquad \text{and} \qquad G_0(z) = \hat{\Phi}\left(\frac{z-\hat{\mu}}{\hat{\sigma}}\right),$$

where $\hat{\mu} = -\theta_0$ and $\hat{\sigma}^2 = \sigma^2/2\mu$. Also note that

$$\hat{\phi}'(z) = -z\hat{\phi}(z) \qquad \text{and} \qquad (1-\hat{\Phi}(z))z \leq \hat{\phi}(z) \qquad \text{for} \qquad z > 0.$$

Then we conclude that

$$\begin{aligned}\left[\frac{G_0(z)}{g_0(z)}\right]' &= \left[\frac{\hat{\sigma}\hat{\Phi}\left(\frac{z-\hat{\mu}}{\hat{\sigma}}\right)}{\hat{\phi}\left(\frac{z-\hat{\mu}}{\hat{\sigma}}\right)}\right]' \\ &= \hat{\sigma}\,\frac{\frac{1}{\hat{\sigma}}\hat{\phi}^2\left(\frac{z-\hat{\mu}}{\hat{\sigma}}\right) + \frac{1}{\hat{\sigma}}\left(\frac{z-\hat{\mu}}{\hat{\sigma}}\right)\hat{\phi}\left(\frac{z-\hat{\mu}}{\hat{\sigma}}\right)\hat{\Phi}\left(\frac{z-\hat{\mu}}{\hat{\sigma}}\right)}{\hat{\phi}^2\left(\frac{z-\hat{\mu}}{\hat{\sigma}}\right)} \\ &= \frac{\hat{\phi}\left(\frac{z-\hat{\mu}}{\hat{\sigma}}\right) + \left(\frac{z-\hat{\mu}}{\hat{\sigma}}\right)\hat{\Phi}\left(\frac{z-\hat{\mu}}{\hat{\sigma}}\right)}{\hat{\phi}\left(\frac{z-\hat{\mu}}{\hat{\sigma}}\right)}.\end{aligned}$$

Defining $y = (z-\hat{\mu})/\hat{\sigma}$, the right-hand side equals

$$\frac{\hat{\phi}(y) + y\hat{\Phi}(y)}{\hat{\phi}(y)}.$$

Clearly, if $y \geq 0$, then the right-hand side is positive. Otherwise, i.e., $y < 0$, then let $x = -y > 0$ and observe that

$$\text{RHS} = \frac{\hat{\phi}(-x) - x\hat{\Phi}(-x)}{\hat{\phi}(-x)} = \frac{\hat{\phi}(x) - x(1-\hat{\Phi}(x))}{\hat{\phi}(x)}.$$

Because $(1-\hat{\Phi}(x))x \leq \hat{\phi}(x)$ for $x > 0$, we conclude that

$$\text{RHS} \geq \frac{\hat{\phi}(x) - \hat{\phi}(x)}{\hat{\phi}(x)} = 0.$$

■

The following corollary is then immediate.

**Corollary 2** *The function $w(\cdot,\gamma)$ is increasing on $(-\infty, x_1(\gamma))$ for $\gamma \geq \underline{\gamma}$. Moreover, we have that*

$$x_1(\gamma) = \begin{cases} \left(\frac{G_0}{g_0}\right)^{-1} \left(\frac{\sigma^2 c_1}{2\gamma}\right), & \text{if } \frac{2\gamma}{\sigma^2}\frac{G_0(0)}{g_0(0)} > c_1, \\ 0, & \text{otherwise.} \end{cases}$$

**Proof.** The monotonicity of $w(\cdot,\gamma)$ is immediate from Lemma 1 and Proposition 5. To conclude the proof, first note from Proposition 5 that $T_1(\gamma) \geq 0$ if and only if $\frac{2\gamma}{\sigma^2}\frac{G_0(0)}{g_0(0)} \leq c_1$, and consider the case $T_1(\gamma) \geq 0$, in which case $x_1(\gamma) = 0$. Otherwise, i.e., $\frac{2\gamma}{\sigma^2}\frac{G_0(0)}{g_0(0)} > c_1$, then it must be that $T_1(\gamma) < 0$, and $x_1(\gamma) = T_1(\gamma)$ by definition. In particular, using the definitions of $x_1(\gamma)$, $T_1(\gamma)$ and Proposition 5, we observe that $x_1(\gamma)$ solves

$$\frac{2\gamma}{\sigma^2}\frac{G_0(x_1(\gamma))}{g_0(x_1(\gamma))} = c_1,$$

which proves the result. ■

Next, we turn to studying the initial value problem on the entire negative real line.

**Lemma 2** *For $\gamma \geq \underline{\gamma}$, the initial value problem IVP$_-(\gamma)$ has a unique solution $w(\cdot,\gamma)$.*

**Proof.** Proposition 5 establishes the result on $(-\infty, x_1(\gamma))$. Assume, without loss of generality, that $x_1(\gamma) < 0$ and consider the initial value problem

$$\gamma = \frac{1}{2}\sigma^2 w'(z) - \mu z w(z) - \mu\phi(w(z)) \qquad \text{for} \qquad z \in [x_1(\gamma), 0],$$

subject to

$$w(x_1(\gamma),\gamma) = c_1.$$

It suffices to show that this initial value problem has a unique solution. To this end, note that $\phi(\cdot)$ is Lipschitz continuous. Then the result follows from Picard's iteration argument, cf. pages 89-98 of Boyce and DiPrima (1992), that there exists a $\delta > 0$ such that we have a unique continuous solution $w(\cdot,\gamma)$ on the interval $[x_1(\gamma), x_1(\gamma)+\delta]$, and $w(\cdot,\gamma)$ is differentiable on that interval. Mimicking the arguments on page 162 of Mandl (1968), we can extend this result to the entire interval $[x_1(\gamma), 0]$.

■

The next result extends Corollary 2 to the entire negative real line, which is a key step in proving that the optimal policy is a nested-threshold policy.

**Proposition 6** *For $\gamma \geq \underline{\gamma}$, $w(\cdot, \gamma)$ is increasing on $(-\infty, 0]$ with $w'(z, \gamma) > 0$ for $z \in (-\infty, 0]$.*

**Proof.** Recall from Corollary 2 that $w(\cdot, \gamma)$ is increasing on $(-\infty, x_1(\gamma)]$. So, we focus on the case $x_1(\gamma) < 0$. (Otherwise, the result follows trivially.) We provide a proof by contradiction. To this end, we first provide a prove that $w(\cdot, \gamma)$ is nondecreasing on $(x_1(\gamma), 0]$. Suppose not. Then there exist $z_1, z_2$ as depicted in Figure 8 such that

$$x_1(\gamma) \leq z_1 < z_2 < 0, \tag{36}$$

$$w(z_1) = w(z_2) = w > 0, \tag{37}$$

$$w'(z_1) > 0 > w'(z_2). \tag{38}$$

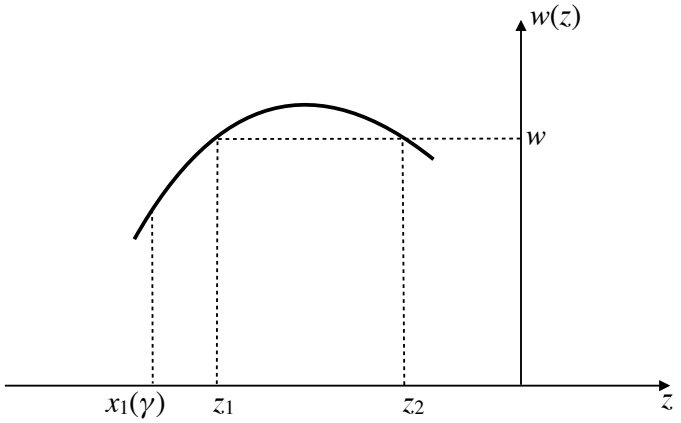


**Figure 8:** An auxiliary figure illustrating Equations (36)-(38).

Recall the Bellman equation at $z_1$ and $z_2$:

$$\gamma = \frac{1}{2}\sigma^2 w'(z_1) - \mu z_1 w(z_1) - \mu\phi(w(z_1)), \tag{39}$$

$$\gamma = \frac{1}{2}\sigma^2 w'(z_2) - \mu z_2 w(z_2) - \mu\phi(w(z_2)). \tag{40}$$

Subtracting (40) from (39) gives

$$0 = \frac{1}{2}\sigma^2[w'(z_1) - w'(z_2)] + \mu(z_2 - z_1)w.$$

Note that the right-hand side is strictly positive because $w'(z_1) > w'(z_2)$ and $z_2 > z_1$, leading to a contradiction, proving that $w(\cdot, \gamma)$ is nondecreasing on $(x_1(\gamma), 0]$.

To establish that $w'(z, \gamma) > 0$ for $z \in (x_1(\gamma), 0]$, we next rule out the three other possibilities: (i) $w(\cdot, \gamma)$ is constant on an interval; (ii) $w(\cdot, \gamma)$ has an inflection point $z_0 \in (x_1(\gamma), 0)$ with $w'(z_0, \gamma) = 0$; and (iii) $w'(0, \gamma) = 0$. We argue by contradiction. First, consider (i) and suppose there exists an interval $(z_1, z_2) \subset (x_1(\gamma), 0]$ such that $w(z) = w$ for all $z \in [z_1, z_2]$. Then we conclude that $w'(z) = 0$ for all $z \in [z_1, z_2]$. Recall the Bellman equation at $z_1$ and $z_2$:

$$\gamma = \frac{1}{2}\sigma^2 w'(z_1) - \mu z_1 w(z_1) - \mu\phi(w(z_1)), \tag{41}$$

$$\gamma = \frac{1}{2}\sigma^2 w'(z_2) - \mu z_2 w(z_2) - \mu\phi(w(z_2)). \tag{42}$$

Using $w'(z_1) = w'(z_2) = 0$ and that $w(z_1) = w(z_2) = w$ yields

$$\gamma = -\mu z_1 w - \mu\phi(w), \tag{43}$$

$$\gamma = -\mu z_2 w - \mu\phi(w). \tag{44}$$

Subtracting (44) from (43) gives $\mu(z_1 - z_2)w = 0$, implying $w = 0$, a contradiction. Thus, $w(\cdot, \gamma)$ cannot be constant on any interval.

Next, we rule out (ii). Suppose $w(\cdot, \gamma)$ has an inflection point $z_0 \in (x_1(\gamma), 0)$ with $w'(z_0, \gamma) = 0$. Then there exists an interval $(z_1, z_2) \subset (x_1(\gamma), 0]$ and $z_0 \in (z_1, z_2)$ such that $w'(z_0) = 0$, but $w'(z) > 0$ for $z \in (z_1, z_2)\backslash\{z_0\}$. To facilitate the proof, we rewrite the Bellman equation as follows:

$$\frac{1}{2}\sigma^2 w'(z) = \gamma - (\mu z w(z) + \mu\phi(w(z))). \tag{45}$$

The left-hand side is zero at $z_0$. Consider the right-hand side at $z_0$, and note that

$$\frac{d}{dz}(\mu z w(z))\Big|_{z_0} = (\mu w(z) + \mu z w'(z))\Big|_{z_0} = \mu w(z_0) > 0.$$

Thus, we conclude that $\mu z w(z) + \mu\phi(w(z))$ is increasing at $z_0$, and hence, the right-hand side of (45) is decreasing at $z_0$ and its value at $z_0$ is zero. Therefore, the right-hand side cannot be positive on $(z_0, z_1)$, a contradiction, which rules out the possibility of (ii).

Lastly, we consider (iii). That is, $w'(0,\gamma) = 0$. To show this cannot happen, we argue by contradiction. Suppose $w'(0,\gamma) = 0$ and consider the Bellman equation at $z = 0$ and $z < 0$ sufficiently small.

$$\frac{1}{2}\sigma^2 w'(z) = \gamma + \mu z w(z) + \mu\phi(w(z)), \tag{46}$$

$$0 = \gamma + \mu\phi(w(0)). \tag{47}$$

Subtracting (47) from (46) gives

$$\frac{1}{2}\sigma^2 w'(z) = \mu\{z w(z) - (\phi(w(0)) - \phi(w(z)))\}, \tag{48}$$

We proved so far that $w(z) < w(0)$ for $z > 0$. Also note from Proposition 1 of Ata et al. (2005) that

$$\phi(y) = \int_0^y \psi(y)du, \ y \geq 0. \tag{49}$$

Then because $\psi(\cdot)$ is left-continuous and piecewise constant, for $z$ sufficiently close to zero, it follows from Equation (49) that

$$\phi(w(0)) - \phi(w(z)) = \psi(w(0))(w(0) - w(z)). \tag{50}$$

Next we consider two subcases:

*Case (iiia):* $\psi(w(0)) \geq 0$. It then follows from (50) that the right-hand side of (49) is negative whereas the left-hand side is positive, a contradiction.

*Case (iiib):* $\psi(w(0)) < 0$. Note from the mean value theorem that there exists $\tilde{z} \in (z, 0)$ such that $w(0) - w(z) = -w'(\tilde{z})z$. Substituting this in (50) and (48) gives

$$\frac{1}{2}\sigma^2 w'(z) = \mu z\{w(z) + \psi(w(0))\, w'(\tilde{z})\}, \tag{51}$$

Because $w(\cdot)$ is continuously differentiable, we can choose $z < 0$ sufficiently close to zero such that

$$w(z) > \frac{w(0)}{2} \text{ and } w'(\tilde{z}) < \frac{w(0)}{4\,|\psi(w(0))|}. \tag{52}$$

Consequently, $w(z, \underline{\gamma}) + \psi(w(0))w'(\tilde{z}) > 0$ so that the right-hand side of (51) is negative because $z < 0$, whereas the left-hand side is positive, a contradiction.

Combining these cases, we can conclude that $w'(z, \gamma) > 0$ for $z \in (-\infty, 0]$ and that $w(\cdot, \gamma)$ is increasing. ■

The following proposition studies $w(\cdot, \gamma)$ at $\gamma = \underline{\gamma}$ and establishes that $w(0, \underline{\gamma}) < c_*$, which is used in the "smooth pasting" argument in constructing the solution to the Bellman equation.

**Proposition 7** *We have that $w(z, \underline{\gamma}) < c_*$ for $z \leq 0$. In particular, $w(0, \underline{\gamma}) < c_*$.*

**Proof.** Note from Proposition 6 that $w(\cdot, \underline{\gamma})$ is increasing. Thus, it suffices to show that $w(0, \underline{\gamma}) < c_*$. Suppose not, i.e., $w(0, \underline{\gamma}) \geq c_*$, and let

$$\tau = \inf\{z \leq 0 : w(z, \underline{\gamma}) \geq c_*\} \leq 0.$$

Also note that at $\gamma = \underline{\gamma}$, the initial value problem $\text{IVP}_-(\gamma)$ becomes

$$\begin{aligned} &\underline{\gamma} = \frac{1}{2}\sigma^2 w'(z, \underline{\gamma}) - \mu\, z w(z, \underline{\gamma}) - \mu\phi(w(z, \underline{\gamma})),\ z < 0, \\ &\text{subject to } \lim_{z \to -\infty} w(z, \underline{\gamma}) = 0, \end{aligned}$$

which gives the following at $z = \tau$:

$$\underline{\gamma} + \mu\tau w(\tau, \underline{\gamma}) + \mu\phi(w(\tau, \underline{\gamma})) = \frac{1}{2}\sigma^2 w'(\tau, \underline{\gamma}).$$

Substituting $\underline{\gamma} = \mu\phi_*$ and $w(\tau, \underline{\gamma}) = c_*$, which follow by definition, gives

$$\mu\phi_* + \mu\tau c_* + \mu\phi(c_*) = \frac{1}{2}\sigma^2 w'(\tau, \underline{\gamma}).$$

Because $\phi(c_*) = -\phi_*$ by definition and $w'(z, \underline{\gamma}) > 0$ by Proposition 6, we conclude that

$$\mu\tau c_* = \frac{1}{2}\sigma^2 w'(\tau, \underline{\gamma}) > 0.$$

Thus, we deduce that $\mu\tau c_* > 0$, which implies $\tau > 0$, leading to a contradiction. ■

Next, we turn to studying the solution $w(z, \gamma)$ as $\gamma$ varies.

**Lemma 3** *For $z \leq 0$ and $\gamma \geq \underline{\gamma}$, $w(z, \gamma)$ is increasing in $\gamma$.*

**Proof.** Recall that

$$x_1(\gamma) = \min\left\{0, \left(\frac{G_0}{g_0}\right)^{-1}\left(\frac{c_1\sigma^2}{2\gamma}\right)\right\} \text{ and } w(z,\gamma) = \frac{2\gamma}{\sigma^2}\frac{G_0(z)}{g_0(z)} \text{ on } (-\infty, x_1(\gamma)).$$

Therefore, $w(z, \gamma)$ increases in $\gamma$ on $(-\infty, x_1(\gamma))$ and $x_1(\gamma)$ decreases with $\gamma$. Let $\gamma_2 > \gamma_1 > 0$. Because we already know that $w(z, \gamma)$ increases in $\gamma$ for $z \in (-\infty, x_1(\gamma))$ and that $x_1(\gamma_2) \leq x_1(\gamma_1)$, it suffices to consider what happens for $z \in (x_1(\gamma_2), 0]$. (Of course, if $x_1(\gamma_2) = 0$, then the proof is complete.) We argue by contradiction: Suppose there exists $z \in (x_1(\gamma_2), 0]$ such that $w(z, \gamma_1) \geq w(z, \gamma_2)$. Then let

$$z^* = \inf\{z > x_1(\gamma_2) : w(z, \gamma_1) \geq w(z, \gamma_2)\}.$$

Note that by definition of $x^*$ that $w(z^*, \gamma_1) = w(z^*, \gamma_2)$. Also, recall the Bellman equation:

$$\gamma = \frac{1}{2}\sigma^2 w'(z) - \mu z w(z) - \mu\phi(w(z)),\ z \leq 0.$$

Define $\tilde{\phi}(y) = \phi(y) - \theta_0 y$ and note that $\tilde{\phi}$ is an increasing function. We can rewrite the Bellman equation as follows:

$$\gamma = \frac{1}{2}\sigma^2 w'(z) - (\mu z + \theta_0) w(z) - \mu\tilde{\phi}(w(z)),\ z \leq 0.$$

There are two cases to consider to complete the proof:

*Case 1:* $z^* > x_1(\gamma_2)$.

*Case 2:* $z^* = x_1(\gamma_2)$.

First, consider Case 1 and note from Equation (34) that

$$\gamma_i = \frac{1}{2}\sigma^2 w'(z,\gamma_i) - (\mu z + \theta_0)w(z,\gamma_i) - \mu\tilde{\phi}(w(z,\gamma_i)).$$

Rearranging the terms gives

$$\frac{2\gamma_i}{\sigma^2} = w'(z,\gamma_i) - \frac{2(\mu z + \theta_0)}{\sigma^2}\, w(z,\gamma_i) - \frac{2\mu}{\sigma^2}\,\tilde{\phi}(w(z,\gamma_i)).$$

Multiplying both sides by $\exp\left(\int_{x_1(\gamma_2)}^{z} -\frac{2}{\sigma^2}(\mu y + \theta_0)dy\right)$ and integrating over $(x_1(\gamma_2), x)$ gives

$$\begin{aligned}
&\frac{2\gamma_i}{\sigma^2}\int_{x_1(\gamma_2)}^{x} \exp\left(\int_{x_1(\gamma_2)}^{z} -\frac{2}{\sigma^2}(\mu y + \theta_0)dy\right) dz \\
&\quad = \int_{x_1(\gamma_2)}^{x} \left[w(z,\gamma_i)\exp\left(\int_{x_1(\gamma_2)}^{z} -\frac{2}{\sigma^2}(\mu y + \theta_0)dy\right)\right]' dz \\
&\quad\quad - \int_{x_1(\gamma_2)}^{x} \frac{2\mu}{\sigma^2}\,\tilde{\phi}(w(z,\gamma_i))\exp\left(\int_{x_1(\gamma_2)}^{z} -\frac{2}{\sigma^2}(\mu y + \theta_0)dy\right) dz.
\end{aligned}$$

Note by definition of $z^*$ that $w(z,\gamma_2) > w(z,\gamma_1)$ for $z \in (x_1(\gamma_2), z^*)$. Putting $x = z^*$ and comparing the preceding equation for $\gamma_1, \gamma_2$ gives:

$$\begin{aligned}
&\frac{2\gamma_2}{\sigma^2}\int_{x_1(\gamma_2)}^{z^*} \exp\left(\int_{x_1(\gamma_2)}^{z} -\frac{2}{\sigma^2}(\mu y + \theta_0)dy\right) dz \\
&\quad = w(z^*,\gamma_2)\exp\left(\int_{x_1(\gamma_2)}^{z^*} -\frac{2}{\sigma^2}(\mu y + \theta_0)dy\right) - w(x_1(\gamma_2),\gamma_2) \\
&\quad\quad - \frac{2\mu}{\sigma^2}\int_{x_1(\gamma_2)}^{z^*} \tilde{\phi}(w(z,\gamma_2))\exp\left(\int_{x_1(\gamma_2)}^{z} -\frac{2}{\sigma^2}(\mu y + \theta_0)dy\right) dz. \qquad (53)
\end{aligned}$$

Similarly,

$$\begin{aligned}
&\frac{2\gamma_1}{\sigma^2}\int_{x_1(\gamma_2)}^{z^*}\exp\left(\int_{x_1(\gamma_2)}^{z}-\frac{2}{\sigma^2}(\mu y+\theta_0)dy\right)dz\\
&\quad=w(z^*,\gamma_1)\exp\left(\int_{x_1(\gamma_2)}^{z^*}-\frac{2}{\sigma^2}(\mu y+\theta_0)dy\right)-w(x_1(\gamma_2),\gamma_1)\\
&\quad-\frac{2\mu}{\sigma^2}\int_{x_1(\gamma_2)}^{z^*}\tilde{\phi}(w(z,\gamma_1))\exp\left(\int_{x_1(\gamma_2)}^{z}-\frac{2}{\sigma^2}(\mu y+\theta_0)dy\right)dz. \qquad (54)
\end{aligned}$$

Subtracting (54) from (53) gives

$$\begin{aligned}
&\frac{2}{\sigma^2}(\gamma_2-\gamma_1)\int_{x_1(\gamma_2)}^{z^*}\exp\left(\int_{x_1(\gamma_2)}^{z}-\frac{2}{\sigma^2}(\mu y+\theta_0)dy\right)dz\\
&\quad=w(x_1(\gamma_2),\gamma_1)-w(x_1(\gamma_2),\gamma_2)\\
&\quad+\frac{2\mu}{\sigma^2}\int_{x_1(\gamma_2)}^{z^*}[\tilde{\phi}(w(z,\gamma_1))-\tilde{\phi}(w(z,\gamma_2))]\exp\left(\int_{x_1(\gamma_2)}^{z}-\frac{2}{\sigma^2}(\mu y+\theta_0)dy\right)dz,
\end{aligned}$$

where $w(x_1(\gamma_2),\gamma_1)-w(x_1(\gamma_2),\gamma_2)<0$ by definition of $z^*$ and the last term on the right-hand side is negative by definition of $z^*$ and the monotonicity of $\tilde{\phi}$. Therefore, the left-hand side is positive whereas the right-hand side is negative, leading to a contradiction in this case.

Next, we turn to the other case.

*Case 2:* $z^*=x_1(\gamma_2)$. We have the following two subcases:

*Case 2a.* $x_1(\gamma_2)=0$. Since $x_1(\gamma_1)\geq x_1(\gamma_2)$, we have $x_1(\gamma_1)=0$. Thus, $z^*=0$. Then we conclude

$$w(z^*,\gamma_2)=w(0,\gamma_2)=\frac{2\gamma_2}{\sigma^2}\frac{G_0(0)}{g_0(0)}>\frac{2\gamma_1}{\sigma^2}\frac{G_0(0)}{g_0(0)}=w(0,\gamma_1)=w(z^*,\gamma_1),$$

which contradicts the definition of $z^*$.

*Case 2b.* $x_1(\gamma_2)<0$. That is, $z^*=x_1(\gamma_2)=T_1(\gamma_2)$. Therefore, we observe that

$$w(z^*,\gamma_2)=w(T_1(\gamma_2),\gamma_2)=c_1. \qquad (55)$$

We proceed by considering the following two further subcases:

*Case 2bi.* $x_1(\gamma_1) < 0$. Then $x_1(\gamma_1) = T_1(\gamma_1)$ and

$$x_1(\gamma_1) = T_1(\gamma_1) > T_1(\gamma_2) = z^*.$$

Since $w(\cdot, \gamma_1)$ is increasing on $(-\infty, T_1(\gamma_1))$ and $w(T_1(\gamma_1), \gamma_1) = c_1$, we conclude that $w(z^*, \gamma_1) < c_1$, which contradicts the definition of $z^*$ and (55).

*Case 2bii.* $x_1(\gamma_1) = 0$. Then because $w(\cdot, \gamma_1)$ is increasing on $(-\infty, 0)$, we write

$$w(z^*, \gamma_1) < w(x_1(\gamma_1), \gamma_1) = w(0, \gamma_1) \leq c_1 = w(z^*, \gamma_2), \tag{56}$$

where the first inequality follows because $x_1(\gamma_2) = z^* < x_1(\gamma_1)$ and $w(\cdot, \gamma_1)$ is increasing, whereas the second inequality follows from the definition of $x_1(\gamma_1)$. The last equality follows from (55). Thus, we note that Equation (56) contradicts the definition of $z^*$.

Combining the cases above yields $w(z, \gamma)$ is increasing in $\gamma$ for $z \leq 0$. ■

The next result is key to pinning down the optimal long-run average cost $\gamma^*$; see Proposition 13 and Corollary 4. The following lemma is a slight modification of the Gronwall inequality and is used crucially in the proof of Proposition 8.

**Lemma 4** *(Gronwall Inequality) Let $f$ be a non-negative function such that*

$$f(x) \leq C + A \int_a^x f(y)\, dy \qquad \text{for} \qquad a \leq x \leq b \tag{57}$$

*for some constants $C$, $A$. Then*

$$f(x) \leq C \mathrm{e}^{A(x-a)}, \ x \in [a, b]. \tag{58}$$

**Proof.** Let $g(x) = \int_a^x f(y)\, dy$. Then it follows from (57) that

$$g'(y) \leq C + Ag(y). \tag{59}$$

Also note that $g(a) = 0$. We rewrite (59) as follows:

$$g'(y) - Ag(y) \leq C.$$

Multiplying both sides of this by $\mathrm{e}^{-Ay}$ gives

$$\left[g(y)\,\mathrm{e}^{-Ay}\right]' \leq C\mathrm{e}^{-Ay}.$$

Integrating both sides on $[a, x]$ for $x \leq b$ gives

$$g(x)\,\mathrm{e}^{-Ax} \leq \frac{C}{A}\left(\mathrm{e}^{-aA} - \mathrm{e}^{-Ax}\right).$$

Or, equivalently,

$$g(x) \leq \frac{C}{A}\left(\mathrm{e}^{A(x-a)} - 1\right).$$

Substituting this in (59) gives (58). ■

**Proposition 8** *We have that $w(0, \gamma)$ is non-negative, continuous and increasing in $\gamma$ for $\gamma \geq \underline{\gamma}$.*

**Proof.** It follows from Proposition 6 and the boundary condition $\lim_{z\to-\infty} w(z, \gamma) = 0$ that $w(0, \gamma) > 0$. Moreover, it is immediate from Lemma 3 that $w(0, \gamma)$ is increasing in $\gamma$. Therefore, what remains to be proved are that $w(0, \gamma)$ is continuous in $\gamma$.

We prove the continuity for $\gamma > \underline{\gamma}$, but the (right) continuity at $\underline{\gamma}$ can be proved similarly.

Let $\gamma_0 > \underline{\gamma}$ be such that $x_1(\gamma_0) < 0$. Otherwise, $x_1(\gamma_0) = 0$ and

$$w(0, \gamma_0) = \frac{2\gamma_0}{\sigma^2}\,\frac{G_0(0)}{g_0(0)},$$

and the result is immediate.

Also recall that $x_1(\gamma)$ is continuous. By definition of $\gamma_0$, there exists $\delta > 0$ such that $x_1(\gamma) < 0$

for $\gamma \in (\gamma_0 - \delta, \gamma_0 + \delta)$ so that

$$w(x_1(\gamma), \gamma) = \frac{2\gamma}{\sigma^2} \frac{G_0(x_1(\gamma))}{g_0(x_1(\gamma))} \tag{60}$$

is continuous. Moreover, note from the Bellman equation that

$$w'(z) = \frac{2\gamma}{\sigma^2} + \frac{2\mu}{\sigma^2} zw(z) + \frac{2\mu}{\sigma^2} \phi(w(z)), \;\; z \le 0.$$

Integrating both sides over $[x_1(\gamma), y]$ for $y \in (x_1(\gamma), 0]$ gives

$$w(y, \gamma) = w(x_1(\gamma), \gamma) - \frac{2\gamma}{\sigma^2} (y - x_1(\gamma)) + \frac{2\mu}{\sigma^2} \int_{x_1(\gamma)}^{y} zw(z)\, dz + \frac{2\mu}{\sigma^2} \int_{x_1(\gamma)}^{y} \phi(w(z, \gamma))\, dz.$$

We let $\gamma_1 \in (\gamma_0 - \delta, \gamma_0 + \delta)$. Hereafter, we also assume $\gamma_1 > \gamma_0$ for concreteness. (The other case, i.e., $\gamma_1 < \gamma_0$, can be handled similarly.) For $y \in (x_1(\gamma_0), 0]$, we write

$$\begin{aligned}
w(y, \gamma_0) &= w(x_1(\gamma_0), \gamma_0) - \frac{2\gamma_0}{\sigma^2} (y - x_1(\gamma_0)) + \frac{2\mu}{\sigma^2} \int_{x_1(\gamma_0)}^{y} zw(z, \gamma_0)\, dz \\
&\quad + \frac{2\mu}{\sigma^2} \int_{x_1(\gamma_0)}^{y} \phi(w(z, \gamma_0))\, dz, \\
w(y, \gamma_1) &= w(x_1(\gamma_1), \gamma_1) - \frac{2\gamma_1}{\sigma^2} (y - x_1(\gamma_1)) + \frac{2\mu}{\sigma^2} \int_{x_1(\gamma_1)}^{y} zw(z, \gamma_1)\, dz \\
&\quad + \frac{2\mu}{\sigma^2} \int_{x_1(\gamma_1)}^{y} \phi(w(z, \gamma_1))\, dz.
\end{aligned}$$

Then taking the difference of these two, we observe that

$$\begin{aligned}
|w(y, \gamma_0) - w(y, \gamma_1)| &\le |w(x_1(\gamma_0), \gamma_0) - w(x_1(\gamma_1), \gamma_1)| + \frac{2|y|}{\sigma^2} |\gamma_0 - \gamma_1| \\
&\quad + \frac{2}{\sigma^2} |\gamma_0 x_1(\gamma_0) - \gamma_1 x_1(\gamma_1)| + \frac{2\mu}{\sigma^2} \int_{x_1(\gamma_0)}^{y} |z|\, |w(z, \gamma_0) - w(z, \gamma_1)|\, dz \\
&\quad + \frac{2\mu}{\sigma^2} \int_{x_1(\gamma_1)}^{x_1(\gamma_0)} |z|\, w(z, \gamma_1)\, dz + \frac{2\mu}{\sigma^2} \int_{x_1(\gamma_0)}^{y} |\phi(w(z, \gamma_1)) - \phi(w(z, \gamma_0))|\, dz \\
&\quad + \frac{2\mu}{\sigma^2} \int_{x_1(\gamma_1)}^{x_1(\gamma_0)} |\phi(w(z, \gamma_1))|\, dz.
\end{aligned} \tag{61}$$

To facilitate the analysis, define the constants

$$
\begin{aligned}
C_1 &= \frac{2\mu}{\sigma^2}\,|x_1(\gamma_0)|,\\
C_2 &= \sup_{x_1(\gamma_1)\le z\le x_1(\gamma_0)} \frac{2\mu}{\sigma^2}\,|zw(z,\gamma_1)|,\\
C_3 &= \sup_{x_1(\gamma_1)\le z\le x_1(\gamma_0)} |\phi(w,z_1)|,\\
C_4 &= \max_{m=0,1,\ldots,M}\{|\theta_m|\},
\end{aligned}
$$

where $C_4$ is the global Lipschitz constant of $\phi$.

By substituting $C_1,\ldots,C_4$ and Equation (60) into Equation (61), and by bounding $y$ observing

$$|y| \le |x_1(\gamma_0)| + |x_1(\gamma_1)|,$$

we write

$$
\begin{aligned}
|w(y,\gamma_0) - w(y,\gamma_1)| \le{}& \frac{2}{\sigma^2}\left|\gamma_0\frac{G_0(x_1(\gamma_0))}{g_0(x_1(\gamma_0))} - \gamma_1\frac{G_0(x_1(\gamma_1))}{g_0(x_1(\gamma_1))}\right|\\
&+ \frac{2}{\sigma^2}\,|x_1(\gamma_0)+x_1(\gamma_1)|\,|\gamma_0-\gamma_1| + \frac{2}{\sigma^2}\,|\gamma_0x_1(\gamma_0)-\gamma_1x_1(\gamma_1)|\\
&+ C_1\int_{x_1(\gamma_0)}^{y} |w(z,\gamma_0)-w(z,\gamma_1)|\,dz + C_2|x_1(\gamma_1)-x_1(\gamma_0)|\\
&+ \frac{2\mu}{\sigma^2}\,C_3|x_1(\gamma_1)-x_1(\gamma_0)| + C_4\,\frac{2\mu}{\sigma^2}\int_{x_1(\gamma_0)}^{y} |w(z,\gamma_0)-w(z,\gamma_1)|\,dz. \qquad (62)
\end{aligned}
$$

Letting $A = C_1 + C_4\,\frac{2\mu}{\sigma^2}$ and

$$
\begin{aligned}
C(\gamma_0,\gamma_1) = \frac{2}{\sigma^2}\left|\gamma_0\frac{G_0(x_1(\gamma_0))}{g_0(x_1(\gamma_0))} - \gamma_1\frac{G_0(x_1(\gamma_1))}{g_0(x_1(\gamma_1))}\right| &+ \frac{2}{\sigma^2}\,|\gamma_0x_1(\gamma_0)-\gamma_1x_1(\gamma_1)|\\
&+ \frac{2}{\sigma^2}\,|x_1(\gamma_0)+x_1(\gamma_1)|\,|\gamma_0-\gamma_1| + \left(C_2 + \frac{2\mu}{\sigma^2}\,C_3\right)|x_1(\gamma_1)-x_1(\gamma_0)|,
\end{aligned}
$$

we arrive at the following

$$|w(y,\gamma_0)-w(y,\gamma_1)| \le C(\gamma_0,\gamma_1) + A\int_{x_1(\gamma_0)}^{y} |w(z,\gamma_0)-w(z,\gamma_1)|\,dz,\ \ y\in[x_1(\gamma_0),0].$$

Then by Gronwall's inequality (see Lemma 4), we conclude that

$$|w(0,\gamma_0) - w(0,\gamma_1)| \leq C(\gamma_0,\gamma_1)\,\mathrm{e}^{-Ax_1(\gamma_0)},$$

which proves that $w(0,\gamma)$ is continuous in $\gamma$ because $C(\gamma_0,\gamma_1)$ can be made arbitrarily small by letting $\gamma_1$ approach $\gamma_0$. ■

The rest of this subsection will help characterize the optimal policy. Recall from Equation (33) the definitions of $T_1(\gamma)$ and $x_1(\gamma)$ for $\gamma > \underline{\gamma}$. Next, we define $T_k(\gamma)$, $x_k(\gamma)$ for $k = 2, ..., M$ inductively as follows: If $x_{k-1}(\gamma) < 0$, then we define

$$T_k(\gamma) = \inf\{z \geq x_{k-1}(\gamma) : w(z,\gamma) \geq c_k\},$$

where $\inf \phi = \infty$, and $x_k(\gamma) = \min\{0, T_k(\gamma)\}$. Otherwise, i.e., $x_{k-1}(\gamma) = 0$, we set $T_k(\gamma) = 0$ and $x_k(\gamma) = \min\{0, T_k(\gamma)\} = 0$.

The following proposition characterizes $w(\cdot,\gamma)$ on $(x_{k-1}(\gamma), x_k(\gamma))$ for $k = 2, ..., M$ and facilitates the characterization of the optimal policy.

**Proposition 9** *For $k = 2, ..., M$, if $x_{k-1}(\gamma) < 0$, then for $z \in (x_{k-1}(\gamma), x_k(\gamma))$, we have that*

$$w(z,\gamma) = c_{k-1}\,\frac{g_{k-1}(T_{k-1}(\gamma))}{g_{k-1}(z)} + \frac{2(\gamma - \mu c(\theta_{k-1}))}{\sigma^2}\,\frac{G_{k-1}(z) - G_{k-1}(T_{k-1}(\gamma))}{g_{k-1}(z)}.$$

**Proof.** Fix $k \in \{2, ..., M\}$ and suppose that $x_{k-1}(\gamma) = T_{k-1}(\gamma) < 0$, and recall the Bellman equation on $(x_{k-1}(\gamma), x_k(\gamma))$:

$$\gamma = \frac{1}{2}\sigma^2 w'(z) - \mu z w(z) - \mu\phi(w(z)),$$
$$w(T_{k-1}(\gamma)) = c_{k-1}.$$

Also note that for $z \in [x_{k-1}(\gamma), x_k(\gamma)]$, we have that $w(z) \in [c_{k-1}, c_k]$ by definition of $x_{k-1}(\gamma)$, $x_k(\gamma)$. Thus, it follows from Equations (18)-(93) that

$$\phi(w(z)) = \theta_{k-1}w(z) - c(\theta_{k-1}) \text{ for } z \in [x_{k-1}(\gamma), x_k(\gamma)].$$

Substituting this into the Bellman equation gives

$$\gamma = \frac{1}{2}\sigma^2 w'(z) - \mu z w(z) - \mu[\theta_{k-1} w(z) - c(\theta_{k-1})].$$

Rearranging the terms gives

$$\frac{2(\gamma - \mu c(\theta_{k-1}))}{\sigma^2} = w'(z) - \mu(z + \theta_{k-1}) w(z).$$

Then we multiply both sides of this by

$$\frac{g_{k-1}(z)}{g_{k-1}(T_{k-1}(\gamma))} = \exp\left( - \int_{T_{k-1}(\gamma)}^{z} \frac{2\mu}{\sigma^2}(y + \theta_{k-1})\, dy \right).$$

(Recall that $g_{k-1}$ is the pdf of a Normal random variable with mean $-\theta_{k-1}$ and variance $\sigma^2/(2\mu)$.)

Then we can write the preceding Bellman equation as follows:

$$\frac{2(\gamma - \mu c(\theta_{k-1}))}{\sigma^2} \frac{g_{k-1}(z)}{g_{k-1}(T_{k-1}(\gamma))} = \left[ w(z) \frac{g_{k-1}(z)}{g_{k-1}(T_{k-1}(\gamma))} \right]'.$$

Integrating both sides over $[T_{k-1}(\gamma), z)$ and using the boundary condition $w(T_{k-1}(\gamma)) = c_{k-1}$ gives

$$\frac{2(\gamma - \mu c(\theta_{k-1}))}{\sigma^2} \frac{G_{k-1}(z) - G_{k-1}(T_{k-1}(\gamma))}{g_{k-1}(T_{k-1}(\gamma))} = \frac{w(z) g_{k-1}(z)}{g_{k-1}(T_{k-1}(\gamma))} - c_{k-1}.$$

Rearranging the terms, we conclude that

$$w(z) = c_{k-1} \frac{g_{k-1}(T_{k-1}(\gamma))}{g_{k-1}(z)} + \frac{2(\gamma - \mu c(\theta_{k-1}))}{\sigma^2} \frac{G_{k-1}(z) - G_{k-1}(T_{k-1}(\gamma))}{g_{k-1}(z)}$$

■

## A.2 Solving IVP$_+(\gamma)$

To facilitate the analysis of IVP$_+(\gamma)$, define $A(\cdot) : (\underline{\gamma}, \infty) \to (0, \infty)$ as follows:

$$A(\gamma) = \frac{\sigma^2}{2} \int_0^p \frac{du}{\gamma + \mu\phi(u)}.$$

The following proposition characterizes useful properties of the function $A(\cdot)$.

**Proposition 10** *The function $A(\cdot)$ is continuous and decreasing on $(\underline{\gamma}, \infty)$ with*

$$\lim_{\gamma \downarrow \underline{\gamma}} A(\gamma) = \infty \qquad \textit{and} \qquad \lim_{\gamma \to \infty} A(\gamma) = 0.$$

**Proof.** First, it is straightforward to see that $A(\cdot)$ is decreasing on $(\underline{\gamma}, \infty)$. Then note that for $\gamma_2 > \gamma_1 > \underline{\gamma}$, it is straightforward to show that

$$\begin{aligned}
|A(\gamma_2) - A(\gamma_1)| &\leq \frac{\sigma^2}{2} \int_0^p \Big| \frac{du}{\gamma_2 + \mu\phi(u)} - \frac{du}{\gamma_1 + \mu\phi(u)} \Big| \\
&= \frac{\sigma^2}{2} |\gamma_2 - \gamma_1| \int_0^p \Big| \frac{du}{(\gamma_1 + \mu\phi(u))(\gamma_2 + \mu\phi(u))} \Big| \\
&= \frac{\sigma^2}{2} |\gamma_2 - \gamma_1| \int_0^p \Big| \frac{du}{(\gamma_1 - \underline{\gamma} + \underline{\gamma} + \mu\phi(u))(\gamma_2 - \underline{\gamma} + \underline{\gamma} + \mu\phi(u))} \Big| \\
&\leq \frac{\sigma^2}{2} |\gamma_2 - \gamma_1| \int_0^p \frac{du}{(\gamma_1 - \underline{\gamma})(\gamma_2 - \underline{\gamma})} \\
&= \frac{\sigma^2}{2} \frac{p|\gamma_2 - \gamma_1|}{(\gamma_1 - \underline{\gamma})(\gamma_2 - \underline{\gamma})},
\end{aligned}$$

which shows that $A(\cdot)$ is continuous. Moreover, note that $1/(\gamma + \mu\phi(u))$ tends to zero monotonically as $\gamma \to \infty$ for all $u \in [0, p]$. Therefore, by the monotone convergence theorem (see Royden 1998) we conclude that $A(\gamma) \to 0$ as $\gamma \to \infty$.

Lastly, we prove that $\lim_{\gamma \downarrow \underline{\gamma}} A(\gamma) = \infty$. To prove this, we consider the following two cases. Case (i) $\theta_0 < 0$, Case (ii) $\theta_0 \geq 0$.

*Case (i):* Recall that $c_*$ is the smallest value such that $\phi(c_*) = -\phi_*$. It is easy to see that $c_* > 0$ in this case. Suppose that $j \geq 1$ is the index such that $c_j = c_*$, and note that

$$\phi(y) = \theta_{j-1} y - c(\theta_{j-1}) \text{ for } y \in [c_{j-1}, c_j]. \tag{63}$$

In particular, we have that

$$\phi(c_j) = \theta_{j-1}c_j - c(\theta_{j-1}) = -\phi_*, \tag{64}$$

$$\phi(c_{j-1}) = \theta_{j-1}c_{j-1} - c(\theta_{j-1}). \tag{65}$$

Moreover, because $\phi(\cdot)$ achieves its minimum at $c_* = c_j$ (and $c_*$ is the smallest minimizer of $\phi(\cdot)$), $\phi$ is decreasing on $[c_{j-1}, c_j]$. In particular, $\theta_{j-1} < 0$, c.f., Equation (63). Then for $\gamma > \underline{\gamma}$, we note that

$$\begin{aligned} A(\gamma) &\geq \frac{\sigma^2}{2}\int_{c_{j-1}}^{c_j} \frac{dy}{\gamma + \mu\phi(u)} \\ &= \frac{\sigma^2}{2}\int_{c_{j-1}}^{c_j} \frac{dy}{\gamma + \mu\theta_{j-1}y - \mu c(\theta_{j-1})} \\ &= \frac{\sigma^2}{\mu\theta_{j-1}} \ln\left(\frac{\gamma + \mu\theta_{j-1}c_j - \mu c(\theta_{j-1})}{\gamma + \mu\theta_{j-1}c_{j-1} - \mu c(\theta_{j-1})}\right) \\ &= \frac{\sigma^2}{\mu\theta_{j-1}} \ln\left(\frac{\gamma + \mu\phi(c_*)}{\gamma + \mu\phi(c_{j-1})}\right). \end{aligned}$$

Since $\underline{\gamma} = -\mu\phi(c_*)$, we conclude that

$$A(\gamma) \geq \frac{\sigma^2}{\mu\theta_{j-1}} \ln\left(\frac{\gamma - \underline{\gamma}}{\gamma + \mu\phi(c_{j-1})}\right).$$

Then, because $\theta_{j-1} < 0$, the right-hand side tends to $\infty$ as $\gamma \downarrow \underline{\gamma}$. Thus, $A(\gamma) \to \infty$ as $\gamma \to \underline{\gamma}$ in Case (i).

*Case (ii):* Because $\theta_0 \geq 0$, $\phi(\cdot)$ is non-negative and nondecreasing. Thus, we conclude that

$$A(\gamma) = \frac{\sigma^2}{2}\int_0^p \frac{dy}{\gamma + \mu\phi(u)} \geq \frac{\sigma^2}{2}\frac{p}{\gamma}. \tag{66}$$

In this case, we also have that $\phi_* = 0$ and $\underline{\gamma} = 0$. Thus, we conclude from (66) that $A(\gamma) \to \infty$ as $\gamma \downarrow \underline{\gamma}$ in Case (ii) as well. ■

The following corollary is then immediate.

**Corollary 3** *There exists a unique $\bar{\gamma}$ such that $A(\bar{\gamma}) = b$.*

The following derivation considers $\text{IVP}_+(\gamma)$ for $\gamma \in (\underline{\gamma}, \bar{\gamma}]$. It closely mimics the analysis in Section 3.2 of Ata et al. (2005) and motivates our definition of the solution to $\text{IVP}_+(\gamma)$:

Note that for $\gamma > \underline{\gamma}$, we can rewrite $\text{IVP}_+(\gamma)$ as follows:

$$\frac{\sigma^2}{2} \frac{u'(t)}{\gamma + \mu\phi(u(t))} = 1 \qquad \text{for} \qquad t \in (0, b].$$

Integrating both sides over $(z, b]$ gives

$$\frac{\sigma^2}{2} \int_z^b \frac{u'(t)}{\gamma + \mu\phi(u(t))} = b - z.$$

Using the boundary condition $u(b) = p$, the change of variable $y = u(t)$, and rearranging terms give

$$z = b - \frac{\sigma^2}{2} \int_{u(z)}^{p} \frac{dy}{\gamma + \mu\phi(y)}.$$

Inverting this relationship yields a formula for $u(z, \gamma)$, which we formalize next. To that end, restricting the domain of the function $H(u, \gamma)$ defined in Equation (30) to $(\underline{\gamma}, \bar{\gamma}]$ and $u \in [0, p]$, recall that

$$H(u, \gamma) = b - \frac{\sigma^2}{2} \int_u^p \frac{dy}{\gamma + \mu\phi(y)}. \tag{67}$$

The function $H(\cdot, \gamma)$ is strictly increasing and continuously differentiable. Therefore, its inverse is well defined. For each $\gamma \in (\underline{\gamma}, \bar{\gamma}]$, let $u(\cdot, \gamma)$ denote that inverse. Then the next proposition follows.

**Proposition 11** *The function $u(\cdot, \gamma)$ is strictly increasing and continuously differentiable. Moreover, $(\gamma, u(\cdot, \gamma))$ solves IVP$_+(\gamma)$.*

**Proof.** Because $H(\cdot, \gamma)$ is strictly increasing and continuously differentiable, its inverse $u(\cdot, \gamma)$ is also strictly increasing and continuously differentiable. To verify that $(\gamma, u(\cdot, \gamma))$ solve $\text{IVP}_+(\gamma)$, first note that

$$u(b, \gamma) = H^{-1}(b, \gamma) = p \qquad \text{because} \qquad H(p, \gamma) = b. \tag{68}$$

Also observe that for $z < b$,

$$u'(z,\gamma) = \frac{d}{dz}[H^{-1}(z,\gamma)] = \left.\frac{1}{\frac{d}{dy}[H(y,p)]}\right|_{y=u(z,p)} = \frac{2}{\sigma^2}\left[\gamma + \mu\phi(u(z,\gamma))\right],$$

so that

$$\gamma = \frac{1}{2}\sigma^2 u'(z,\gamma) - \mu\phi(u(z,\gamma)). \tag{69}$$

Combining (68)-(69), we conclude that $(\gamma, u(z,\gamma))$ solve $\text{IVP}_+(\gamma)$. ■

Lastly, Proposition 12 (stated below) will help us pin down the optimal long-run average cost $\gamma^*$. The following lemma will facilitate the proof of Proposition 12 and can be proved along the lines of Proposition 10.

**Lemma 5** *The function $H(u,\gamma)$ is increasing and continuous in $\gamma$ on $(\underline{\gamma},\infty)$.*

**Proof.** First, it is easy to see that $H(u,\gamma)$ is increasing in $\gamma$. Then note that for $\gamma_2 > \gamma_1 \geq \underline{\gamma}$, it is straightforward to show that

$$\begin{aligned}
|H(u,\gamma_2) - H(u,\gamma_1)| &\leq \frac{\sigma^2}{2}\int_u^p \left|\frac{du}{\gamma_2+\mu\phi(u)} - \frac{du}{\gamma_1+\mu\phi(u)}\right| \\
&= \frac{\sigma^2}{2}|\gamma_2-\gamma_1|\int_u^p \frac{du}{(\gamma_1+\mu\phi(u))(\gamma_2+\mu\phi(u))} \\
&= \frac{\sigma^2}{2}|\gamma_2-\gamma_1|\int_u^p \frac{du}{(\gamma_1-\underline{\gamma}+\underline{\gamma}+\mu\phi(u))(\gamma_2-\underline{\gamma}+\underline{\gamma}+\mu\phi(u))} \\
&\leq \frac{\sigma^2}{2}|\gamma_2-\gamma_1|\int_u^p \frac{du}{(\gamma_1-\underline{\gamma})(\gamma_2-\underline{\gamma})} \\
&= \frac{\sigma^2}{2}\frac{(p-u)|\gamma_2-\gamma_1|}{(\gamma_1-\underline{\gamma})(\gamma_2-\underline{\gamma})},
\end{aligned}$$

which shows that $H(u,\gamma)$ is continuous on $\gamma$ on $(\underline{\gamma},\infty)$. ■

**Proposition 12** *For $z \in [0,b]$ and $\gamma \in (\underline{\gamma},\bar{\gamma}]$, $u(z,\gamma)$ is continuous and decreasing in $\gamma$. Moreover, $u(0,\bar{\gamma}) = 0$ and $\lim_{\gamma\downarrow\underline{\gamma}} u(0,\gamma) \geq c_*$.*

**Proof.** We first show that $u(z,\gamma)$ is decreasing in $\gamma$. Let $\gamma_2 > \gamma_1 > \underline{\gamma}$. It is clear from (67) that

$H(u, \gamma_2) > H(u, \gamma_1)$ for all $u$. This is illustrated in Figure 9, from which it is also clear that

$$H^{-1}(y, \gamma_2) < H^{-1}(y, \gamma_1) \qquad \text{for all } y.$$

Because $u$ is the inverse of $H$, we conclude that

$$u(z, \gamma_2) < u(z, \gamma_1) \qquad \text{for all } z.$$

That is, $u(z, \gamma)$ is decreasing in $\gamma$.

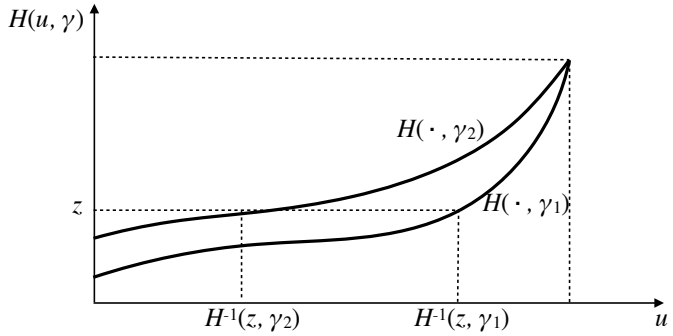


**Figure 9:** An illustrative $H$ function.

Next, we prove that $u(z, \gamma)$ is continuous in $\gamma$. Fix $\gamma > \underline{\gamma}$. We prove that $u(z, \cdot)$ is continuous at $\gamma$ in two steps:

(a) it is right-continuous at $\gamma$;

(b) it is left-continuous at $\gamma$.

*Proof of (a)*: Take an arbitrary decreasing sequence $\{\gamma_n\}_{n=1}^{\infty}$ such that $\gamma_n \downarrow \gamma$ as $n \to \infty$. By the first part of the proof, $u(z, \gamma_n)$ is increasing in $n$. So the limit $u^*(z) = \lim_{n\to\infty} u(z, \gamma_n)$ exists, and $u^*(z) \leq u(z, \gamma)$ by monotonicity of $u(z, \cdot)$. Suppose $u^*(z) < u(z, \gamma)$. Then

$$H(u^*(z), \gamma) < H(u(z, \gamma), \gamma) = z. \tag{70}$$

Also, because $u^*(z) > u(z, \gamma_n)$ for all $n$, we have that

$$H(u^*(z), \gamma_n) \geq H(u(z, \gamma_n), \gamma_n) = z \qquad \text{for all } n.$$

Passing to the limit as $n \to \infty$ gives $H(u^*(z), \gamma) \geq z$ because $H(u^*(z), \cdot)$ is continuous by Lemma 5. However, this contradicts (70), and that $u^*(z) = u(z, \gamma)$ so that $u(z, \cdot)$ is right-continuous at $\gamma$.

*Proof of (b)*: Take an arbitrary increasing sequence $\{\gamma_n\}_{n=1}^{\infty}$ such that $\gamma_n \uparrow \gamma$ as $n \to \infty$. Clearly, $u(z, \gamma_n)$ is decreasing. So the limit $u_*(z) = \lim_{n\to\infty} u(z, \gamma_n)$ exists, and $u_*(z) \geq u(z, \gamma)$ by monotonicity of $u(z, \cdot)$. Suppose $u_*(z) > u(z, \gamma)$. Then

$$H(u_*(z), \gamma) > H(u(z, \gamma), \gamma) = z. \tag{71}$$

Also, because $u_*(z) \leq u(z, \gamma_n)$, we have

$$H(u_*(z), \gamma_n) \leq H(u(z, \gamma_n), \gamma_n) = z \qquad \text{for all } n.$$

Passing to the limit as $n \to \infty$ gives $H(u_*(z), \gamma) \leq z$ because $H(u_*(z), \cdot)$ is continuous by Lemma 5. However, this contradicts (71), and thus $u_*(z) = u(z, p)$ so that $u(z, \cdot)$ is left-continuous at $\gamma$.

Lastly, we prove that $u(0, \bar{\gamma}) = 0$ and $\lim_{\gamma \downarrow \underline{\gamma}} u(0, \gamma) \geq c_*$. Proving the former is equivalent to showing that $H(0, \bar{\gamma}) = 0$, which follows from Corollary 3. For the latter, we consider two cases: Case (i) $\theta_0 \geq 0$, Case (ii) $\theta_0 < 0$.

In Case (i), $\phi(\cdot)$ is nondecreasing so that $\phi_* = 0$ and $c_* = 0$. Thus, $u(0, \gamma) \geq c_* = 0$ by definition for all $\gamma \geq \underline{\gamma}$. Consequently, we trivially have $\lim_{\gamma \downarrow \underline{\gamma}} u(0, \gamma) \geq c_* = 0$ in Case (i).

Consider Case (ii) $\theta_0 < 0$. It is easy to see in this case that $c_* > 0$. We proceed by contradiction. Suppose

$$\lim_{\gamma \downarrow \underline{\gamma}} u(0, \gamma) < c_*. \tag{72}$$

In particular, there exists $\tilde{\gamma} > \underline{\gamma}$ such that

$$u(0, \gamma) < c_* \text{ for all } \gamma \in (\underline{\gamma}, \tilde{\gamma}). \tag{73}$$

We restrict attention to such $\gamma \in (\underline{\gamma}, \tilde{\gamma})$ below. Note that because $u(\cdot, \gamma)$ is the inverse of $H(\cdot, \gamma)$:

$$0 = H(u(0, \gamma), \gamma) \text{ for all } \gamma \in (\underline{\gamma}, \tilde{\gamma}).$$

Then by definition of $H(\cdot,\gamma)$ (see Equation (67)), we write

$$0 = b - \frac{\sigma^2}{2}\int_{u(0,\gamma)}^{p} \frac{dy}{\gamma + \mu\phi(y)} \text{ for all } \gamma \in (\underline{\gamma}, \tilde{\gamma}).$$

In particular, because $u(0,\gamma) < c_* < p$ for $\gamma \in (\underline{\gamma}, \tilde{\gamma})$, we write

$$b = \frac{\sigma^2}{2}\int_{u(0,\gamma)}^{p} \frac{dy}{\gamma + \mu\phi(y)} \geq \frac{\sigma^2}{2}\int_{u(0,\gamma)}^{c_*} \frac{dy}{\gamma + \mu\phi(y)}. \tag{74}$$

Suppose $j$ is the index such that $c_j = c_*$ and note that

$$\phi(y) = \theta_{j-1}y - c(\theta_{j-1}) \text{ for } y \in [c_{j-1}, c_j]. \tag{75}$$

Moreover, because $\phi(\cdot)$ achieves its minimum at $c_* = c_j$ (and $c_*$ is the first such value), $\phi$ is decreasing on $[c_{j-1}, c_j]$. In particular, $\theta_{j-1} < 0$, c.f. Equation (75). Substituting (75) in Equation (74) and noting that $x \vee y = \max\{x, y\}$ yields

$$\begin{aligned}
b &\geq \frac{\sigma^2}{2}\int_{u(0,\gamma)\vee c_{j-1}}^{c_j} \frac{dy}{\gamma + \mu\phi(y)} \\
&= \frac{\sigma^2}{2}\int_{u(0,\gamma)\vee c_{j-1}}^{c_j} \frac{dy}{\gamma + \mu\theta_{j-1}y - \mu c(\theta_{j-1})} \\
&\geq \frac{\sigma^2}{2}\frac{1}{\mu\theta_{j-1}} \ln\left(\frac{\gamma + \mu\theta_{j-1}c_j - \mu c(\theta_{j-1})}{\gamma + \mu\theta_{j-1}(u(0,\gamma)\vee c_{j-1}) - \mu c(\theta_{j-1})}\right) \\
&= \frac{\sigma^2}{2}\frac{1}{\mu\theta_{j-1}} \ln\left(\frac{\gamma + \mu\phi(c_j)}{\gamma + \mu\phi(u(0,\gamma)\vee c_{j-1})}\right) \\
&= \frac{\sigma^2}{2}\frac{1}{\mu\theta_{j-1}} \ln\left(\frac{\gamma - \bar{\gamma}}{\gamma + \mu\phi(u(0,\gamma)\vee c_{j-1})}\right),
\end{aligned}$$

where the last equality follows since $\underline{\gamma} = -\mu\phi_* = -\mu\phi(c_j)$. That is,

$$b \geq \frac{\sigma^2}{2}\frac{1}{\mu\theta_{j-1}} \ln\left(\frac{\gamma - \bar{\gamma}}{\gamma + \mu\phi(u(0,\gamma)\vee c_{j-1})}\right). \tag{76}$$

Letting $\gamma \downarrow \underline{\gamma}$ and noting that $\theta_{j-1} < 0$, we conclude from Equation (76) that $b \geq \infty$, a contradiction. Thus, we have that $\lim_{\gamma\downarrow\underline{\gamma}} \geq c_*$ in Case (ii) as well. ■

### A.3 Solving the Bellman Equation

For $\gamma \in (\underline{\gamma}, \bar{\gamma}]$, let $\Delta(\gamma) = u(0,\gamma) - w(0,\gamma)$. The following result follows from Propositions 8 and 12.

**Proposition 13** *The function $\Delta(\cdot)$ is continuous and decreasing with $\Delta(\bar{\gamma}) < 0$ and $\Delta(\underline{\gamma}) > 0$.*

The following corollary is then immediate.

**Corollary 4** *There exists a unique $\gamma^*$ such that $\Delta(\gamma^*) = 0$.*

Thus, $\gamma^*$ satisfies Equation (28). Then defining $v(z,\gamma^*)$ as in Equation (29), the pair $(\gamma^*, v(z,\gamma^*))$ solve the Bellman equation as formalized next.

**Proposition 14** *The pair $(\gamma^*, v(z,\gamma^*))$ solve the Bellman equation (20)-(21).*

**Proof.** It follows from Lemma 2 and Proposition 6 that $w(\cdot,\gamma^*)$ solves $\text{IVP}_-(\gamma)$ on $(-\infty, 0]$ and that it is increasing and continuously differentiable. Propositions 5 and 9 characterize $w(\cdot,\gamma^*)$ explicitly. Moreover, it follows from Proposition 11 that $u(\cdot,\gamma^*)$ solves $\text{IVP}_+(\gamma)$ on $[0, b]$ and that it is increasing and continuously differentiable.

To complete the proof, we next argue that $v(z,\gamma^*)$, as defined in Equation (29), is continuously differentiable at the origin. Note that Corollary 4 ensures that $v(z,\gamma^*)$ is continuous at the origin (and hence on $(-\infty, b]$) and increasing on $(-\infty, b]$. Combining this with the differential equations of $\text{IVP}_-(\gamma)$ and $\text{IVP}_+(\gamma)$ shows that its left- and right-derivatives match at the origin as well, proving that $v(\cdot,\gamma^*)$ is continuously differentiable. ■

# B Proofs

**Proof of Proposition 1.** First consider $m_n(z,t)$ when $z \geq 0$, i.e., there are jobs waiting in the queue, and note that

$$\begin{aligned}
m_n(z,t) &= \lim_{h\downarrow 0} \frac{1}{h}\frac{1}{\sqrt{n}} \left[ \sum_{i=1}^{I}\sum_{j=1}^{J_i}\sum_{l=1}^{k_{ij}^n(z)} \lambda_{ij}^n l\, \mathbb{P}(N_{ij}(k_{ij}^n(z)) = l)h - n\mu h + o(h) \right] \\
&= \frac{1}{\sqrt{n}} \left[ \sum_{i=1}^{I}\sum_{j=1}^{J_i} \lambda_{ij}^n q k_{ij}^n(z) - n\mu \right] \\
&= \frac{1}{\sqrt{n}} \left[ \sum_{i=1}^{I}\sum_{j=1}^{J_i} q\lambda_{ij}^n k_{ij}^* \left(1 - \frac{\theta_{ij}(t)}{\sqrt{n}}\right) - n\mu \right] \\
&= \frac{\sum_{i=1}^{I}\sum_{j=1}^{J_i} q\lambda_{ij}^n k_{ij}^* - n\mu}{\sqrt{n}} - \frac{1}{n} q \sum_{i=1}^{I}\sum_{j=1}^{J_i} \lambda_{ij}^n k_{ij}^* \theta_{ij}(t) \\
&= -(1-\rho^n)\sqrt{n}\mu - \frac{1}{n} q \sum_{i=1}^{I}\sum_{j=1}^{J_i} \lambda_{ij}^n k_{ij}^* \theta_{ij}(t).
\end{aligned}$$

Then, by the heavy traffic assumption, in particular that $\lambda_{ij}^n/n \to \mu\rho_{ij}/(k_{ij}^* q)$ as $n \to \infty$, we conclude that when $z \geq 0$:

$$m_n(z,t) \to -\mu\beta - \mu \sum_{i=1}^{I}\sum_{j=1}^{J_i} \rho_{ij}\theta_{ij}(t) \quad \text{as } n \to \infty.$$

Next, consider $m_n(z,t)$ when $z < 0$. Repeating the above steps gives

$$m_n(z,t) = \lim_{h\downarrow 0} \frac{1}{h}\frac{1}{\sqrt{n}} \left[ \sum_{i=1}^{I}\sum_{j=1}^{J_i}\sum_{l=1}^{k_{ij}^n(z)} \lambda_{ij}^n l\, \mathbb{P}(N_{ij}(k_{ij}^n(z)) = l)h - (n\mu + z\mu\sqrt{n})h + o(h) \right].$$

Following the same steps as above gives that when $z < 0$:

$$m_n(z,t) \to -\mu\beta - \mu z - \mu \sum_{i=1}^{I}\sum_{j=1}^{J_i} \rho_{ij}\theta_{ij}(t) \text{ as } n \to \infty.$$

Next, we turn our attention to studying $\sigma_n^2(z,t)$. First, consider the case $z \geq 0$ and note that

$$\begin{aligned}
\sigma_n^2(z,t) &= \lim_{h\downarrow 0} \frac{1}{h}\frac{1}{n}\left[\sum_{i=1}^{I}\sum_{j=1}^{J_i}\sum_{l=1}^{k_{ij}^n(z)} \lambda_{ij}^n l^2\, \mathbb{P}(N_{ij}(k_{ij}^n(z)) = l)h + n\mu h + o(h)\right] \\
&= \frac{1}{n}\sum_{i=1}^{I}\sum_{j=1}^{J_i}\left(k_{ij}^n(z)q(1-q) + (k_{ij}^n(z)q)^2\right)\lambda_{ij}^n + \mu \\
&= \sum_{i=1}^{I}\sum_{j=1}^{J_i}\left[k_{ij}^*\left(1-\frac{\theta_{ij}(t)}{\sqrt{n}}\right)q(1-q) + \left(k_{ij}^*\left(1-\frac{\theta_{ij}(t)}{\sqrt{n}}\right)q\right)^2\right]\frac{\lambda_{ij}^n}{n} + \mu.
\end{aligned}$$

Recall from the heavy traffic assumption that $\lambda_{ij}^n/n \to \mu\rho_{ij}/(k_{ij}^* q)$ as $n \to \infty$. Thus, we conclude that as $n \to \infty$,

$$\begin{aligned}
\sigma_n^2(z,t) &\to \sum_{i=1}^{I}\sum_{j=1}^{J_i}\left[k_{ij}^* q(1-q) + (k_{ij}^* q)^2\right]\frac{\mu\rho_{ij}}{k_{ij}^* q} + \mu \\
&= \sum_{i=1}^{I}\sum_{j=1}^{J_i}\left[(1-q) + qk_{ij}^*\right]\mu\rho_{ij} + \mu \\
&= \sum_{i=1}^{I}\sum_{j=1}^{J_i}\left[1 + (k_{ij}^*-1)q\right]\mu\rho_{ij} + \mu \\
&= \mu\sum_{i=1}^{I}\sum_{j=1}^{J_i}\rho_{ij} + \mu\sum_{i=1}^{I}\sum_{j=1}^{J_i}\rho_{ij}(k_{ij}^*-1)q + \mu \\
&= 2\mu + \mu\sum_{i=1}^{I}\sum_{j=1}^{J_i}\rho_{ij}(k_{ij}^*-1)q,
\end{aligned}$$

where we used Equation (4) to deduce the last step. Therefore, we conclude that when $z \geq 0$:

$$\sigma_n^2(z,t) \to \mu\left[2 + q\sum_{i=1}^{I}\sum_{j=1}^{J_i}\rho_{ij}(k_{ij}^*-1)\right] \text{ as } n \to \infty.$$

Lastly, we consider the case $z < 0$:

$$\sigma_n^2(z,t) = \lim_{h\downarrow 0} \frac{1}{h}\frac{1}{n}\left[\sum_{i=1}^{I}\sum_{j=1}^{J_i}\sum_{l=1}^{k_{ij}^n(z)} \lambda_{ij}^n l^2\, \mathbb{P}(N_{ij}(k_{ij}^n(z)) = l)h + n\mu h + z\mu\sqrt{n}h + o(h)\right].$$

Following the same steps as above yields that for $z < 0$,

$$\sigma_n^2(z,t) \to \sigma^2 = \mu \left[ 2 + q \sum_{i=1}^{I} \sum_{j=1}^{J_i} \rho_{ij}(k_{ij}^* - 1) \right] \text{ as } n \to \infty.$$

■

**Proof of Proposition 2.** As a preliminary, we first show that

$$\begin{aligned} c(x) = \min_{\zeta_{ij}^d} \Bigg\{ & \sum_{i=1}^{I} \sum_{j=1}^{J_i} \pi_{ij}^l \zeta_{ij}^l \bar{\theta}_{ij} \rho_{ij} + \sum_{i=1}^{I} \sum_{j=1}^{J_i} \pi_{ij}^r (1 - \zeta_{ij}^r) |\underline{\theta}_{ij}| \rho_{ij} : \\ & \theta_0 + \sum_{i=1}^{I} \sum_{j=1}^{J_i} \zeta_{ij}^l \bar{\theta}_{ij} \rho_{ij} + \sum_{i=1}^{I} \sum_{j=1}^{J_i} (1 - \zeta_{ij}^l) |\underline{\theta}_{ij}| \rho_{ij} = x, \\ & 0 \le \zeta_{ij}^d \le 1 \text{ for } (i,j,d) \in \mathscr{A} \Bigg\}, \ x \in A = [\theta_0, \theta_M]. \end{aligned} \tag{77}$$

First note that $c(\theta_0) = 0$ and the right-hand side of (77) is also zero. Moreover, at $x = \theta_0$, we have that $\zeta_{ij}^l = 0$ and $\zeta_{ij}^r = 1$ for all $ij$, and as $x$ increases, some $\zeta_{ij}^l$'s will increase (to one) and $\zeta_{ij}^r$'s will decrease (to zero). Eventually, at $x = \theta_M$ we have that $\zeta_{ij}^l = 1$ and $\zeta_{ij}^r = 0$ for all $ij$. We prove (77) by using induction on $m = 1, ..., M$. As the induction basis ($m = 0$), consider $x \in (\theta_0, \theta_1]$. In this case, $c(x) = c_1 x$, where $c_1$ is the smallest element of the set $\{\pi_{ij}^d : (i,j,d) \in \mathscr{A}\}$ by definition; see Equation (14). Consider the right-hand side of (77) for $x \in (\theta_0, \theta_1]$ and recall that $\pi_{ij}^r < \pi_{ij}^l$ for all $ij$. The minimum on the right-hand side of (77) is achieved by setting

$$(1 - \zeta_{ij}^r) |\underline{\theta}_{ij}| \rho_{ij} = x$$

for the index $ij$ such that $\pi_{ij}^r = \min\{\pi_{ij}^d : (i,j,d) \in \mathscr{A}\}$ and setting all other $\zeta_{ij}^r = 1$; and also setting $\zeta_{ij}^l = 0$ for all $ij$.

As the induction hypothesis, suppose (77) holds for $x \in [\theta_0, \theta_{m-1}]$ and consider $x \in (\theta_{m-1}, \theta_m]$. Note that at $x = \theta_{m-1}$, the minimization operation on the right-hand side of (77) picks the $(m-1)$ indices $(i,j,d) \in \mathscr{A}$ for which $\pi_{ij}^d$ is the smallest. For $x \in (\theta_{m-1}, \theta_m]$, it picks, in addition, the index for which $\pi_{ij}^d$ is the $m^{th}$ smallest, i.e., it is equal to $c_m$ by Equation (14). Thus, for $x \in (\theta_{m-1}, \theta_m]$, the right-hand side of (77) increases at rate $c_m$ as $x$ increases, from which and the induction

hypothesis we conclude that (77) holds for $x \in [\theta_0, \theta_m]$.

To facilitate the proof, define $\zeta(\cdot) = (\zeta_{ij}^d(\cdot) : (i,j,d) \in \mathscr{A})$ as the minimizer in Equation (77). That is,

$$\zeta(x) = \arg\min_{\zeta_{ij}^d} \left\{ \sum_{i=1}^{I}\sum_{j=1}^{J_i} \pi_{ij}^l \zeta_{ij}^l \bar{\theta}_{ij}\rho_{ij} + \sum_{i=1}^{I}\sum_{j=1}^{J_i} \pi_{ij}^r (1-\zeta_{ij}^r)|\underline{\theta}_{ij}|\rho_{ij} : \right.$$
$$\theta_0 + \sum_{i=1}^{I}\sum_{j=1}^{J_i} \zeta_{ij}^l \bar{\theta}_{ij}\rho_{ij} + \sum_{i=1}^{I}\sum_{j=1}^{J_i} (1-\zeta_{ij}^r)|\underline{\theta}_{ij}|\rho_{ij} = x,$$
$$\left. 0 \le \zeta_{ij}^d \le 1 \text{ for } (i,j,d) \in \mathscr{A} \right\},\ x \in A = [\theta_0, \theta_M]. \tag{78}$$

Because we have $\pi_{ij}^r < \pi_{ij}^l$ for all $i, j$ and that $\zeta_{ij}^d(\cdot)$ are the minimizers, we conclude that

$$\zeta_{ij}^r(x)\zeta_{ij}^l(x) = 0 \text{ for all } i,j \text{ and } x \in [\theta_0, \theta_M]. \tag{79}$$

Then, given a feasible policy $\theta(\cdot)$ for $(P)$, let

$$\tilde{\theta}_{ij}(s) = \underline{\theta}_{ij}\zeta_{ij}^r(\theta(s)) + \bar{\theta}_{ij}\zeta_{ij}^l(\theta(s)), \tag{80}$$

and note that this policy is feasible for $(\tilde{P})$ and that

$$\begin{aligned}
&\sum_{i=1}^{I}\sum_{j=1}^{J_i} \hat{\pi}_{ij}(\rho_{ij}\tilde{\theta}_{ij}(s)) - \sum_{i=1}^{I}\sum_{j=1}^{J_i} \pi_{ij}^r \rho_{ij}\underline{\theta}_{ij} \\
&= \sum_{i=1}^{I}\sum_{j=1}^{J_i} (\pi_{ij}^l \zeta_{ij}^l(\theta(s))\bar{\theta}_{ij}\rho_{ij} + \pi_{ij}^r \zeta_{ij}^r(\theta(s))\underline{\theta}_{ij}\rho_{ij}) - \sum_{i=1}^{I}\sum_{j=1}^{J_i} \pi_{ij}^r \rho_{ij}\underline{\theta}_{ij} \\
&= \sum_{i=1}^{I}\sum_{j=1}^{J_i} (\pi_{ij}^l \zeta_{ij}^l(\theta(s))\bar{\theta}_{ij}\rho_{ij} + \sum_{i=1}^{I}\sum_{j=1}^{J_i} \pi_{ij}^r (1-\zeta_{ij}^r)|\underline{\theta}_{ij}|\rho_{ij} \\
&= c(\theta(s)),
\end{aligned}$$

where the first equality follows from (79) and the last equality follows from Equations (77) and (78). Thus, the policy $\tilde{\theta}_{ij}(\cdot)$ given in (80) for $(\tilde{P})$ has the same cost as the policy $\theta(\cdot)$ for $(P)$.

Given a feasible policy $\tilde{\theta}_{ij}(s)$ for $(\tilde{P})$, define the policy $\theta(\cdot)$ for $(P)$ as follows:

$$\theta(s) = \sum_{i=1}^{I} \sum_{j=1}^{J_i} \rho_{ij} \tilde{\theta}_{ij}(s), \ s \geq 0,$$

which is feasible for $(P)$. Moreover, it is clear from (77) that

$$\begin{aligned} c(\theta(s)) &\leq \sum_{i=1}^{I} \sum_{j=1}^{J_i} \pi_{ij}^l \frac{[\tilde{\theta}_{ij}(s)]^+}{\bar{\theta}_{ij}} \bar{\theta}_{ij} \rho_{ij} + \sum_{i=1}^{I} \sum_{j=1}^{J_i} \pi_{ij}^r \left(1 - \frac{[\tilde{\theta}_{ij}(s)]^-}{|\underline{\theta}_{ij}|}\right) |\underline{\theta}_{ij}| \rho_{ij} \\ &= \sum_{i=1}^{I} \sum_{j=1}^{J_i} \pi_{ij}^l [\tilde{\theta}_{ij}(s)]^+ \rho_{ij} + \sum_{i=1}^{I} \sum_{j=1}^{J_i} \pi_{ij}^r (-[\tilde{\theta}_{ij}(s)]^-) \rho_{ij} - \sum_{i=1}^{I} \sum_{j=1}^{J_i} \pi_{ij}^r \rho_{ij} \underline{\theta}_{ij} \\ &= \sum_{i=1}^{I} \sum_{j=1}^{J_i} \hat{\pi}_{ij} (\rho_{ij} \tilde{\theta}_{ij}(s)) - \sum_{i=1}^{I} \sum_{j=1}^{J_i} \pi_{ij}^r \rho_{ij} \underline{\theta}_{ij}. \end{aligned}$$

Therefore, the policy $\theta(\cdot)$ (for $(P)$) has lower cost than the policy $\tilde{\theta}_{ij}(s)$ (for $(\tilde{P})$).

What remains to show to conclude the proof is that $\tilde{\theta}_{ij}(\cdot)$ proposed in (80) coincides with the one given in Equation (15). Recall that $\pi_{ij}^r < \pi_{ij}^l$ so that $r_1(i,j) < r_2(i,j)$ for all $ij$. Thus, we proceed by considering the different possibilities of where $m$ falls relative to $r_1(i,j) < r_2(i,j)$. We have the following five cases: Case (i) $r_2(i,j) \leq m$; Case (ii) $r_2(i,j) = m+1$; Case (iii) $r_2(i,j) > m+1$ and $r_1(i,j) \leq m$; Case (iv) $r_1(i,j) = m+1$; Case (v) $r_1(i,j) > m+1$. Next we discuss each case.

*Case (i):* $r_2(i,j) \leq m$. In this case, we have that $\pi_{ij}^r < \pi_{ij}^l \leq c_m$. Thus, it follows from Equation (77) that $\zeta_{ij}^r = 0$ and $\zeta_{ij}^l = 1$. It then follows from (80) that $\tilde{\theta}_{ij}(s) = \bar{\theta}_{ij}$ in this case.

*Case (ii):* $r_2(i,j) = m+1$. In this case, we have that $\pi_{ij}^r \leq c_m < c_{m+1} = \pi_{ij}^l$. So it follows from Equation (77) that $\zeta_{ij}^r = 0$ and $\zeta_{ij}^l = (\theta(s) - \theta_m)/(\bar{\theta}_{ij}\rho_{ij}) \in (0,1]$. Thus, it follows from Equation (80) that $\tilde{\theta}_{ij}(s) = (\theta(s) - \theta_m)/\rho_{ij}$ in this case.

*Case (iii):* $r_2(i,j) > m+1$ and $r_1(i,j) \leq m$. In this case, we have that $\pi_{ij}^r \leq c_m$ and $\pi_{ij}^l > c_{m+1}$. Thus, it follows from (77) that $\zeta_{ij}^r = \zeta_{ij}^l = 0$. It then follows from (80) that $\tilde{\theta}_{ij}(s) = 0$.

*Case (iv):* $r_1(i,j) = m+1$. In this case, $\pi_{ij}^r = c_{m+1}$ and $\pi_{ij}^l > c_{m+1}$. Thus, it follows from (77) that $\zeta_{ij}^l = 0$ and $1 - \zeta_{ij}^r = (\theta(s) - \theta_m)/(\rho_{ij}|\underline{\theta}_{ij}|)$. It then follows from Equation (80) that $\tilde{\theta}_{ij}(s) = \underline{\theta}_{ij} + (\theta(s) - \theta_m)/\rho_{ij}$.

*Case (v):* $r_1(i,j) > m+1$. In this case, $\pi_{ij}^l > \pi_{ij}^r > c_{m+1}$. Thus, it follows from Equation (77) that $\zeta_{ij}^l = 0$ and $\zeta_{ij}^r = 1$. It then follows from Equation (80) that $\tilde{\theta}_{ij}(s) = \underline{\theta}_{ij}$. ■

**Proof of Proposition 3.** Letting $\gamma^*$ be as in Corollary 4 and $v(z) = v(z, \gamma^*)$ for $z \in (-\infty, b]$, where $v(z, \gamma^*)$ is given by Equation (29), the result is immediate from Proposition 14. ■

The following lemma will be used in the proof of Theorem 1.

**Lemma 6** *Under any admissible policy $\theta(\cdot)$, we have that*

$$\frac{\mathbb{E}Z(t)}{t} \to 0 \qquad as \qquad t \to \infty.$$

**Proof.** Let $K = \theta_M > 0$ and observe that for $x < -K$, the following holds:

$$m(x) - \mu\theta(x) = -\mu x - \mu\theta(x) \geq -\mu x - \mu\theta_M > \mu\theta_M - \mu\theta_M = 0. \tag{81}$$

Then define

$$Y(t) = \min\{Z(t), -K\},$$

and note that for any admissible policy $\theta(\cdot)$:

$$Y(t) \leq Z(t) \leq b. \tag{82}$$

In what follows, we will show that $\{Y(t), t \geq 0\}$ is a submartingale so that

$$\mathbb{E}Y(0) \leq \mathbb{E}Y(t) \leq b,$$

and therefore,

$$\frac{\mathbb{E}Y(t)}{t} \to 0 \qquad \text{as} \qquad t \to \infty. \tag{83}$$

Combining Equations (82) and (83) gives $\mathbb{E}[Z(t)]/t \to 0$ as $t \to \infty$, as desired.

Thus, to complete the proof, we turn to proving $\{Y(t), t \geq 0\}$ is a submartingale. To that end,

define the stopping times

$$S_1 = \inf\{t \geq 0 : Z(t) < -K\},$$
$$S_2 = \inf\{t \geq S_1 : Z(t) > -K\}.$$

Similarly, for $k = 1, 2, \ldots,$ define

$$S_{2k+1} = \inf\{t \geq S_{2k} : Z(t) < -K\},$$
$$S_{2k+2} = \inf\{t \geq S_{2k+1} : Z(t) > -K\}.$$

Note that

$$Y(t) = \begin{cases} Z(t), & \text{if } t \in [S_{2k-1}, S_{2k}] \text{ for some } k \geq 0, \\ -K, & \text{otherwise.} \end{cases}$$

Therefore, to show $\{Y(t), t \geq 0\}$ is a submartingale, it suffices to show that for any two stopping times $\hat{S}_1 \leq \hat{S}_2$ such that

$$S_{2k-1} \leq \hat{S}_1 \leq \hat{S}_2 \leq S_{2k} \qquad \text{for some } k,$$
$$\mathbb{E}[Y(\hat{S}_2) \,|\, Z(t), t \in [0, \hat{S}_1]] \geq Y(\hat{S}_1).$$

Also note that $Y(\hat{S}_i) = Z(\hat{S}_i)$ for $i = 1, 2$ and $Z(t) < -K$ for $t \in [\hat{S}_1, \hat{S}_2]$. Thus we write

$$Z(\hat{S}_2) = Z(\hat{S}_1) + \int_{\hat{S}_1}^{\hat{S}_2} [m(Z(t)) - \mu\theta(Z(t))]\, dt + \sigma[B(\hat{S}_2) - B(\hat{S}_1)].$$

Taking the conditional expectation of both sides and using Equation (81) gives

$$\mathbb{E}[Z(\hat{S}_2) \,|\, Z(t) : t \in [0, \hat{S}_1]] \geq Z(\hat{S}_1).$$

completing the proof. ■

**Proof of Theorem 1.** Note from Equations (23)-(25) that the candidate policy $\theta^*(\cdot)$ satisfies the following; also see Equations (18), (19), and (20).

$$\gamma^* = \frac{1}{2}\sigma^2 f''(z) + [m(z) - \mu\theta^*(z)]f'(z) + \mu c(\theta^*(z)), \;\; z \leq b. \tag{84}$$

Similarly, for an arbitrary admissible policy $\theta(\cdot)$, we have

$$\gamma^* \leq \frac{1}{2}\sigma^2 f''(z) + [m(z) - \mu\theta(z)]f'(z) + \mu c(\theta(z)), \;\; z \leq b. \tag{85}$$

Also, for any admissible policy $\theta(\cdot)$, applying Ito's lemma to $f(Z(t))$ gives

$$\begin{aligned} f(Z(t)) - f(Z(0)) = &\int_0^t \left( [m(Z(t)) - \mu\theta(Z(t))]f'(Z(t)) + \frac{\sigma^2}{2} f''(Z(t)) \right) dt \\ &+ \int_0^t \sigma f'(Z(t))\, dB(t) - f'(b)\mu\, U(t), \end{aligned}$$

see Chapters 4 and 6 of Harrison (2013). Because $\{f'(Z(t))\}$ is a bounded process, taking the expectations of both sides gives

$$\begin{aligned} \mathbb{E}[f(Z(t))] - \mathbb{E}[f(Z(0))] = \mathbb{E}&\int_0^t \left( [m(Z(t)) - \mu\theta(Z(t))]f'(Z(t)) + \frac{\sigma^2}{2} f''(Z(t)) \right) dt \\ &- f'(b)\mu\, \mathbb{E}[U(t)]. \end{aligned} \tag{86}$$

For any admissible policy $\theta(\cdot)$, combining Equations (85) and (86) gives

$$\mathbb{E}[f(Z(t))] - \mathbb{E}[f(Z(0))] \geq \mathbb{E}\left[ \int_0^t (\gamma^* - \mu c(\theta(Z(s))))\, ds \right] - p\mu\, \mathbb{E}[U(t)].$$

Rearranging the terms gives

$$\mathbb{E}\left[ \int_0^t \mu c(\theta(Z(s)))\, ds + \mu p U(t) \right] \geq \gamma^* t + \mathbb{E}[f(Z(0))] - \mathbb{E}[f(Z(t))]. \tag{87}$$

Also note from Equation (22) that

$$\mathbb{E}|f(Z(t))| \leq \mathbb{E}\int_{Z(t)}^b v(y)\, dy \leq p(b - \mathbb{E}Z(t)).$$

Combining this with Lemma 6 gives

$$\frac{\mathbb{E}[f(Z(t))]}{t} \to 0 \qquad \text{as } t \to \infty. \tag{88}$$

Then, we conclude from Equations (87)-(88) that

$$\underline{\lim}_{t\to\infty} \frac{1}{t}\, \mathbb{E}\left[\int_0^t \mu c(\theta(Z(s))\, ds + \mu p U(t)\right] \geq \gamma^*$$

for any admissible policy $\theta(\cdot)$.

Similarly, for the candidate policy $\theta^*(\cdot)$, combining (84) and (86) gives

$$\mathbb{E}[f(Z(t))] - \mathbb{E}[f(Z(0))] = \mathbb{E}\left[\int_0^t (\gamma^* - \mu c(\theta^*(Z(s))))\, ds\right] + \mu p\, \mathbb{E}[U(t)].$$

Rearranging the terms gives

$$\mathbb{E}\left[\int_0^t \mu c(\theta^*(Z(s)))\, ds + \mu p U(t)\right] = \gamma^* t + \mathbb{E}[f(Z(0))] - \mathbb{E}[f(Z(t))].$$

Then it follows from Equation (88) that

$$\lim_{t\to\infty} \frac{1}{t}\, \mathbb{E}\left[\int_0^t \mu c(\theta^*(Z(s))\, ds + \mu p U(t)\right] = \gamma^*.$$

Therefore, the candidate policy is optimal and its long-run average cost is $\gamma^*$. ■

**Proof of Proposition 4.** Note from Corollary 2 that if $\gamma^* \leq \frac{c_1\sigma^2}{2}\frac{g_0(0)}{G_0(0)}$, then $x_1(\gamma^*) = 0$, implying that $w(0, \gamma^*) \leq c_1$. Thus the value function $v(\cdot)$ reaches $c_1, ..., c_M$ at the thresholds $\tau_1, ..., \tau_M$, respectively, where $0 \leq \tau_1 < ... < \tau_M$. In particular, because $v(z) = u(z, \gamma^*)$ for $z \geq 0$, we must have

$$u(\tau_i, \gamma^*) = c_i, \;\; i = 1, ..., M.$$

Recall from Equation (67) that the inverse of $u(\cdot, \gamma^*)$ is given by $H(\cdot, \gamma^*)$. Thus,

$$\tau_i^* = H(c_i, \gamma^*) \text{ for } i = 1, ..., M,$$

proving the result in Case 0.

Next, we consider Case $j$, where $j = 1, ..., M-1$. In that case, it follows from $2\gamma^* > c_1\sigma^2 \frac{g_0(0)}{G_0(0)}$ and Corollary 2 that $x_1(\gamma^*) < 0$. Thus,

$$w(0, \gamma^*) = v(0, \gamma^*) > c_1. \tag{89}$$

Moreover, it follows from $H(c_{j+1}, \gamma^*) > 0 \geq H(c_j, \gamma^*)$ that

$$c_j < w(0, \gamma^*) = u(0, \gamma^*) = v(0) < c_{j+1}. \tag{90}$$

Thus, combining (89) and (90), we conclude that

$$\tau_1^* < ... < \tau_j^* < 0 < \tau_{j+1}^* < ... < \tau_M^*.$$

Then it follows from Proposition 5 that

$$w(\tau_1^*, \gamma^*) = \frac{2\gamma^*}{\sigma^2} \frac{G_0(\tau_1^*)}{g_0(\tau_1^*)} = c_1,$$

which yields (31), whereas for $i = j+1, ..., M$, we have that

$$u(\tau_i, \gamma^*) = v(\tau_i) = c_i$$

and inverting this gives $\tau_i = H(c_i, \gamma^*)$. On the other hand, for $i = 1, ..., j$, we have that $w(\tau_i, \gamma^*) = c_i$, or equivalently that

$$\tau_i = w^{-1}(c_i, \gamma^*) \text{ for } i = 1, ..., j,$$

from which (32) follows by virtue of Proposition 9. ■

# C Supplemental Analysis for the Heavy Traffic Approximation

## C.1 Imposing delay constraints for every class

In the heavy traffic regime, by virtue of the state-space collapse results, imposing an overall delay constraint as done by Equation (7) also imposes the same delay constraint for every class $ij$ separately; see for example Bramson (1998), Plambeck et al. (2001), and Ata and Kumar (2005) for rigorous proofs of state-space collapse results.

To see this, first let $Q_{ij}^n(t)$ denote the class $ij$ queue length (expressed in units of volunteer job equivalents) at time $t$ for $i = 1, ..., I$ and $j = 1, ..., J_i$ (note that $Q_{ij}^n(t) \geq 0$). The state-space collapse (under the first-come-first-serve scheduling of the gleaning trips of various classes) suggests that

$$Q_{ij}^n(t) \approx \frac{\lambda_{ij}^n k_{ij}^*}{\sum_{i=1}^{I} \sum_{j=1}^{J_i} \lambda_{ij}^n k_{ij}^*} [Q^n(t) - n]^+, \;\; t \geq 0. \tag{91}$$

Suppose now that we wish to impose a delay constraint of $D^n$ in the $n^{th}$ system for every class $ij$. This can be done by imposing the upper bound $b_{ij}^n = \lambda_{ij}^n k_{ij}^* q D^n$ on $Q_{ij}^n(t)$ for all $ij$; see Plambeck et al. (2001), Ata (2006), and Rubino and Ata (2009) for a justification of this. However, it follows from Equation (91) that this can be achieved by setting

$$b^n = \left( \sum_{i=1}^{I} \sum_{j=1}^{J_i} \lambda_{ij}^n k_{ij}^* \right) q D^n$$

in Equation (7), which therefore implies a delay constraint of $D^n$ for all classes.

## C.2 Relaxing Assumption 2

If Assumption 2 does not hold then an optimal policy for that setting can be derived from our analysis above as follows. Let $p = \min_{ij} \tilde{p}_{ij}/k_{ij}^*$ and find the optimal policy $\theta_{ij}(\cdot)$ for all $ij$ as if the preceding assumption is satisfied with this parameter $p$. Suppose that the planner uses this policy with one modification: she turns away only those classes of donations for which $\tilde{p}_{ij}/k_{ij}^* = p$ and no others. Then this policy is optimal for the setting where the assumption fails. For a justification of this assertion in a closely related setting, see Plambeck et al. (2001) and Rubino and Ata (2009).

## C.3 An approximation of the planner's expected payoff in the heavy traffic regime

Fixing a large $n$, consider the cumulative net payoff up to time $t$, denoted by $\xi(t)$, and note that

$$\begin{aligned}\mathbb{E}[\xi(t)] &= \mathbb{E}\int_0^t \sum_{i=1}^{I}\sum_{j=1}^{J_i} \lambda_{ij}^n \pi_{ij}(k_{ij}^n(s))\,ds - \sum_{i=1}^{I}\sum_{j=1}^{J_i} \tilde{p}_{ij}\,\mathbb{E}[R_{ij}^n(t) - R_{ij}^n(t-U_{ij}^n(t))] \\ &= \sum_{i=1}^{I}\sum_{j=1}^{J_i} \lambda_{ij}^n \mathbb{E}\int_0^t [\pi_{ij}(k_{ij}(s)) - \pi_{ij}(k_{ij}^*)]\,ds - \sum_{i=1}^{I}\sum_{j=1}^{J_i} \tilde{p}_{ij}\,\lambda_{ij}^n\,\mathbb{E}U_{ij}^n(t) + \sum_{i=1}^{I}\sum_{j=1}^{J_i} \lambda_{ij}^n \pi_{ij}(k_{ij}^*)t \\ &= \sum_{i=1}^{I}\sum_{j=1}^{J_i} \lambda_{ij}^n \mathbb{E}\int_0^t \tilde{\pi}_{ij}\left(\frac{k_{ij}^*\theta_{ij}(s)}{\sqrt{n}}\right) ds - \sum_{i=1}^{I}\sum_{j=1}^{J_i} \tilde{p}_{ij}\,\lambda_{ij}^n \mathbb{E}U_{ij}^n(t) + \sum_{i=1}^{I}\sum_{j=1}^{J_i} \lambda_{ij}^n \pi_{ij}(k_{ij}^*)t.\end{aligned}$$

Then using the approximations $\lambda_{ij}^n \approx n\mu\rho_{ij}/(k_{ij}^* q)$ and $\sqrt{n}\,U_{ij}^n(t) \approx U_{ij}(t)$ and Assumption 2, the planner's cumulative expected payoff can be approximated as follows:

$$\begin{aligned}&\mathbb{E}\sum_{i=1}^{I}\sum_{j=1}^{J_i}\int_0^t \frac{n\mu}{k_{ij}^* q}\frac{k_{ij}^*}{\sqrt{n}}\tilde{\pi}_{ij}(\rho_{ij}\theta_{ij}(s))ds - \sum_{i=1}^{I}\sum_{j=1}^{J_i}\frac{pk_{ij}^*}{q}\frac{\sqrt{n}\mu\rho_{ij}}{k_{ij}^*}\mathbb{E}U_{ij}(t) \\ &= \sqrt{n}\frac{\mu}{q}\mathbb{E}\left[\sum_{i=1}^{I}\sum_{j=1}^{J_i}\int_0^t \tilde{\pi}_{ij}(\rho_{ij}\theta_{ij}(s))ds\right] - \sqrt{n}\frac{p\mu}{q}\mathbb{E}\left[\sum_{i=1}^{I}\sum_{j=1}^{J_i}\rho_{ij}U_{ij}(t)\right].\end{aligned}$$

Recall that $U(t) = \sum_{i=1}^{I}\sum_{j=1}^{J_i}\rho_{ij}U_{ij}(t)$ by definition, which yields the following expression for the planner's cumulative expected net payoff:

$$\sqrt{n}\left\{\frac{\mu}{q}\mathbb{E}\left[\int_0^t \sum_{i=1}^{I}\sum_{j=1}^{J_i}\tilde{\pi}_{ij}(\rho_{ij}\theta_{ij}(s))ds\right] - p\frac{\mu}{q}\mathbb{E}U(t)\right\}.$$

## C.4 Descriptions of the $\phi(\cdot)$ and $\psi(\cdot)$ functions

Using (19), it is easy to check that for $y \geq 0$,

$$\psi(y) = \begin{cases} \theta_0, & \text{if } 0 \leq y \leq c_1, \\ \theta_{k-1}, & \text{if } c_{k-1} < y \leq c_k,\ k = 2, ..., M, \\ \theta_M, & \text{if } y > c_M. \end{cases} \tag{92}$$

The function $\psi$ captures all relevant aspects of the cost function $c(\cdot)$ for our analysis. Because $\phi(y) = y\psi(y) - c(\psi(y))$, we conclude that

$$\phi(y) = \begin{cases} \theta_0 y, & \text{if } 0 \leq y \leq c_1, \\ \theta_{k-1} y - c(\theta_{k-1}), & \text{if } c_{k-1} < y \leq c_k,\ k = 2, ..., M, \\ \theta_M y - c(\theta_M), & \text{if } y > c_M. \end{cases} \tag{93}$$

Figure 10 depicts illustrative $\psi(\cdot)$ and $\phi(\cdot)$ functions with $M = 4$, for the case of $\theta_0 < 0$. Note that the analysis in Section 5 allows for the case where $\theta_0 \geq 0$ as well.

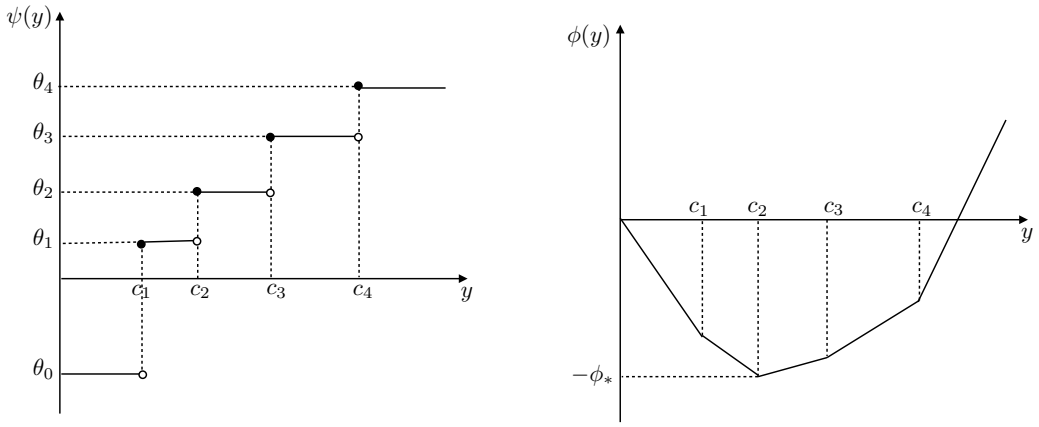


(a) An illustrative $\psi(\cdot)$ function.

(b) An illustrative $\phi(\cdot)$ function.

**Figure 10:** Illustrative $\psi(\cdot)$ and $\phi(\cdot)$ functions.

# D Simulation Parameters

This section specifies the parameters used in the simulation study presented in Section 6.

### General Parameters

The parameters below are based on estimates from the Boston Area Gleaners (Caldwell et al. 2017).

- $q = 0.8$
- $\mu = 0.0253$
- gleaning window = 7 days

**Table 1:** Crop type $i = 1$ (corn)

| Donation size, $j$ | 1 | 2 | 3 |
|---|---|---|---|
| Pounds | 1360 | 2040 | 2720 |
| $\lambda^n_{1j}$ | 0.2657 | 0.1328 | 0.0664 |
| $\tilde{k}_{1j}$ | 8 | 12 | 16 |
| $k^*_{1j} = \tilde{k}_{1j}/q$ | 10 | 15 | 20 |
| $\underline{k}_{1j}$ | 8 | 12 | 16 |
| $\bar{k}_{1j}$ | 12 | 18 | 24 |
| $\pi^l_{1j}$ | 95 | 102 | 106 |
| $\pi^r_{1j}$ | 33 | 30 | 28 |

**Table 2:** Crop type $i = 2$ (apple)

| Donation size, $j$ | 1 | 2 | 3 | 4 |
|---|---|---|---|---|
| Pounds | 1680 | 2520 | 3360 | 4200 |
| $\lambda^n_{2j}$ | 0.0664 | 0.0664 | 0.0664 | 0.0664 |
| $\tilde{k}_{2j}$ | 8 | 12 | 16 | 20 |
| $k^*_{2j} = \tilde{k}_{2j}/q$ | 10 | 15 | 20 | 25 |
| $\underline{k}_{2j}$ | 8 | 12 | 16 | 20 |
| $\bar{k}_{2j}$ | 12 | 18 | 24 | 30 |
| $\pi^l_{2j}$ | 117 | 126 | 131 | 135 |
| $\pi^r_{2j}$ | 41 | 37 | 34 | 31 |

- $n = 400$ (based on BAG volunteer pool size in 2016)

### Crop Types and Volunteer Gleaner Productivity

Volunteer gleaner productivity was calculated from BAG gleaning trips in 2014.

- $i = 1$: Corn, $r_1 = 170$ pounds per volunteer per 3-hour trip
- $i = 2$: Apple, $r_2 = 210$ pounds per volunteer per 3-hour trip
- $i = 3$: Chard, $r_3 = 55$ pounds per volunteer per 3-hour trip

### Crop Specific Parameters

The distribution of the classes of donation arrivals (i.e., crop type and size) in Tables 1, 2, and 3 are based on the distribution of donation arrivals from BAG's 2016 season (BAG 2016).

**Table 3:** Crop type $i = 3$ (chard)

| Donation size, $j$ | 1 | 2 | 3 |
|---|---|---|---|
| Pounds | 220 | 440 | 660 |
| $\lambda_{3j}^n$ | 0.0664 | 0.0664 | 0.0664 |
| $\tilde{k}_{3j}$ | 4 | 8 | 12 |
| $k_{3j}^* = \tilde{k}_{3j}/q$ | 5 | 10 | 15 |
| $\underline{k}_{3j}$ | 4 | 8 | 12 |
| $\bar{k}_{3j}$ | 6 | 12 | 18 |
| $\pi_{3j}^l$ | 26 | 31 | 33 |
| $\pi_{3j}^r$ | 12 | 11 | 10 |

**Table 4:** BAG Data from 2014 gleaning season

| Class | Total pounds gleaned [pounds/season] | Total number of trips [trips/season] | Total number of volunteers attending trips [volunteer attendance/season] | Average number of pounds gleaned by one volunteer on a 3-hour trip |
|---|---|---|---|---|
| Class 1 | 12,905 | 6 | 25 | 509 |
| Class 2 | 21,878 | 14 | 61 | 360 |
| Class 3 | 24,451 | 17 | 102 | 239 |
| Class 4 | 26,361 | 27 | 161 | 163 |
| Class 5 | 12,417 | 27 | 197 | 63 |

# E Comparison of Simulation Output to 2014 BAG Gleaning Season Output

To check that our simulation model produces the same output as the actual gleaning operation, we use input parameters from the Boston Area Gleaners' 2014 gleaning season, run our simulation, and compare the output of the simulation to the actual output in 2014. We received gleaning trip data on 5 crop types, gleaned over a span of the 220-day gleaning season in 2014, during which there were $n = 200$ volunteers in the volunteer pool. An estimate from BAG indicated a volunteer service rate of $\mu = 0.0253$ (Caldwell et al. 2017) (i.e., the volunteer becomes available approximately every 40 days). Table 4 shows the actual trip numbers and output of the 2014 season.

We compared the performance of the gleaning operation predicted by our simulation with the actual output from the 2014 season. In particular, we compared by class and in total, the number of pounds gleaned, the number of trips scheduled, and the number of volunteers that attended trips. Tables 5, 6, and 7 show that the actual performance metrics from the 2014 season fall within the boundaries of the 95% confidence intervals for each metric predicted by our simulation model.

**Table 5:** Total pounds gleaned

| Total pounds gleaned | Actual | Simulation Average | 95% Confidence Interval Lower Bound | 95% Confidence Interval Upper Bound |
|---|---|---|---|---|
| Total | 98,012 | 98,868 | 96,911 | 100,825 |
| Class 1 | 12,905 | 13,369 | 12,311 | 14,428 |
| Class 2 | 21,878 | 22,276 | 21,103 | 23,448 |
| Class 3 | 24,451 | 24,549 | 23,435 | 25,663 |
| Class 4 | 26,361 | 26,621 | 25,522 | 27,720 |
| Class 5 | 12,417 | 12,051 | 11,617 | 12,484 |

**Table 6:** Total number of trips scheduled

| Number of trips | Actual | Simulation Average | 95% Confidence Interval Lower Bound | 95% Confidence Interval Upper Bound |
|---|---|---|---|---|
| Total | 91 | 91.30 | 89.54 | 93.06 |
| Class 1 | 6 | 6.20 | 5.71 | 6.69 |
| Class 2 | 14 | 14.24 | 13.51 | 14.97 |
| Class 3 | 17 | 17.18 | 16.42 | 17.94 |
| Class 4 | 27 | 27.37 | 26.22 | 28.52 |
| Class 5 | 27 | 26.31 | 25.40 | 27.22 |

**Table 7:** Total number of volunteers that attended trips

| Number of volunteers attending trips | Actual | Simulation Average | 95% Confidence Interval Lower Bound | 95% Confidence Interval Upper Bound |
|---|---|---|---|---|
| Total | 547 | 545.39 | 534.83 | 555.95 |
| Class 1 | 25 | 26.25 | 24.17 | 28.33 |
| Class 2 | 61 | 61.96 | 58.70 | 65.22 |
| Class 3 | 102 | 102.79 | 98.13 | 107.45 |
| Class 4 | 161 | 163.1 | 156.37 | 169.83 |
| Class 5 | 197 | 191.29 | 184.41 | 198.17 |

# F Sensitivity Analysis on the Staffing Level Range

In this sensitivity analysis, we investigate how the staffing level range affects the performance of the dynamic policy. To facilitate this analysis, we define the following parameters: $\underline{\delta}_{ij} \equiv k^* - \underline{k}_{ij}$ and $\bar{\delta}_{ij} \equiv \bar{k}_{ij} - k^*_{ij}$. For example, the simulation study in Section 6, $\underline{\delta}_{ij} = \bar{\delta}_{ij} = 0.2k^*_{ij}$, so that the entire range of staffing levels is $k^*_{ij} \pm 0.2k^*_{ij}$. For this sensitivity analysis, we consider the following values for $\underline{\delta}_{ij}$ and $\bar{\delta}_{ij}$: $\underline{\delta}_{ij}, \bar{\delta}_{ij} \in \{0.1k^*_{ij}, 0.2k^*_{ij}, 0.3k^*_{ij}, 0.6k^*_{ij}\}$.

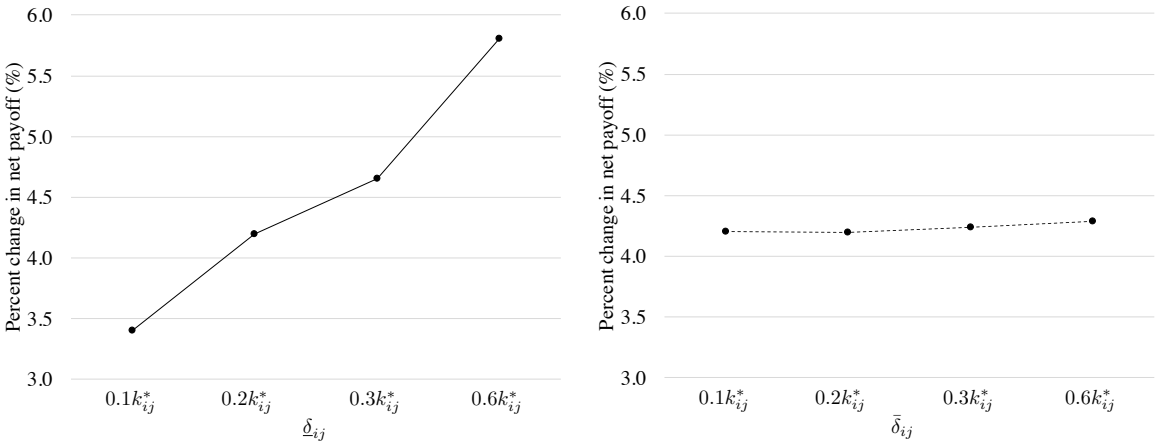


(a) Changing $\underline{\delta}_{ij}$, holding constant $\bar{\delta}_{ij} = 0.2k^*_{ij}$.

(b) Changing $\bar{\delta}_{ij}$, holding constant $\underline{\delta}_{ij} = 0.2k^*_{ij}$.

**Figure 11:** Percent change in net payoff achieved by the dynamic policy over the static policy for various staffing level ranges; $n = 400$, $q = 0.8$, $\mu = 0.0253$, $p = 160$.

Figure 11 shows the percentage change in net payoff of the dynamic policy compared to static policy as we change $\underline{\delta}_{ij}$ and $\bar{\delta}_{ij}$, for penalty value $p = 160$. Comparing Figures 11(a) and 11(b) shows that $\underline{\delta}_{ij}$ has more impact on performance than $\bar{\delta}_{ij}$. Specifically, increasing $\underline{\delta}_{ij}$ from $0.1k^*_{ij}$ to $0.6k^*_{ij}$ increases the relative performance of the dynamic policy from 3.4% to 5.8%, whereas the relative performance of the dynamic policy remains relatively constant at approximately 4.2% for the same range of $\bar{\delta}_{ij}$.

Figures 12 and 13 shed light on why $\underline{\delta}_{ij}$ is more effective than $\bar{\delta}_{ij}$. Comparing Figures 12(a) and 12(b) shows that the increase in net payoff relative to the static policy comes from reducing the number of rejected donations. For this purpose, the $\underline{\delta}_{ij}$ lever is more effective than $\bar{\delta}_{ij}$. By increasing $\underline{\delta}_{ij}$, every time the staffing level is set to $\underline{k}_{ij}$, more volunteers are "saved" for later trips, thereby reducing the probability of a later donation being rejected. Moreover, each $\underline{k}_{ij}$ trip saves more volunteers as $\underline{\delta}_{ij}$ increases. Thus, fewer trips have to be designated $\underline{k}_{ij}$ trips (see Figure 13(a)), but

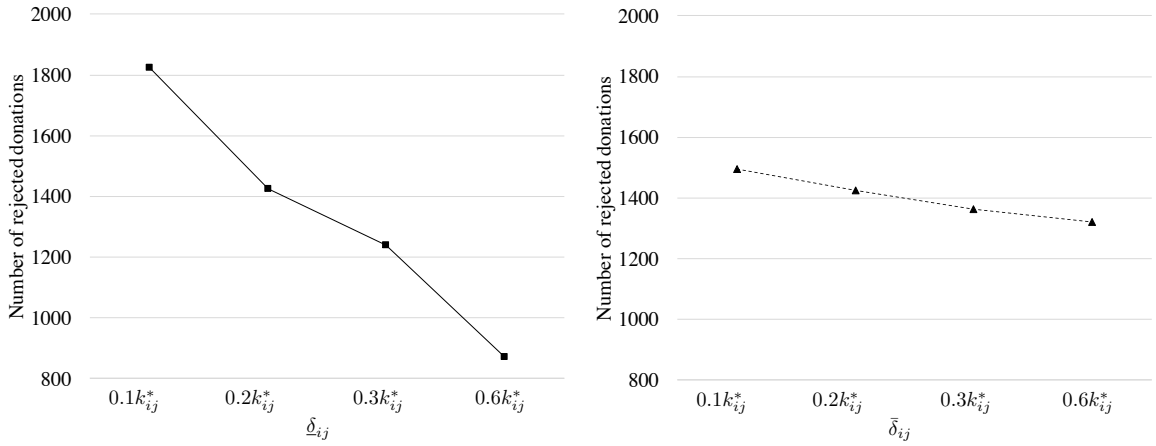


(a) Changing $\underline{\delta}_{ij}$, holding constant $\bar{\delta}_{ij} = 0.2k^*_{ij}$.

(b) Changing $\bar{\delta}_{ij}$, holding constant $\underline{\delta}_{ij} = 0.2k^*_{ij}$.

**Figure 12:** Average number of rejected donations in a season for various staffing level ranges; $n = 400$, $q = 0.8$, $\mu = 0.0253$, $p = 160$.

those trips have very low staffing level. Those few $\underline{k}_{ij}$ staffing level trips provide a two-fold benefit to the system: 1) donations that would have been rejected for lack of volunteers (or equivalently, a large backlog of jobs) are accepted, and 2) trips that would have been assigned the $\underline{k}_{ij}$ staffing level are bumped up to the $k^*_{ij}$ or $\bar{k}_{ij}$ staffing level.

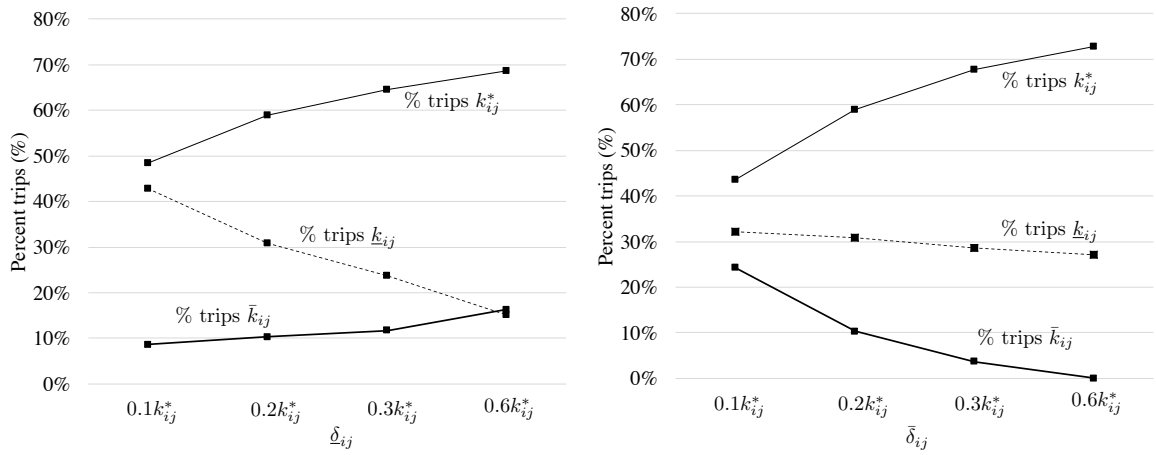


(a) Changing $\underline{\delta}_{ij}$, holding constant $\bar{\delta}_{ij} = 0.2k^*_{ij}$.

(b) Changing $\bar{\delta}_{ij}$, holding constant $\underline{\delta}_{ij} = 0.2k^*_{ij}$.

**Figure 13:** Percentage breakdown of trips at each staffing level for various staffing level ranges; $n = 400$, $q = 0.8$, $\mu = 0.0253$, $p = 160$.

Conversely, Figure 12(b) shows that as we increase $\bar{\delta}_{ij}$, the number of rejected donations decreases only slightly. The dynamic policy shifts the allocation of trips from $\underline{k}_{ij}$ and $\bar{k}_{ij}$ to $k^*_{ij}$ as $\bar{\delta}_{ij}$ increases (see Figure 13(b)). Clearly, as $\bar{\delta}_{ij}$ increases, it becomes more inefficient to choose the $\bar{k}_{ij}$

staffing level because the value of the marginal volunteer on a given trip decreases. Reducing the number of $\bar{k}_{ij}$ trips frees up some volunteers, but since the number of $\bar{k}_{ij}$ trips was low to begin with, this has limited impact on increasing the availability of volunteers for future trips. Thus, there is only a small decrease in the number of rejections. However, the "freed up" volunteers can be used to shift $\underline{k}_{ij}$ trips to $k^*_{ij}$ trips.

The results from this sensitivity analysis would seem to suggest that $\underline{k}_{ij}$ should be very low. However, it should be noted that $\underline{k}_{ij}$ cannot be so low that it is not worthwhile for the gleaning organization to organize and manage the $\underline{k}_{ij}$ trip. For example, suppose the gleaning organization measured the value of the crop using the farm-gate price, and the cost of organizing a gleaning trip consists of the cost of the staff and truck needed for the trip. An estimate for the fixed cost of a trip is \$22 for transportation (40 miles at \$0.55 per mile) and \$128 for staff (4 hours at \$32 per hour), for a total fixed cost of \$150. To make the trip worthwhile, the value of the produce gleaned should total at least \$150. For the apple crop, the farm gate price is \$0.376 per pound (USDA 2018). Therefore, if a volunteer can harvest 210 pounds per trip, the minimum number of volunteers required to make an apple gleaning trip worthwhile is $2.5 \sim 3$ volunteers. Therefore, for apples, $\underline{k}_{ij} \geq 3$. The lower bound for $\underline{k}_{ij}$ for each class would vary depending on how the value of the crop is assessed and what it costs to organize the gleaning trip.